Field Training Course Notebook

Structural analysis of Earthquake Archaeological Effects (EAE): Baelo Claudia Examples (Cádiz, South Spain)

Editors

J.L. Giner-Robles, M.A. Rodríguez-Pascua, R. Pérez-López, P.G. Silva, T. Bardají, C. Grützner and K. Reicherter

1st INQUA-IGCP 567 International Workshop on Earthquake Archaeology and Palaeoseismology

VOL 2

7-13 September 2009

Baelo Claudia (Cádiz, Spain)

Field Training Course Notebook

Structural analysis of Earthquake Archaeological Effects (EAE): Baelo Claudia Examples (Cádiz, South Spain)

Editors
J.L. Giner-Robles, M.A. Rodríguez-Pascua, R. Pérez-López,P.G. Silva
T. Bardají, C. Grützner, and K. Reicherter

Focus Area on Paleoseismology and Active Tectonics

INQUA

IUGS UNESCO IGCP 567

Earthquake Archaeology
Archaeoseismology along the Alpine-Himalayan seismic zone

This **Notebook Volume** 2 has been produced for the **1st INQUA-IGCP 567 International Workshop on Earthquake Archaeology and Palaeoseismology** held in Baelo Claudia Roman ruins (Cádiz, Southern of Spain). The event has been organized together by the INQUA Focus Area on Paleoseismology and Active Tectonics and the IGCP-567: Earthquake Archaeology.

This scientific meeting has been supported by the Spanish Research Projects ACI2008-0726, CGL08-03998BTE, CGL08-04000BTE and ACTISIS CGL2006-05001/BTE and UNED grant.

RWTH AACHEN UNIVERSITY · VNiVERSiDAD D SALAMANCA · UNED · Instituto Geológico y Minero de España · INQUA · IUGS UNESCO IGCP · AEQUA · JUNTA DE ANDALUCIA CONSEJERIA DE CULTURA · CSIC · GOBIERNO DE ESPAÑA · MINISTERIO DE CIENCIA E INNOVACIÓN

Index

1. Introduction 5

Traces of Archaeoearthquakes

Questions to be solved before the structural analysis will be performed

Cautions and uncertainties

Contributions of the 1st INQUA-IGCP 567 Workshop on Earthquake Archaeology

2. Classification of Earthquake Archaeological Effects (EAE) 13

PRIMARY COSEISMIC EFFECTS

SECONDARY POSTSEISMIC EFFECTS

STRAIN STRUCTURES GENERATED BY GROUND DEFORMATION 17

2.1a FOLDED MORTAR PAVEMENTS

2.1b FRACTURES, FOLDS AND POP-UPS ON "REGULAR PAVEMENTS"

2.1c FRACTURES, FOLDS AND POP-UPS ON "IRREGULAR PAVEMENTS"

2.2a SHOCK BREAKOUTS IN FLAGSTONES

2.2b FRACTURE PATTERNS IN FLAGSTONES

2.3 ROTATED AND DISPLACED BUTTRESS WALLS

2.4 TILTED WALLS

2.5 FOLDED AND DISPLACED WALLS

STRAIN STRUCTURES GENERATED IN THE BUILDING FABRIC 28

2.6 PENETRATIVE FRACTURES IN MASONRY BLOCKS

2.7 FALLEN AND ORIENTED COLUMNS

2.8 DISPLACED MASONRY BLOCKS

2.9 DROPPED KEY STONES IN ARCHES OR LINTELS IN WINDOWS AND DOORS

2.10 FOLDED STEPS AND KERBS

2.11 IMPACT BLOCK MARKS

2.12 DIPPING BROKEN CORNERS

BASCULATED AND COLLAPSED WALLS

SUMMARY OF THE GEOLOGICAL STRUCTURAL ANALYSIS OF DAMAGED STRUCTURES

3. Quantification of the strain data 39

3.1 DATA CONSTRAINT 39

Orientation data

Type of data

Complementary data

Comparing poblational dataset

3.2 ORIENTATION OF THE HORIZONTAL STRAIN TENSOR 43

A brief background of the strain tensor

Regional and local strain tensor

3.3 INDIVIDUAL EAE ANALYSIS 45

I. Fracture, Folds and Pop-Ups in Pavements

II. Tilted, Displaced and Folded Walls

III. Fallen and Oriented Columns

IV. Dropped Keystone in Arch or Lintel in Windows and Doors

V. Impact Block Marks

VI. Dipping Broken Corner-Blocks

3.4 STRAIN FIELD *VS* PREVIOUS ANISOTROPY 61

3.4a Geological data

3.4b Anisotropy induced by archaeological structures

3.5 CONCEPTUAL EXAMPLE OF THE FINAL OUTCOME OF THIS COURSE 64

4. Field sheets for selected EAE 67

4.1 FOLDED MORTAR PAVEMENTS, FRACTURES, FOLDS & POP-UPS

4.2 SHOCKS BREAKOUTS IN FLAGSTONES

4.3 TILTED WALLS

4.4 FOLDED WALLS

4.5 FALLEN AND ORIENTED COLUMNS

4.6 DROPPED KEYSTONES IN ARCHES OR LINTELS IN WINDOWS AND DOORS

4.7 DIPPING BROKEN CORNERS

4.8 BUILDING RECONSTRUCTION

5. References

Appendix

Work plans of Baelo Claudia

Key map

1.1 Theatre 1 (west side)

1.2 Theatre 2 (east side)

2. West Decumanus maximus
3. Center Decumanus maximus
4. East Decumanus maximus. Market. South Place. Curia
5. Baths
6. West Foro. Temple. Archive
7. East Foro. Shops
8. Foro. Basilica
9. Capitolium. Temples of Minerva, Jupiter and Juno
10. Temple of Isis

1. INTRODUCTION

1. Introduction

In recent years, the Archaeoseismology has passed from being a new term to an own discipline known in the study of earthquakes. The different effort made in the 80s by some authors was directed to release this multidisciplinary branch of science (Rapp, 1982; Zang et al., 1986; Stiros, 1988a y b; Nikonov, 1988; Guidoboni, 1989) and begins to be taken into account. Although, other authors had introduced before the earthquakes in archaeological interpretations (e.g. Lanciani, 1918), Stiros and Jones (1996) made a compilation of the state of the art in Archaeoseismology and recommended a multidisciplinary collaboration among Archaeology, Seismology, Geology, Engineering, Architecture and History. Nowadays this statement is widely accepted and the multidisciplinary work is strongly required for the advance in Archaeoseismology. Furthermore, these authors made a question: *What criteria are necessary to identify seismic effects on an archaeological site?* At present, this question is not fully answered, being actually one of the objectives of the IGCP 567 (Earthquake Archaeology along the Alpine-Himalayan seismic zone), to formulate an appropriate standardize methodology on Archaeoseismology. In this sense, the work of Sintubin and Stewart (2008) has gone beyond proposing a methodology based on the logical-tree structure to quantify a potential archaeoseismological factor (AF) of an archaeological site. However, at present there is not a precise and specific methodology for distinguishing seismic effects from other destructive agents.

This Field Training Course Notebook appears with the aim of establishing a methodology for the recognition and measurement of deformations, with the purpose to discriminate between coseismic processes from other energetic processes. The deformation generated in an ancient city should be conditioned by the trigger mechanism that generated these features. In this sense, the deformation produced by an earthquake is strongly conditioned by the orientation of the seismic wave arrival, whereas wars, explosions or simply ruin normally generate random not uniformly oriented collapses of the architectural fabrics. Thus, if we could see Tenochtitlan after the attack of Hernán Cortés using artillery, we would not find oriented structures of deformation. However, the seismic waves produce an oriented impulse, which may trigger the arrangement of the deformations.

In this course, we propose a reverse problem, by means of the observed deformations it is possible to calculate the strain ellipsoid produced by the earthquake in the ancient buildings. The trend of the strain axis of different deformation structures must be similar if the trigger mechanism was a single earthquake. Otherwise, a relevant dispersion of the calculated strain ellipsoids will be obtained, like the effect of the artillery in a devastating city. The classification of the structures of deformation according to the EAE standardized classification (i.e. Rodríguez-Pascua et al., 2009) is recommended with the purpose of normalizing or regulating further analyses.

The classic techniques of geological structural analysis are shown as tools for calculating the strain ellipsoids of seismic origin by deformations located in archaeological sites. We have chosen the ancient Roman City of Baelo Claudia to test this methodology, because it was the first archaeological site in Spain analyzed from modern archaeoseismological techniques (Silva et al., 2005; 2009). The richness and variety of deformed structures in this ancient city make it suitable the application of analytical techniques in Structural Geology. The result has been this Field Training Course Notebook in which the assistants may acquire skills about how to analyze some of these architectural disruptions and deformations *in situ* as well as their subsequent treatment in the laboratory. These approaches will make possible to obtain data about the origin of these deformations in order to integrate them with other data obtained from Archaeology, Seismology, Geology, Engineering, Architecture and History, to reach a checked solution.

Whatever the case, we have to take into account that the recorded deformations in an archaeological site may hold different sources, and in most of the cases they are the summation of several ones. The natural slope of the site, additional landsliding events, natural subsidence, severe storms or hurricanes, and even the ruin and burial history of the site has to be largely considered during and after the analysis of deformed archaeological sites. Some of these processes can also produce similar oriented arrangements of architectural fabrics, therefore the geomorphological context (coastal site, valley site, mountainous site, etc.), the climatic context and even the climatic history (for the most ancient sites) have to be taken into account to assist the scientific discussion of the obtained data. Finally, other post-burial interferences must be considered, such as a complete knowledge of the history of the archaeological excavations, works for the consolidation of ruins , etc.

Traces of Archaeoearthquakes

An historic view and state of the art of archaeoseismology

Detecting earthquakes in ancient remains and archaeological findings is an attractive argument for researchers. The history of humankind is the history of catastrophes that have affected all cultures around the world. In Archaeology, the reconstruction of the past obviously includes these catastrophes and, in general, is described under superstitious or even religious frames. However, in Geology there are not catastrophes, the history of the Earth is the knowledge of the Geodynamics of an evolving Earth. Extinctions and human catastrophes are the consequence of living on a living planet.

Archaeoseismology addresses the possibility to detect earthquakes affecting ancient remains. Evans (1928) defined the *earthquake horizon* from his own experience of an earthquake shaking while he was working in an archaeological site (Stiros, 1996). This horizon of destruction was soon adopted by the archaeology community although with more enthusiasm than a strict scientific methodology.

One of the first cooperative works to develop the foundations of this new discipline is the volume of Archaeoseismology, edited by Stiros and Jones (1996). In the introduction of this volume, both authors underlined the relevance of the archaeoseismic information for seismic hazard assessments. Perhaps the most notorious argument supporting the archaeoseismology provided in that volume is the multidisciplinary approach to evaluate correctly ancient earthquakes from archaeology findings. Moreover, Stiros (1996) introduced a systematic guideline to assign earthquake destruction in archaeological sites (Peloponnese and Gulf of Corinth area). This guideline includes a detailed description of structural damage affecting fallen columns, tilted walls, chipped corners, arches and vaults, etc.

The oriented damage of structures is also considered as a strong argument to support the seismic destruction but with some considerations: use of multiple damaged structures, absence of anthropic destruction, etc. Nur and Ron (1996) and Korres (1996) also introduced structural damage affecting other archaeological sites in the Jordan area and Greece (Athenian Acropolis) respectively. Buck and Stewart (2000) and Jones and Stiros (2000) pointed out the ambiguity of archaeoseismic evidence for earthquakes in Greece and the Mediterranean zone, Guidonobi et al. (2000)

introduced a methodological classification in archaeology applied for strong ancient earthquakes.

Other interesting volumes focused on Archaeoseismology are The Archaeology of Geological Catastrophes, edited by McGuire, Griffiths, Hancock and Stewart (2000) and the Special Issue on Archaeoseismology at the Beginning of the 21st Century, edited by Galadini, Hinzen and Stiros (2006). Deformed structures or arches and walls are described by Hancock et al. (2000) and Galadini et al. (2006) proposed a methodological issue and procedure for Archaeoseismology. Modelling of structural damage is performed by Mistler et al. (2006) and Poursoulis et al. (2006).

Kovach (2004) compiled several archaeoseismic findings in his outstanding book Early Earthquakes of the Americas, finding a lot of archaeoseismic evidence from Azteca, Inca and Maya ancient cultures. Moreover, this author agreed with a systematic approach for Archaeoseismology in similar terms than Stiros (1996) and Nur and Ron (1996). This author also described structural damage from seismic shaking and affecting corbelled arches, prehispanical pyramids, walls, tombs *stelae*, etc.

Two of the most interesting epoch-analyses were performed at the San Francisco earthquake (1906) by Lawson (1908) and at the Acambay earthquake (1912) by Urbina y Camacho (1913). Both works described structural damage on modern buildings by two instrumental strong earthquakes (both greater than Ms 7). We have included this references in those structures analysed here that present similar damage than those described by these authors.

Questions to be solved before the structural analysis will be performed.

Stiros (1996) pointed out several interesting questions to solve before the archaeoseismic argument will be widely accepted.

When? The question addresses whether we can date the archaeoearthquake or not. Several techniques on geochronology can help us to date the earthquake, although a more deep explanation goes beyond the focus of this course (i.e. 14C, K-Ar, U-Th Series, 210 Pb, dendrochronology, lichenometry, termoluminescence, tephrochronology, etc.). However, some concepts are needed to say here: first, numerical aging is relevant only if we well-know *what has to be dated*. Furthermore, we have to well-know the constraints and age interval of the dating technique, and finally, we have to obtain the errors of the measurement to evaluate the reality of the numerical age.

Where? One thing is to state that one earthquake has hit one ancient city and other is locating potential epicentres. Studies on seismotectonics and tectonic geomorphology into the area can help us to understand the geodynamics of the area and the seismic potential of geological features near to the archaeological site.

How? Once the potential seismic source is identified (seismogenic fault or seismogenic area), palaeoseismology help us to identify the history of this fault, period of recurrence, slip-rate for seismogenic faults, evidences of paleoearthquakes and even material to be dated. Other arguments to be used: archaeological evidence of earthquakes, ancient writings and chronicles, ceramic and mosaic iconography, etc. (e.g. Nur and Cline 2000; Ambraseys, 2006).

Cautions and uncertainties

Several works strongly recommend that cautions and uncertainties should be considered before the seismic theory will be accepted. A great variety of these cautions and methodologies applied to reduce uncertainties can be consulted at: Stiros (1996), Jones and Stiros (2000), Buck and Stewart (2000), Guidoboni et al. (2000), Kovach (2004), Ambraseys (2006), Marco (2008), Sintubin and Stewart (2008).

Contributions of the 1st INQUA-IGCP 567 Workshop on Earthquake Archaeology and Palaeoseismology to Archaeoseismology

Towards a comprehensive classification of Earthquake Archaeological Effects and quantification of the deformation. This sentence resumes the aim of the Organization Committee regarding the Structural Course of Earthquakes Archaeological Effects. During the previous workshop, several works regarding the topic claimed here were presented. Archaeoseismic evidence along the word was presented by Chatzipetros and Pavlides (2009) and Ferry et al. (2009) in the Dead Sea zone, meanwhile Da-Quan et al. (2009) and Jin et al., (2009) worked on Archaseismology in China and Korea, respectively and Rodríguez-Pascua et al. (2009b) and Silva et al., (2009b) have introducing historic earthquakes from archaeoseismic evidence in Spain. Hinzen, (2009), Schaub et al., (2009), Schereiber et al. (2009) and Yerli et al. (2009) have modelled the structural damage affecting ancient constructing by using modern techniques as LIDAR survey and numeric modelling. Regarding the methods in Archaeoseismology, Hinzen et al. (2009) proposed a *quantitative method* to test the seismogenic hypothesis based on laser scanner, geotechnical models, ground motion and structure models. In this way, Rodríguez-Pascua et al. (2009) introduce a comprehensive classification of the so-called Earthquake Archaeological Effects (EAE) and their use to obtain strain data related with the seismic source. Finally, Sintubin et al. (2009) pointed out the future trends in Archaeoseismology, with spatial focus on the development of quantitative multidisciplinary methodologies.

Acknowledgements
The Organizers of the field course on Structural analysis of Earthquakes Archaeological Effects acknowledge the support given by the responsible people of "Conjunto Arqueológico Romano de Baelo Claudia (Junta de Andalucía)" in assisting our initiative by giving us access to different facilities of the Museum of Baelo Claudia, as well as all the institutions involved in the organization, and all the people of the Bolonia Bay (Cádiz) around the conference.

Organization

P.G. Silva (ESP) and K. Reicherter (GER)

Organization Committee

T. Bardají (ESP), A. Cabero (ESP), P. Carrasco (ESP), T.Fernández-Steeger (GER), I. García (ESP), J.L. Giner-Robles (ESP), J.L. Goy (ESP), C. Grützner (GER), P. Huertas (ESP), J. Lario (ESP), A. Muñoz (ESP), R. Pérez-López, (ESP), M.A. Rodríguez-Pascua (ESP), C. Zazo (ESP)

After Bonsor 1919.

2. CLASSIFICATION OF EARTHQUAKE ARCHAEOLOGICAL EFFECTS (EAE)

Aim:
During the workshop held at Baelo Claudia (Spain, 2009), the authors have presented a work entitled: A COMPREHENSIVE CLASSIFICATION OF EARTHQUAKE ARCHAEOLOGICAL EFFECTS (EAE) FOR STRUCTURAL STRAIN ANALYSIS IN ARCHAEOSEISMOLOGY, by Rodríguez-Pascua et al. (2009). The second chapter of the Field course Notebook is based on this publication, extracting those relevant parts and being increased with various photographs from Baelo Claudia. The main objective of this chapter is to introduce the Earthquake Archaeological Effects (EAE) to the reader. The next chapter consists to evaluate the strain field deduced from these EAEs with the purpose to establish the seismic anisotropy, the seismic ray potential direction and therefore, the congruence with the interpretation of an earthquake-damage affecting to the archaeological site.
One of the key arguments in Archaeoseismology consists to identify how quantity of the observed damage is related with ancient earthquakes. Abandonments, ruins or wars are general causes assumed by archaeologists and natural disasters are rarely considered. In this chapter, we propose and develop a comprehensive classification of Earthquakes Archaeological Effects (EAE) with the aim of carry out geological structural analysis. The objective of this classification is to recognize the tectonic strain field responsible of the buildings damage and the relationship with the potential earthquake or related-earthquake natural disaster. Several examples at Baelo Claudia of such EAEs are shown.

2. Classification of Earthquake Archaeological Effects (EAE)

The interest of in the characterization of EAE is to recognize potential archaeoseismic damage due to earthquake deformation from other damage assigned to ruins, wars or abandonment, among others. Furthermore, a good establishment of potential EAE in a particular archaeological site supports indirect information of the seismic source for earthquake hazard assessment. Following the recent classification of earthquake environmental effects (EEE) established in the ESI-07 Intensity Scale (Michetti, et al., 2007) we introduce a classification of EAE based on strain structures due to "coseismic effects" (*direct or primary effects*) and structures generated by "postseismic effects" (indirect or secondary effects) (Fig. 1). This subdivision classifies those coseismic archaeological effects from those post-seismic effects "as a consequence" of the large earthquake affecting a populated site.

PRIMARY COSEISMIC EFFECTS

We have divided the primary coseismic effects in (1) geological effects and (2) building fabric effects (Fig. 1) (Rodríguez-Pascua et al., 2009).

(1) Geological effects: These effects are well described from the macroseismic scale of environmental earthquake effect (ESI07, Michetti et al., 2007). This scale separates primary effects as fault scarp, surface rupture, and tectonic uplift/subsidence from secondary effects as liquefaction, landslides, tsunamis, etc.

Geological effects recognized as EAE are referred a fault planes crossing the ancient town, soil displacements due to seismic shaking, city damage for landslides and rockfalls, liquefaction generating tilted monuments, remains buried by seismites and tsunamites within the archaeological stratigraphic sections. This kind of effects is the traditionally cited ones in the still young archaeoseismological literature.

(2) Building fabric coseismic effects: These effects indicate direct damage on buildings associated to ground deformation and/or seismic waves. We have focused the Structural Course on practise the recognition and quantification of these EAEs in different parts of the roman city of Baelo Claudia.

First of all, a complete understanding of the type of construction (masonry, mortar type, column type, arch construction etc.) used by ancient cultures in each particular archaeological site is needed. This architectural knowledge allows recognizing those potential buildings to find archaeoseismic effects and discards those other ones damaged by secondary effects (antiseismic reconstruction, recycling blocks in reconstructions, etc.). In this case the differentiation of damage produced by (a) natural ground instability or (b) seismic ground shacking is a starting key point.

Some good examples of probable ground shacking deformations are folded pavements, shocks and oriented fracturing in pavement flagstones, folded mortar floors, pop up-like structures on pavements, titled and folded masonry walls, etc. Other deformations exclusively affecting to the building fabrics will be: penetrative fractures on masonry blocks, displaced or differentially rotated arches or, broken pottery found in fallen position, etc.

SECONDARY POSTSEISMIC EFFECTS

Other common deformations observed in present damaged archaeological remains are typically linked to the abandonment and eventual ruin of the site. Roof and vault collapses of inhabited houses commonly trigger fires by the burning of the wood fabric of most of the pre-modern roofs. Flash flood events triggered by earthquake severe damage on ancient earth dams is also a source of information but, complicate for decoding and interpretation.

Eventually the development of ancient antiseismic either structures or building designs are a key feature talking about previous strong seismic shaking events.

Destructive horizons within the geoarchaeological record tell about histories of city reconstruction. In this case the identification of demolition horizons linked to city reconstruction after severe earthquake damage is also a common feature in archaeoseismological sites. In the same way the analyses of recycled and reutilized architectural elements also can indicate the nature and age of city reconstruction.

Eventually, the burial history of the archaeological site can introduce complementary deformation and/or amplify the existing ones. An analysis of the present geomorphology of the area, operating geomorphic process during burial and the urban geology of the studied site are necessary to understand the existing deformation, if deformation is coeval and finite.

All the aforementioned structures of deformation are listed in the table of Figure 1, which illustrate most of the deformational structures we can see today in archaeological sites formerly affected by at least one earthquake. As in classical palaeoseismic analysis the building fabric coseismic effects has to be ascribed to a particular geoarchaeological horizon, which will be the earthquake horizon. In this sense before the structural analysis of building deformation we have to collect the complete geoarchaeological history of the city.

The simplest analysis of orientation of many of the building fabric effects can help to put constrains on the directivity or not of related ground deformation (e.g. Silva et al., 2009). Consistently oriented building deformation will indicate the sense of ground movement, but also to differentiate it for other non-oriented deformations caused by other phenomena. The determination of the geographical quadrant in which presumably a seismic source (NE, SW, etc.) was located for an historic, non-documented, event is a quality step provided by the archaeoseismology.

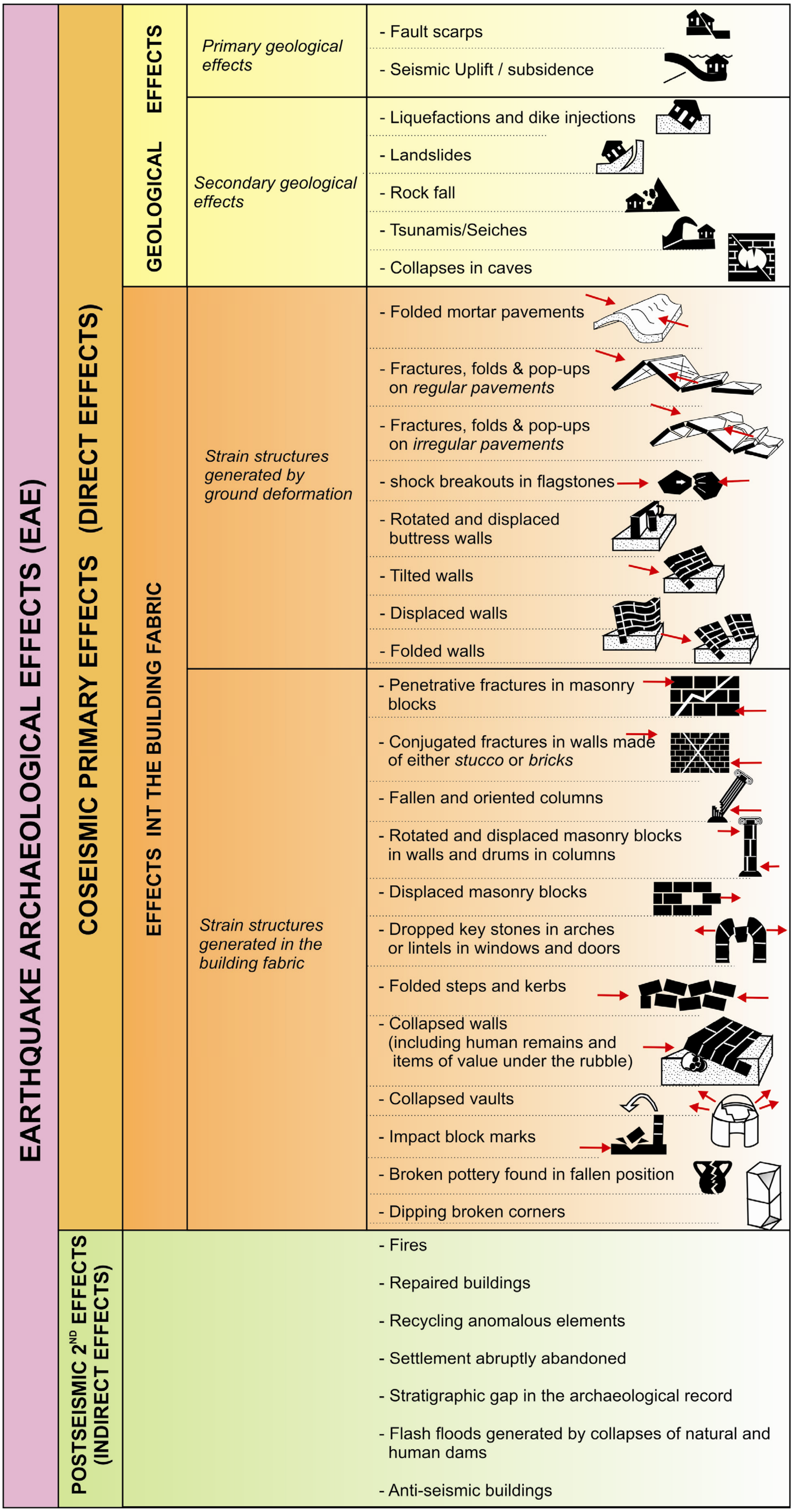

Fig. 1: A comprehensive classification of Earthquake Archaeological Effects (EAE), based on primary and secondary geological effects of earthquakes (After ESI07 macroseismic scale, Michetti et al., 2007) and building damage. Red arrows indicate the possible seismic wave orientation. After Rodríguez-Pascua et al., 2009.

Photographic examples at Baelo Claudia for EFFECTS IN BUILDING FABRIC

STRAIN STRUCTURES GENERATED BY GROUND DEFORMATION

2.1a FOLDED MORTAR PAVEMENTS

***Photo 1*.** Temple of Juno

Photo 2. Market (*Macellum*)

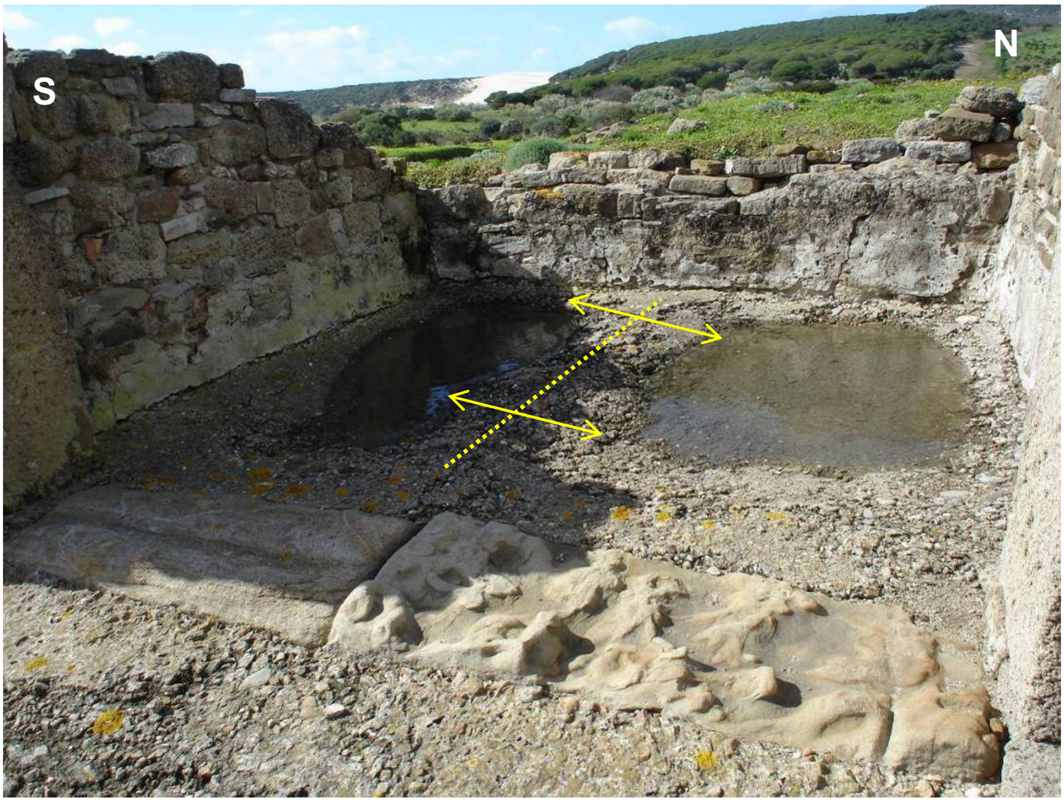

Photo 3. A detailed floor of one shop in the MARKET (*macellum*)

2.1b FRACTURES, FOLDS AND POP-UPS ON "REGULAR PAVEMENTS"

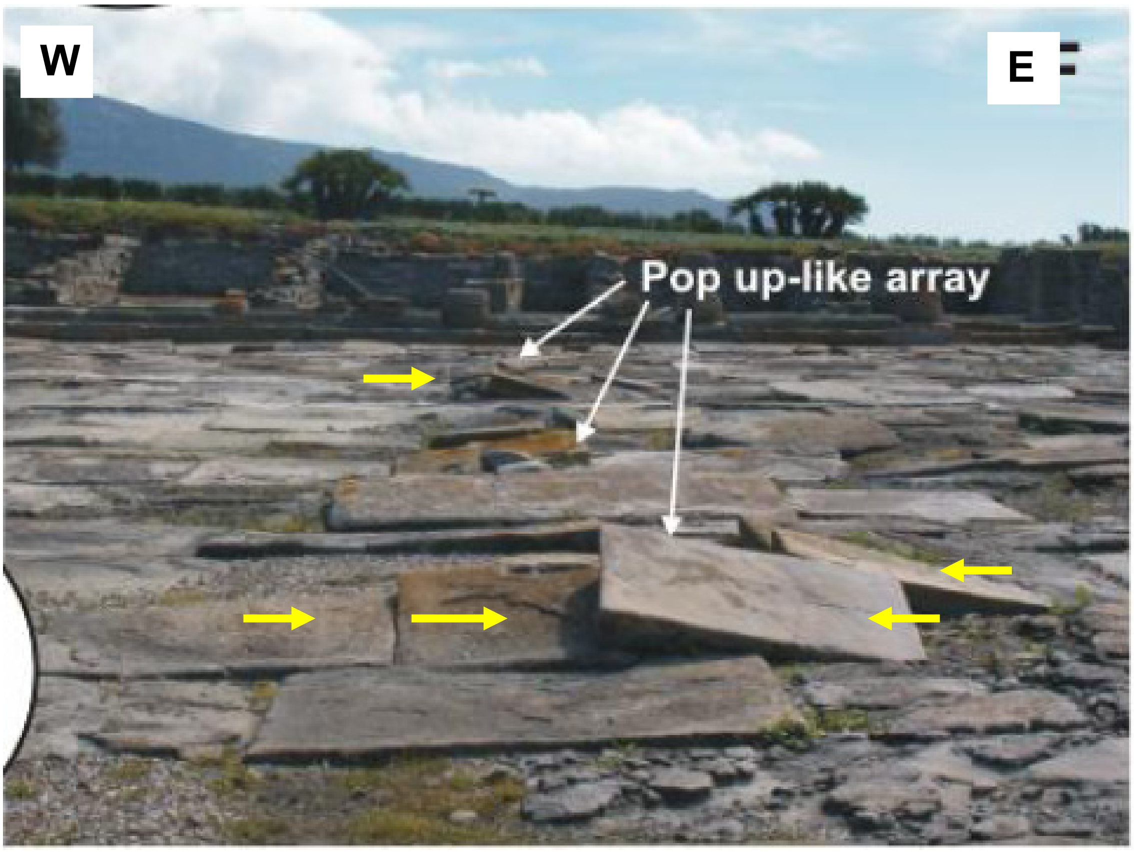

Photo 4. Pop-ups affecting the regular pavement of the FORO

Photo 5. Folded regular pavement and pop-ups (FORO). Yellow lines anticlines, red lines synclines axes.

Photo 6. Folded regular pavement (Principal Street in the THEATRE). Yellow dashed line indicates the anticline axis

2.1c FRACTURES, FOLDS AND POP-UPS ON "IRREGULAR PAVEMENTS"

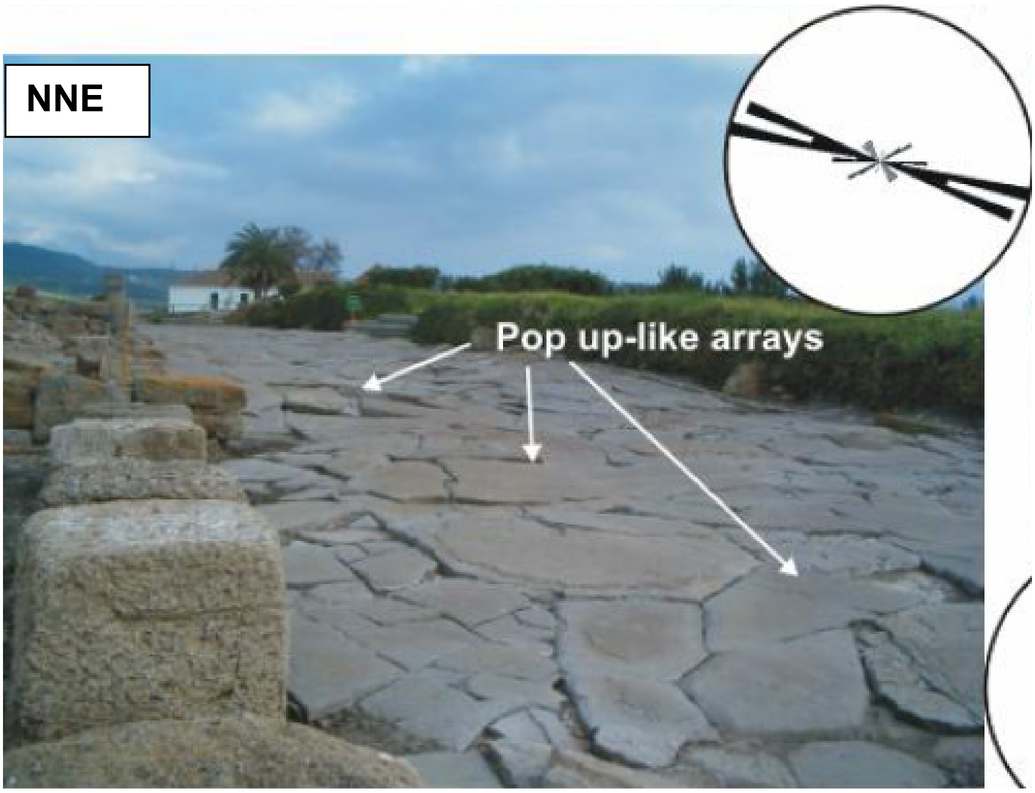

Photo 7. West DECUMANUS MAXIMUS

Photo 8. West-Central DECUMANUS MAXIMUS. Yellow dashed lines indicate anticline axis

2.2a SHOCK BREAKOUTS IN FLAGSTONES

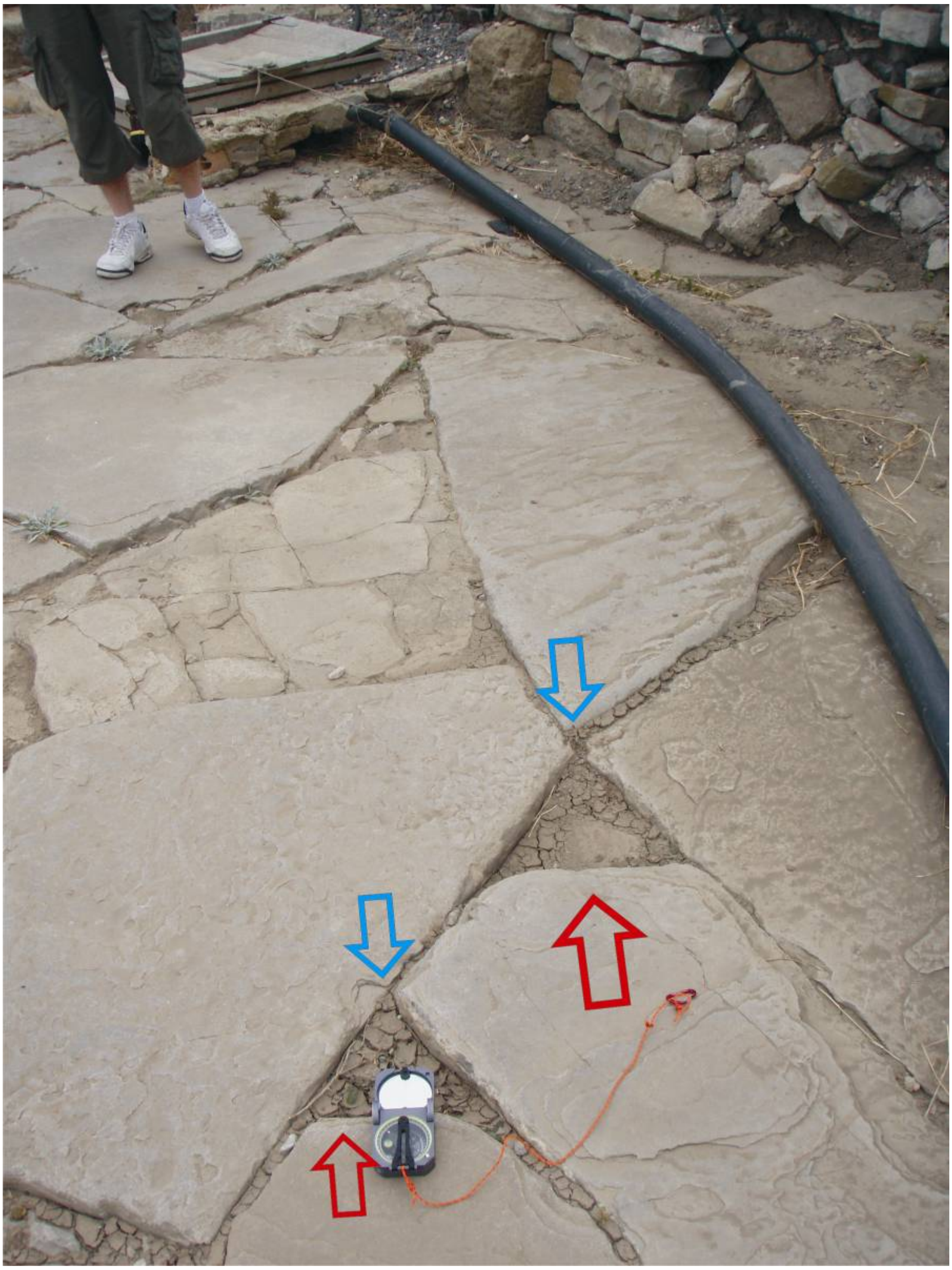

Photo 9. Shocks affecting irregular pavement at West DECUMANUS MAXIMUS. Blue and red arrows show the direction of shock. The red arrow is the probably seismic incoming azimuth

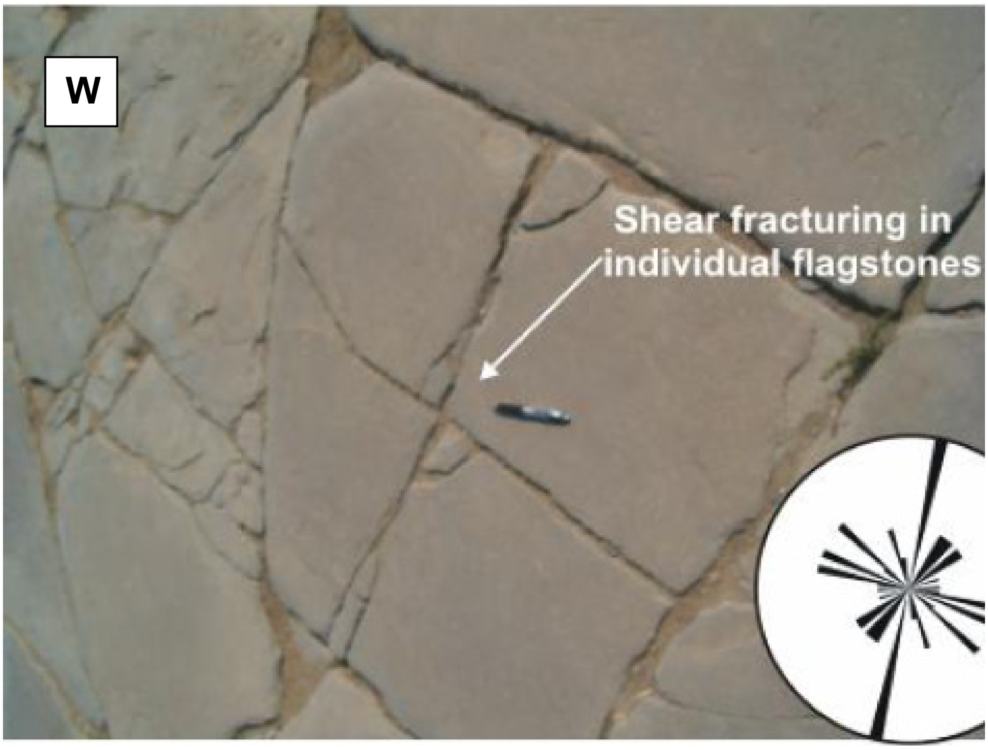

Photo 10. DECUMANUS MAXIMUS

Photo 11. DECUMANUS MAXIMUS

2.2b FRACTURE PATTERNS IN FLAGSTONES

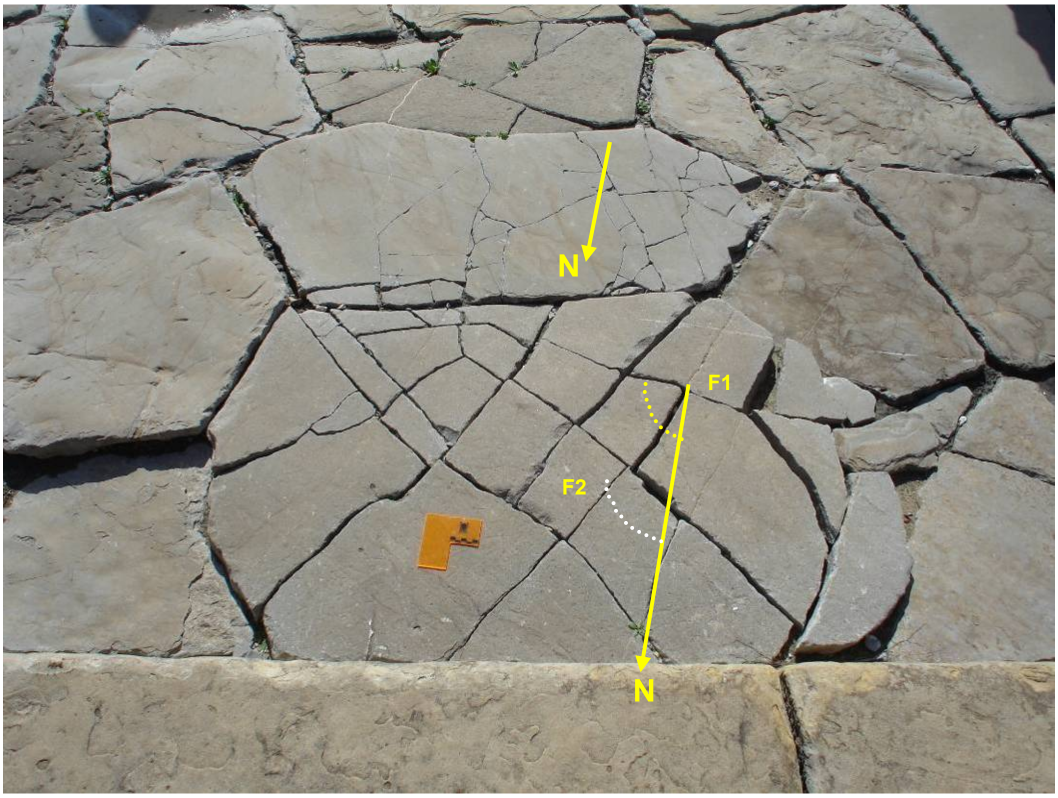

Photo 12a and 12b. Irregular pavement in the WEST DECUMANUS MAXIMUS, conjugated fracture sets oriented NW-SE and ESE-WNW (*up and down*)

2.3 ROTATED AND DISPLACED BUTTRESS WALLS

Photo 13. Rotated and displaced buttress affecting the water cistern at the Northern part of Baelo Claudia

Photo 14. Displaced masonry block (right, detailed view)

2.4 TILTED WALLS

Photo 15. Tilted north wall in the inner part of the ISIS TEMPLE

Photo 16. Tilt angle (α) of the tilted EAST DEFENSIVE WALL (BASTION)

2.5 FOLDED AND DISPLACED WALLS

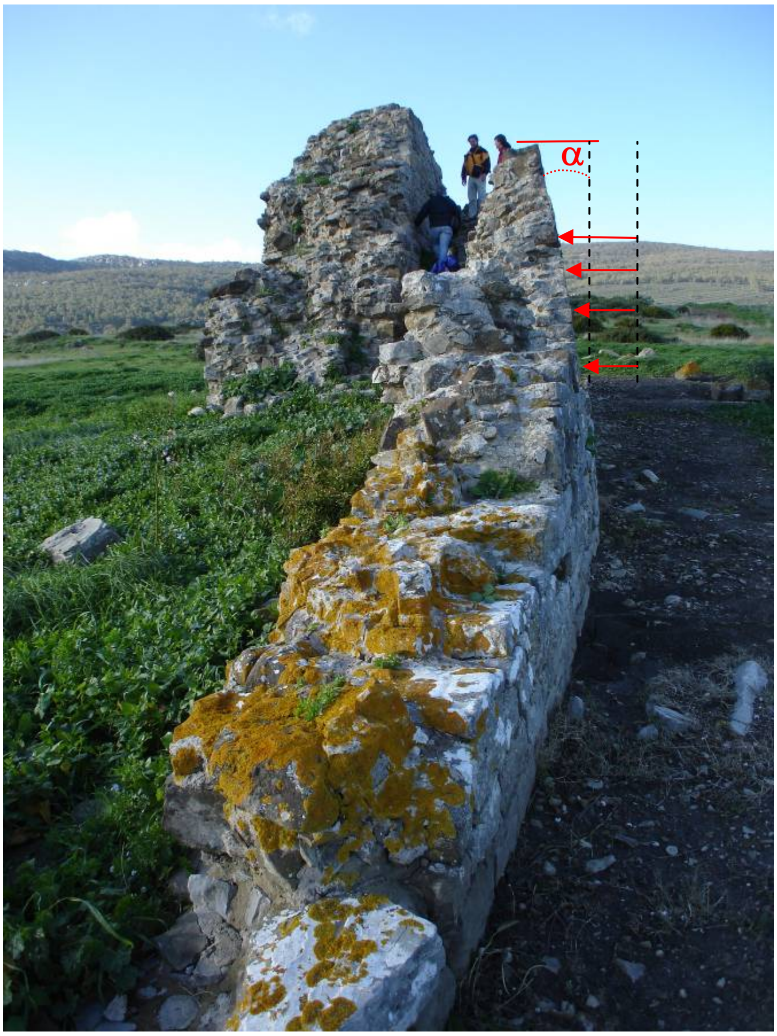

Photo 17. Folded and tilted defensive wall of the NORTH BASTION

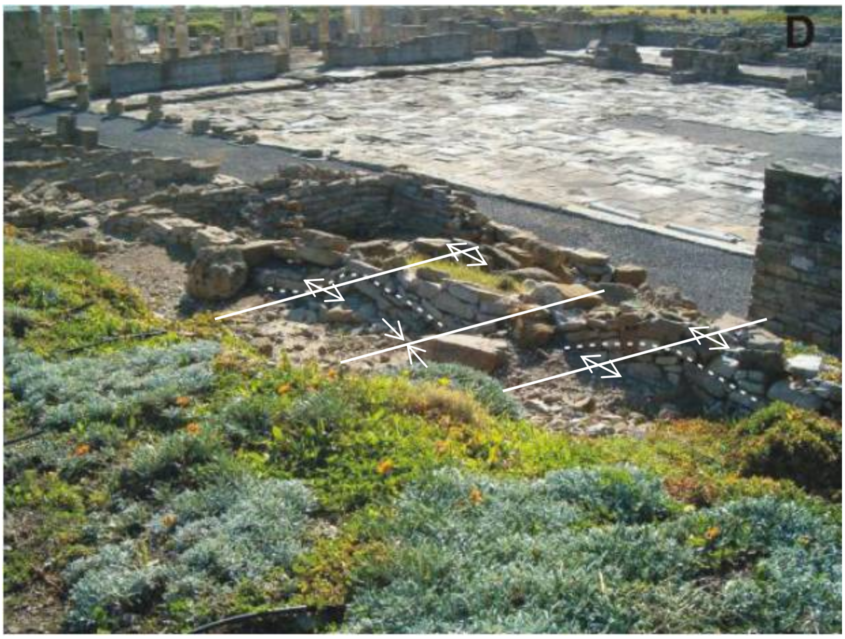

Photo 18. Folded walls in the East Street of the FORO. White lines are fold axes

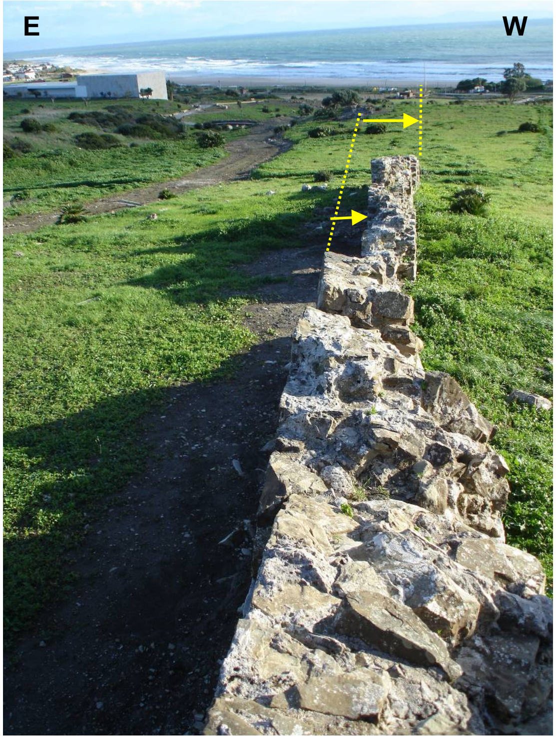

Photo 19. *Left*: Displaced walls of the roman aqueduct. *Right*: Displaced East Defensive Wall

Photo 20. Differential movement throughout a defensive wall at the West side of Baelo Claudia

STRAIN STRUCTURES GENERATED IN THE BUILDING FABRIC

2.6 PENETRATIVE FRACTURES IN MASONRY BLOCKS

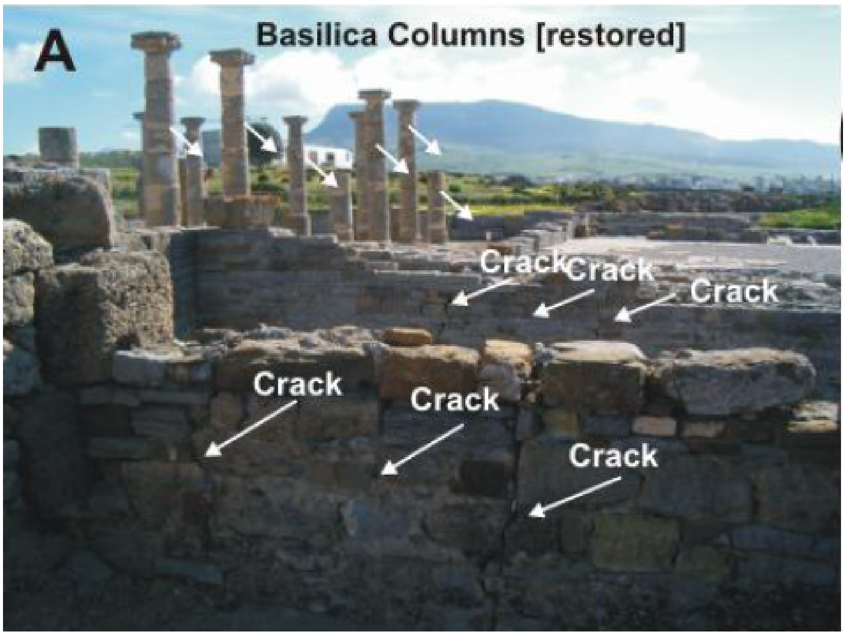

Photo 21. Cracked walls in the MARKET (*Macellum*). See the propagation of the crack through both walls

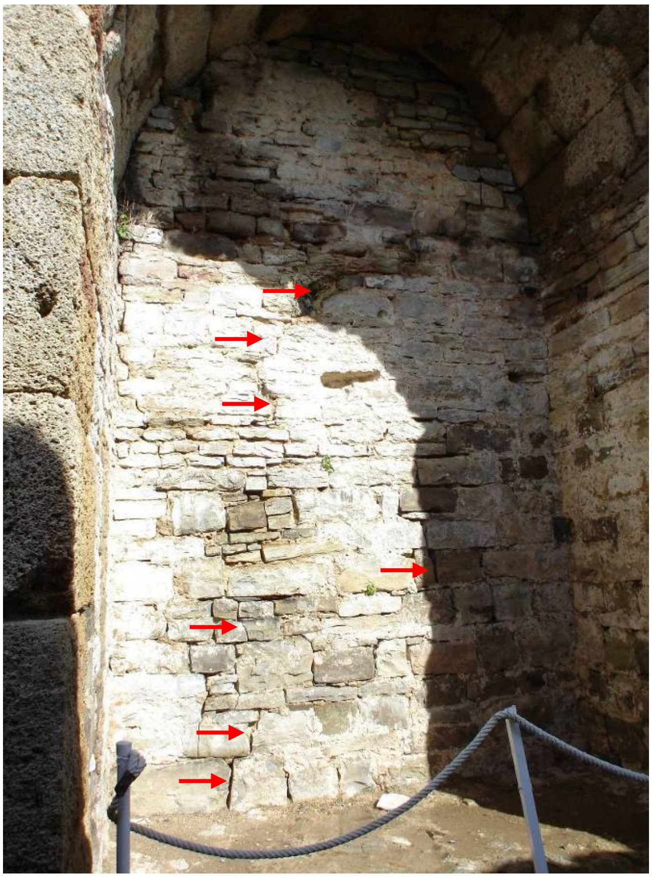

Photo 22. Penetrative crack affecting brick joints and breaking bricks. Building at the East entrance of the Theatre.

Photo 23. Penetrative propagated cracks affecting masonry blocks of the tower basement in the entrance at the East DECUMANUS MAXIMUS

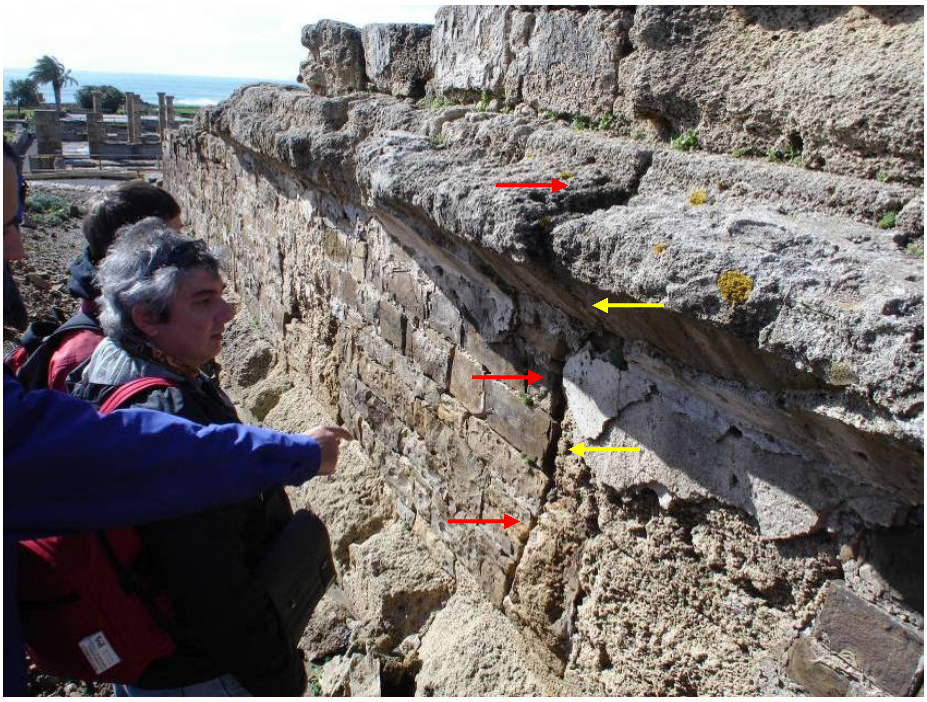

Photo 24. Penetrative cracks affecting the Temple of Jupiter.

2.7 FALLEN AND ORIENTED COLUMNS

Photo 25. Toppled columns of the Basilica (Silva et al., 2009a)

2.8 DISPLACED MASONRY BLOCKS

Photo 26. Displaced masonry block at the MARKET (*Macellum*)

2.9 DROPPED KEY STONES IN ARCHES OR LINTELS IN WINDOWS AND DOORS

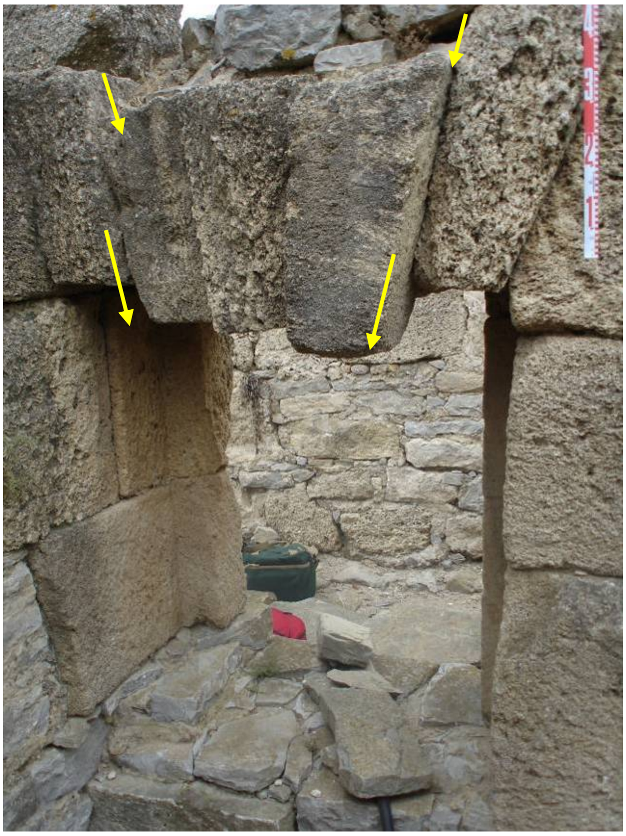

Photo 27. Dropped stones of the window lintel (BASILICA)

Photo 28. Dropped key stone of the arch door at the defensive wall of the North Bastion

Photo 29. Relative displacement of blocks in the east arch of the Theatre.

2.10 FOLDED STEPS AND KERBS

Photo 30. Folded steps affecting the stairs of the BASILICA

2.11 IMPACT BLOCK MARKS

Photo 31. Fallen block affecting the pavement in the FORO

Photo 32. Detailed view of an impact block mark (Regular flagstone of the FORO)

2.12 DIPPING BROKEN CORNERS

Photo 33. Different views of dipping corners. Measure of the dip angle and sense by using a compass

BASCULATED AND COLLAPSED WALLS (not included in the EAE Table)

Photo 34. (BOTH VIEWS) Collapsed walls, isolated megablocks and horizon of demolition.

SUMMARY OF THE GEOLOGICAL STRUCTURAL ANALYSIS OF DAMAGED STRUCTURES

The application of classical techniques on geological structural analysis for ductile and brittle deformations affecting buildings is a second quality step in the study of Archaeoseismology. The analysis of the strain may allow the calculation of the strain ellipsoid associated with the arrival of the seismic wave. For the interpretation of the results derived from structural analysis is important the previous classification of the structures following the aforementioned EAE guidelines.

The strain solutions obtained from the structural analysis of damaged building and pavement fabrics can be compared to those obtained from instrumental seismicity, Quaternary tectonic structures around the studied zones, etc. The similarity between the strain ellipsoid derived by pure geological analysis and by archaeoseismological analysis will point to the seismic origin of the analysed structures, although strongly depending on the time/date of the deformation. This should be established as a standard to be applied in archaeological sites to determine possible seismic deformation.

Therefore the application of the classification EAE and strain measurements proposed in this course will help to formalize archaeoseismological investigations, putting some quality steps to undertake a more comprehensive parameterization of ancient earthquakes.

3. QUANTIFICATION OF THE STRAIN DATA

3. Quantification of the strain data

The next step once the EAE (Earthquake Archaeological Effect) are described consists to make a classification of those EAEs that could provide information about the seismic strain field. Those EAEs which provides more strain information are the *coseismic primary effects* or *direct effects* (Fig.1, Rodríguez-Pascua et al., 2009a). These EAEs comprise structural information about the seismic strain field and the purpose of this course is extracting this information. To do this, we can apply classic modern techniques on Structural Geology and obtain then various parameters of the strain ellipsoid generated from earthquake shaking. These parameters are the main axes of the strain ellipsoid, ey (*maximum horizontal shortening*), ex (*minimum horizontal shortening*) and ez (*vertical axis*) (see below). Even information about the path of the seismic ray that passed through the ancient city can be inferred and discussed. Of course, all of these have sense whether the deformations into the archaeological site are due to earthquake phenomena. Indeed, the relevance of this analysis consists to discriminate seismic deformations from others.

3.1 DATA CONSTRAINT

Some aspects should be considered before to perform the strain classification of the EAE. These aspects include the type of data, the orientation of the data, the nature of the data (single or complementary) and comparisons among them. The following paragraphs describe each consideration.

Orientation data

We can take directional measurements for EAE in two forms.

- PLANE: Defined by the direction and dip of the EAE (e.g. folds, spatial orientation of flagstones in folded pavements, etc.).
- LINE: Defined by a vector, we can measure three different types.
  - a) Only direction (L1)
  - b) Direction and azimuth (e.g. vector of fallen column) (L2)
  - c) Direction, azimuth and magnitude (e.g. a slip vector) (L3)

Type of data

The type of data can be either a single value as the orientation of a vector, or an interval of oriented dataset, for instance.

- *Single orientation:* The measurement of the shock direction in flagstones is a vector defined by the strike and plunge.
- *Range of orientations:* In this case, we take various measurements of one EAE. For example, we take several data in a tilted wall, by using a compass in different parts of the wall.

Complementary data

- *Single data*: This data is a direct measurement of the EAE and is not evaluated with other complementary data of the same EAE.
- *Complementary data (walls, arch blocks,):* In this case, we can analyse a dataset of similar structural data from one EAE. For example, we can take dataset measurements from tilted walls (Fig. 3.1). Each tilted wall exhibits a data set of azimuths about 180º. In the particular case of Baelo Claudia, showing an orthogonal distribution of walls (parallel to the *Decumanus Maximus*, E-W and *Cardos*, N-S), we can define the dataset of tilted walls in one building with a common interval of directions for all walls of the building (Fig. 3.1b). By overlapping the complementary dataset in a rose-type diagram, we can estimate the range of the possible shock direction (grey zone of Fig. 3.1b).

Considering that each single EAE data includes structural information on the seismic strain field, we can assign a structural measurement to each EAE. Depending of the nature of the EAE and the involved architectural element (wall, floor, flagstone, etc.), we have assigned an oriented data following the aforementioned classification.

Accordingly, the Fig. 3.2 defines the type of structural data assigned to each EAE. Data orientation means plane or line, data type means single orientation or range of orientations and Data com. means single or complementary data. The EAE can be divided into two groups: (1) deformations by ground shacking and (2) by building fabric deformation.

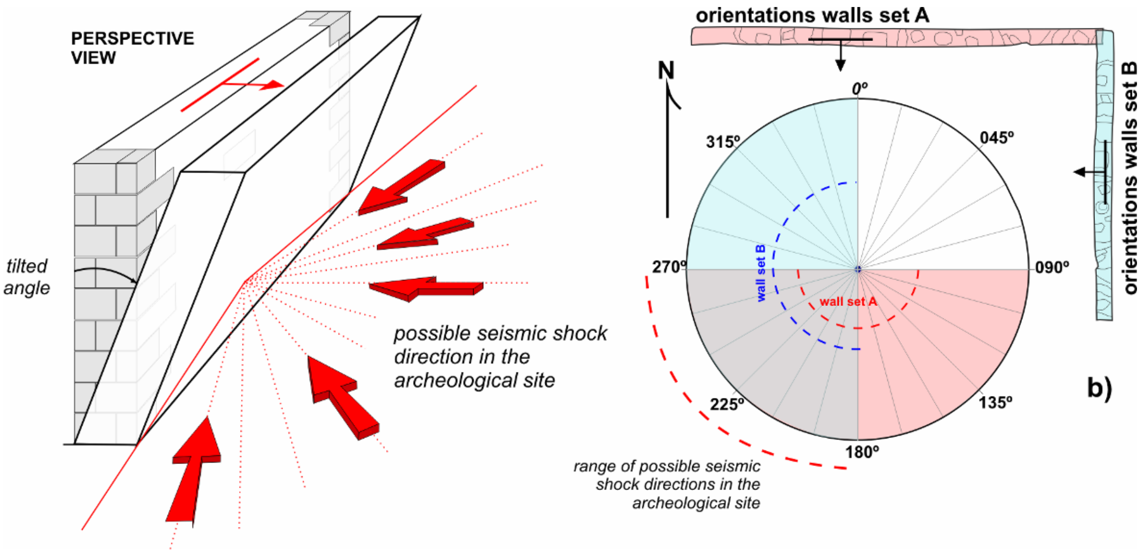

Fig 3.1: *(a) If we assume that the tilted wall is a consequence of the incoming seismic ray (Nikonov, 1988; Stiros, 1996, see Appendix 1 of Stiros, 1996; Walls in dry masonry buildings and walls in rigid constructions) the range of potential directions is 180°. (b) By the combination of dataset in a rose diagram from parallel tilted walls (blue range) with orthogonal tilted walls (pink range), we can estimate the possible seismic shock direction (grey area).*

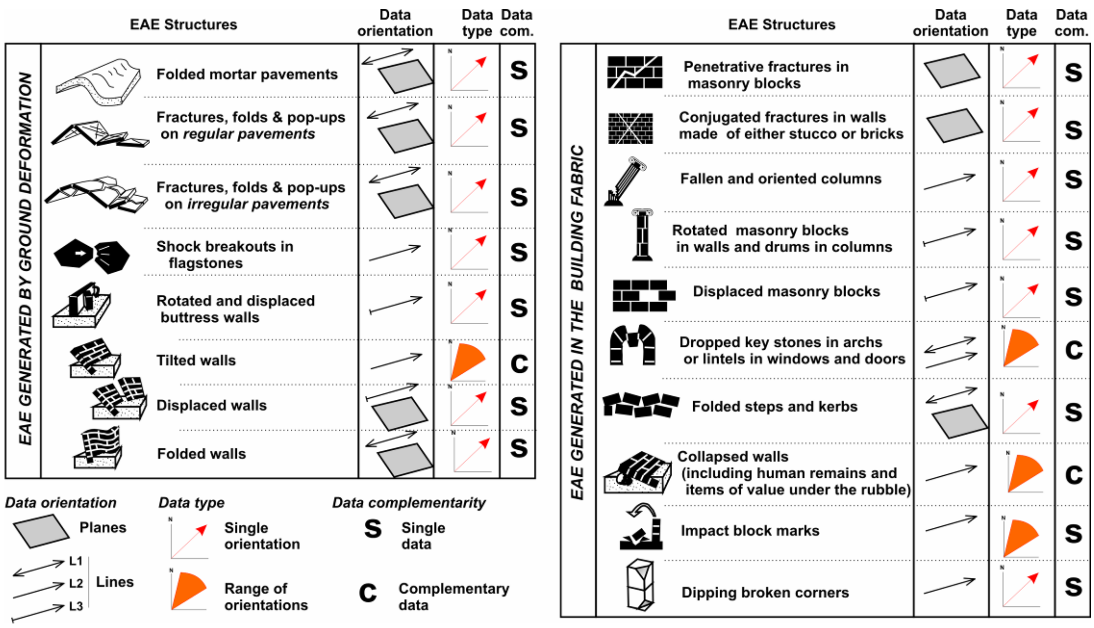

Fig 3.2: *Proposed table of structural data associated to EAE (see text for further explanation).*

Comparing poblational data

The final step of the archaeoseismic structural analysis proposed here is to perform a statistical analysis of all of the structural dataset. From this analysis, we can interpretate a possible seismic origin for the strain data extracted from an archaeological site. Therefore, the interpretation of data obtained from the structural archaeoseismic analysis is based on a poblational-type analysis. We have to obtain the mean orientation with its statistics for each EAE interpreted in one archaeological site (Fig. 3.3a, b). We have used rose-type diagram to show oriented data and stereographic net for planes (Wulff equiangular stereonet): folds and fractures. The use of rose-diagrams has been demonstrated to be an useful tool for the analysis of deformations in Baelo Claudia (Silva et al., 2009a).

Finally, to obtain the strain ellipsoid, we use the whole structural data derived from EAE (Fig. 3.3c). The key point to validate this analysis consists in the comparison of the strain field interpreted from the structural archaeoseismic analysis, with the strain field obtained from the geological classical analyses on faults (Fig. 3.3d). Therefore, we can estimate the quality of the analysis and its congruence with any seismic interpretation about the origin of the deformation at the archaeological site.

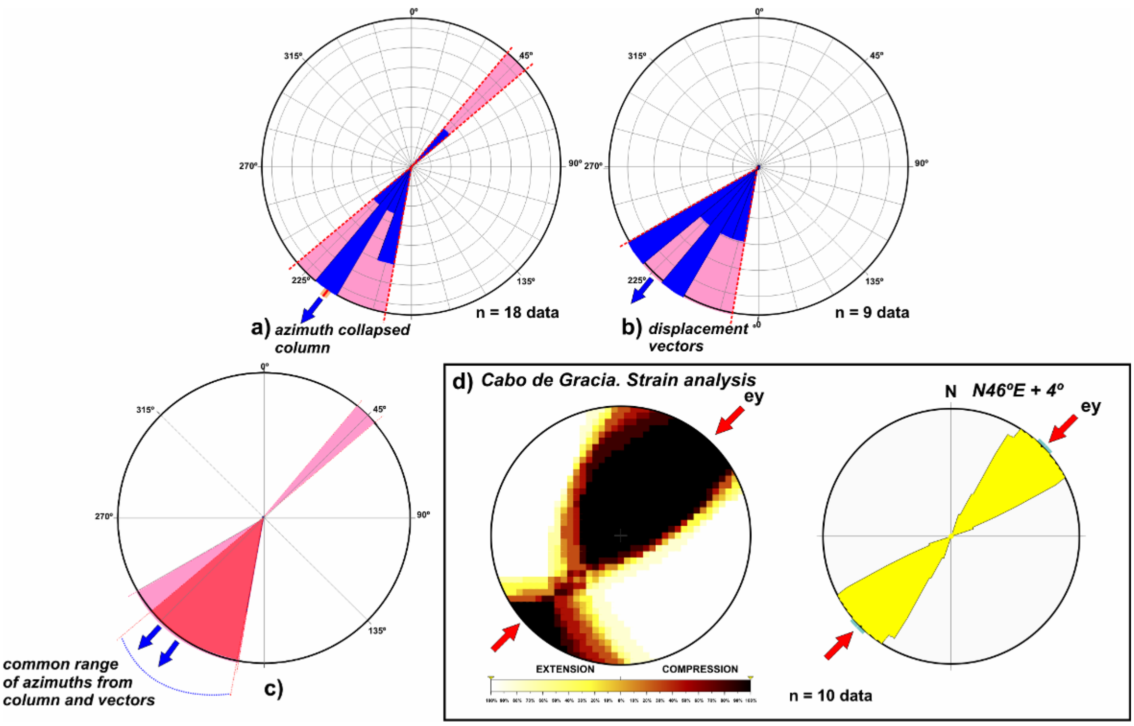

Fig. 3.3: *Preliminary results of the structural analysis of EAE applied in Baelo Claudia: (a) collapsed columns at the Basilica (Photo 25, all references hereafter of photos correspond to photos of chapter 2 of this volume) and (b) slip vectors for the displacement measured in the Foro. We assume that in both cases (fallen columns and slip vectors) the azimuth is opposite to the seismic shock direction (Lawson, 1909; Urbina y Camacho, 1913; Stiros, 1996; Kovach, 2000; Silva et al., 2009a). (c) The comparison between both results from (a) and (b) displays a range of interval for the seismic shock direction between SW and SSW. (d) Strain analysis of slickensides measured in the fault plane of the Cabo de Gracia Fault, right dihedral diagram (left) (Angelier and Mechler, 1977) and rose-type diagram of the maximum horizontal shortening (ey)(right) obtained from the Slip Model of strain analysis (Reches, 1983; De Vicente, 1988).*

3.2 ORIENTATION OF THE HORIZONTAL STRAIN TENSOR

A brief background of the strain tensor

We use the strain tensor to consider the strain field derived for the EAE structural analysis. The strain tensor is defined by an ellipsoid and this ellipsoid is defined by the orientation and the magnitude of three principal orthogonal axes: ey, ex and ez. The axes of the horizontal deformation are ey and ex (ey $\geq$ ex), and ez is the vertical deformation. The shape of the strain ellipsoid is defined by the relative magnitude value of these principal axes.

Most of the analyses are difficult to obtain the absolute value of these axes. Instead these techniques apply the relative magnitude value to define the shape of the ellipsoid. However, in the case of the archaeoseismic structural analysis we can obtain neither the absolute nor relative magnitude value for the principal axes. Therefore we only have considered the orientation of the strain tensor in a horizontal plane (Fig. 3.4).

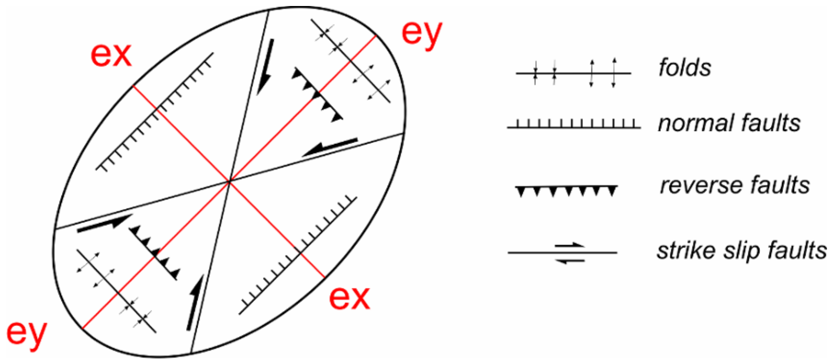

Fig. 3.4: Horizontal strain ellipse (ey maximum horizontal shortening, ex minimum horizontal shortening). Faults included indicate the main structures that could be generated and/or reactivated for this orientation of the strain tensor (ey trending N45°E, with the North arrow from down to up the page).

Regional and local strain tensor

One important point to consider when we are performing a strain analysis is the occurrence of local effects that may introduce changes in the resulting strain tensor. These local variations are normally related with the scale of the analysis introducing small changes on the geometry of the strain ellipsoid but important modifications for the shape factor of the ellipsoid.

Basically, the changes of the strain ellipsoid are commonly related to either the oriented and deformed structures (walls, main streets etc.), or to the differential behaviour of the architectonic structures (masonry walls, mortar pavements, type of brick, different size of brick, etc.). Nevertheless and independent of the shape of the strain tensor, the orientation and position of the strain axes are constants (ey and ex). Therefore, we can estimate the seismic deformation mainly from the strain axes orientation.

Then, we represent the strain trajectories by interpolating ey and ex orientation of each EAE from its spatial location. Obviously, the strain trajectory does not display a unique orientation, depending on the type of EAE and differential behaviour under the strain field. As example, Fig. 3.5 shows the preliminary result obtained for the Foro at Baelo Claudia.

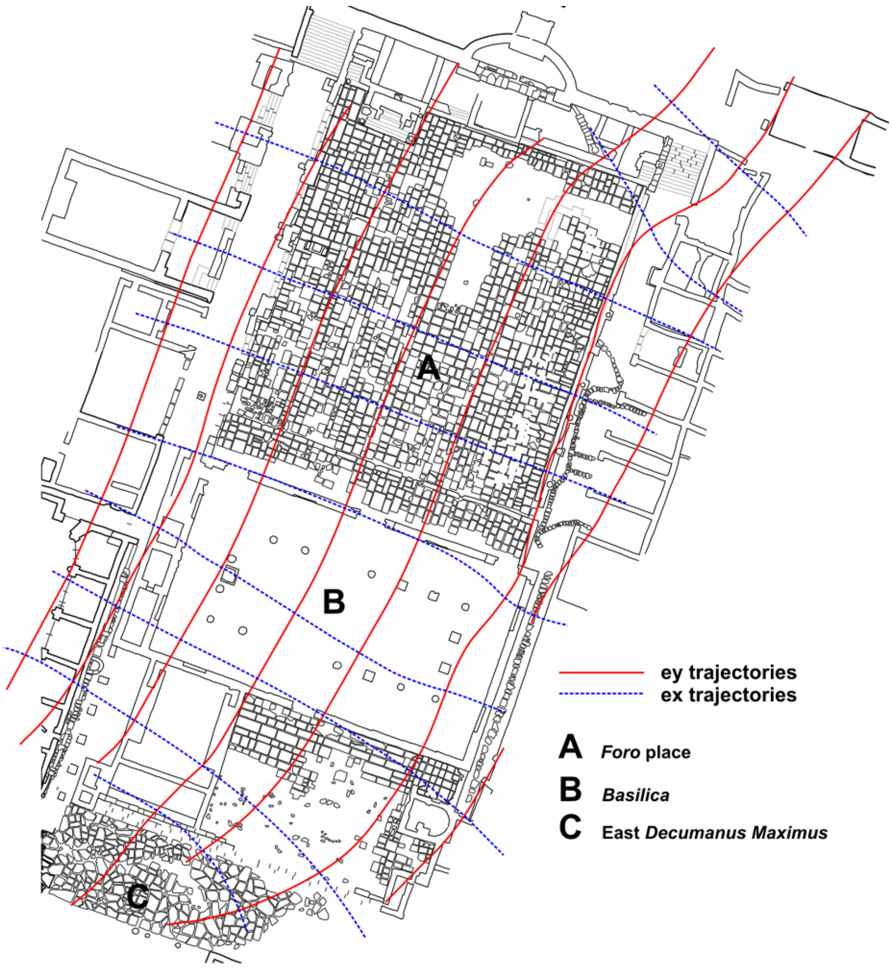

Fig. 3.5: Preliminary map of the strain trajectories for the Foro and surroundings at Baelo Claudia. These trajectories are obtained from the interpolation of the EAE measured, being the red line the ey trajectory and the blue one the ex trajectory. See that the ey trajectory is parallel to the principal flagstone direction. This is an effect of the regular pavement, which rotates the strain tensor according to the anisotropy of the pavement (Silva et al., 2005; 2009a). Also, the Decumanus Maximus exhibits an important strain tensor rotation interpreted as an effect of the underground water drainage-line.

3.3 INDIVIDUAL EAE ANALYSIS

First of all, we have to know the nature of each possible EAE and what type of data we can measure. Then, we have to locate the spatial position of the EAE in order to orientate the strain tensor later. We have analysed in detail the most frequent EAEs recorded at Baelo Claudia.

I. Fracture, Folds and Pop-Ups in Pavements

Pavement constitutes a very sensible structure under a strain field and can be deformed both as brittle as ductile behaviour (Altunel, 1998). We have distingued three types of pavements, in relationship with the differential behaviour and fabric:

- *Mortar pavements* (1). For example the Temple of Juno (Photo 1), the floor of the Market (Photos 2, 3), etc.
- *Flagstone pavements*. This floor is constructed by putting flagstones on and horizontal sand plain. Moreover, we have subdivided two types:

  Irregular flagstone pavements (2), (*Decumanus Maximus,* work plans 2, 3 and 4; Photos 7,8)

  Regular flagstone pavements (3) (*Foro* Place, work plan 8*;* Photos 4,5,6).

Both *mortar pavements* (1) as *Irregular flagstone pavements* (2) are isotropic under the strain field. In this case, there are no rotations of the strain tensor and the ey trajectory does not change following previous structural orientations. Instead, the main orthogonal orientations of the *regular flagstone pavements* (3), introduce an anisotropy that produce ey rotations (Figs. 3.25 and 3.6). Other factors that introduce strain tensor rotation are previous structures as buried older building foundations (*Market, work plan 4;* Photo 3), drainages and sewers as well (*Decumanus Maximus, work plans 3 and 4;* Photo 8).

Fig. 3.5 shows the ey trajectory trending NE-SW in the Basilica (mortar pavement, work plan nº 8), whereas the regular flagstone pavement of the Foro place (work plan nº 8) the ey trajectory rotates being parallel to the principal flagstone orientation trending NNE-SSW.

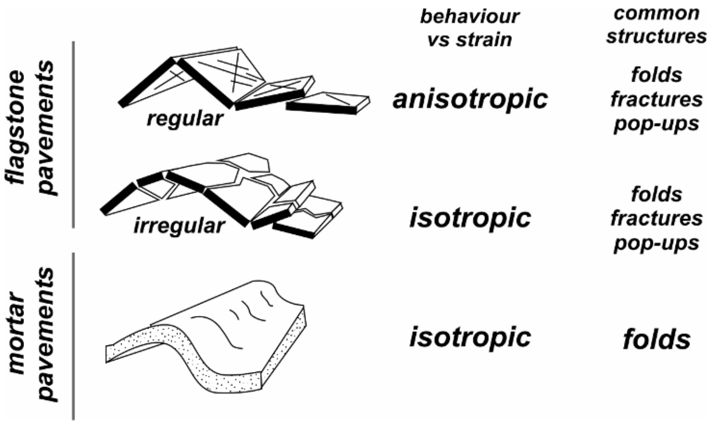

Fig. 3.6: Strain behaviour for different pavements and structure generated (folds and/or fractures).

The most common deformations affecting the pavements are folds, although flagstone pavements commonly display pop-ups and fracture arrays as well (Fig. 3.6). The Baelo Claudia case is an outstanding example of several types of folds, pop-ups and fractures in regular and irregular flagstone pavements (Silva et al., 2005; 2009a).

Folded Pavements

The analysis for folds in pavements is the same independent the type of pavement. Nevertheless, the orientation of the data could be biased by the isotropic inherent behaviour of the structure (regular flagstone pavement) and the presence of other structures (sewers, drainage, ancient foundations, etc.). The ey trajectory is perpendicular to the axis fold (Fig. 3.7). Therefore, we estimate the axis fold of the pavement and the ey trajectory is inferred (L1, see Fig. 3.2 and Fig. 3.7).

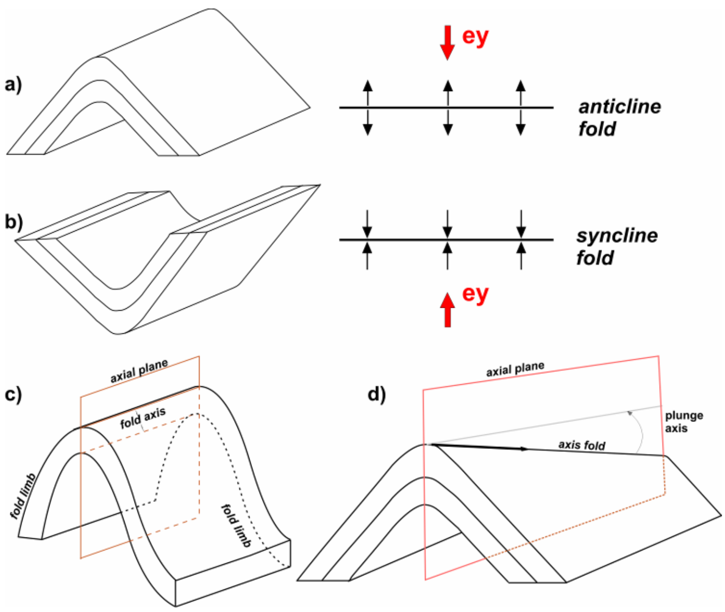

Fig. 3.7: Type and cartographic symbol for folds. Ey is perpendicular to the horizontal projection of the axis fold. (a) Anticline fold and (b) syncline fold. The geometry of a fold is defined by the limbs, hinge, axial plane and plunge of the axis fold. (c) Horizontal axis fold. (d) Inclined axis fold, the plunge of the axis fold is 30° in this case).

We can take the direct measurement of the axis fold (L1, see Fig. 3.2) or from the dip and dip-direction of the limbs of the fold. However, if we decide to obtain the axis of the fold from the limbs, we have to consider that both limbs are defined by rigid flagstones and these flagstones act as stiff material under the seismic strain field. This means that the axis fold will appear with an irregular trace and the plunge direction of the axis fold could be in opposite azimuths (Figs. 3.8b and 3.25).

Moreover, this irregularity of the axis fold conditioned by the fabric of the pavement could appear affecting steps as within the South steps at the Foro place and the kerbs of the East part of the Foro place (see Photo 30.).

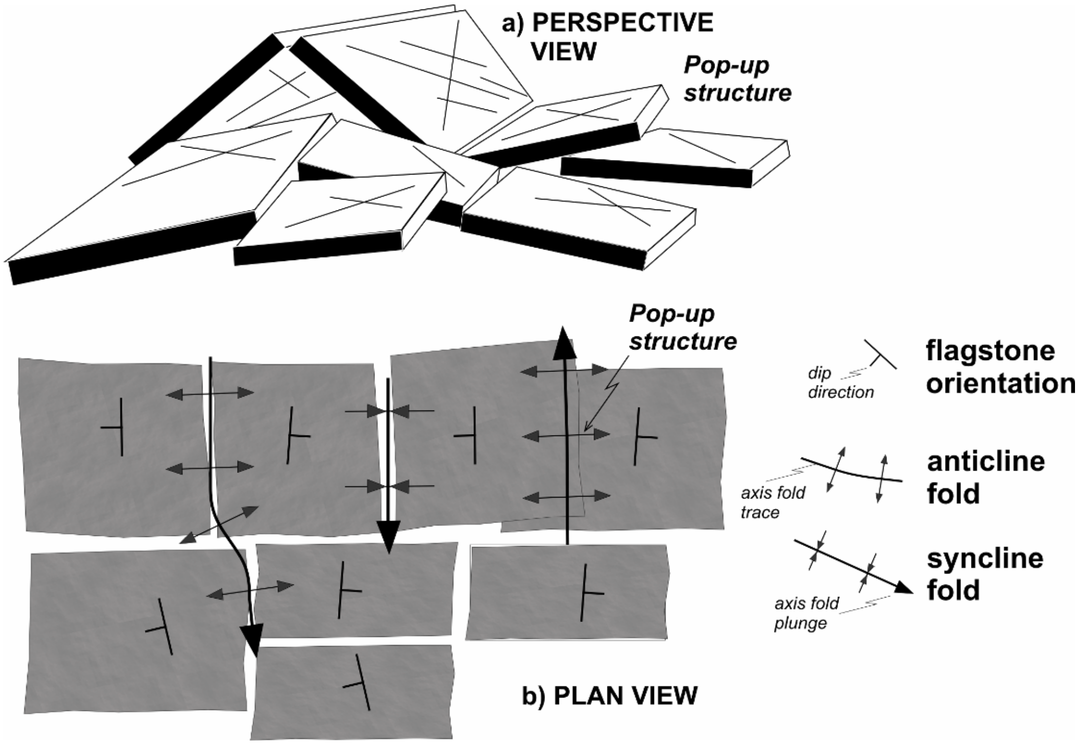

Fig. 3.8: Idealised sketch in 3D perspective (a) and plan view (b) of folding affecting irregular flagstone pavement and pop-up structures (Photo 4). In this case the axis fold is adapted to the flagstone joint.

Pop-ups

Pop-up structure is developed in flagstones, either with regular or with irregular shape (Photos 4, 5, 7). This structure indicates the horizontal shortening direction (Fig. 3.8b).

As a general rule, when the ground shakes the pavement is folded. However, if the horizontal vibration increases the flagstones are horizontally displaced each other. In this case, the ey orientation is parallel to the flagstone overlapping direction (L2 and L3, see Fig. 3.2).

Fractures

Fractures are common in flagstones due to the seismic shaking. Of course, others fractures can be appear due to the ordinary use of the pavement. However, fracture sets due to seismic shaking appear as conjugated sets and the ey direction can be estimated from the different position of the minor angle between these conjugated sets (Boer and Hale, 2000; Monaco and Tortorici, 2004)(Figs. 12a and b). We represent the plane orientation of the fractures in stereogram plots.

Shock breakouts

Shock breakout is a typical fracture produced from the horizontal vibration of the flagstones, crashing the corner of the corner of the flagstone *(Fig. 3.9 Decumanus Maximus*, work plans 2, 3 and 4; Photos 9-11).

This EAE shows a triangular-shaped rupture in the corner-edge of the flagstones (Silva et al., 2009a). For a better interpretation *in situ* preservation of the broken piece will be required (Fig.3.9; Photo 10). The size of the shock breakout is usually centimetric and exceptionally decametric. Horizontal movement due to seismic waves induces the collision between flagstones giving place to the rupture of their corner-edges. The rectilinear rupture outlines a quasi-perfect triangle. The movement of flagstones is perpendicular to the base of the triangle pointing to the undamaged flagstone.

We assume that the orientation (L2, see Fig. 3.2) of the base of the triangular fracture for the broken flagstone, is orthogonal to the ey trajectory (Fig.3.9).

The most concluding results are obtained in irregular flagstone-pavements, with variable size and geometry of flagstones. Results will not depend on the pre-existing fabric orientations displayed by regular pavements.

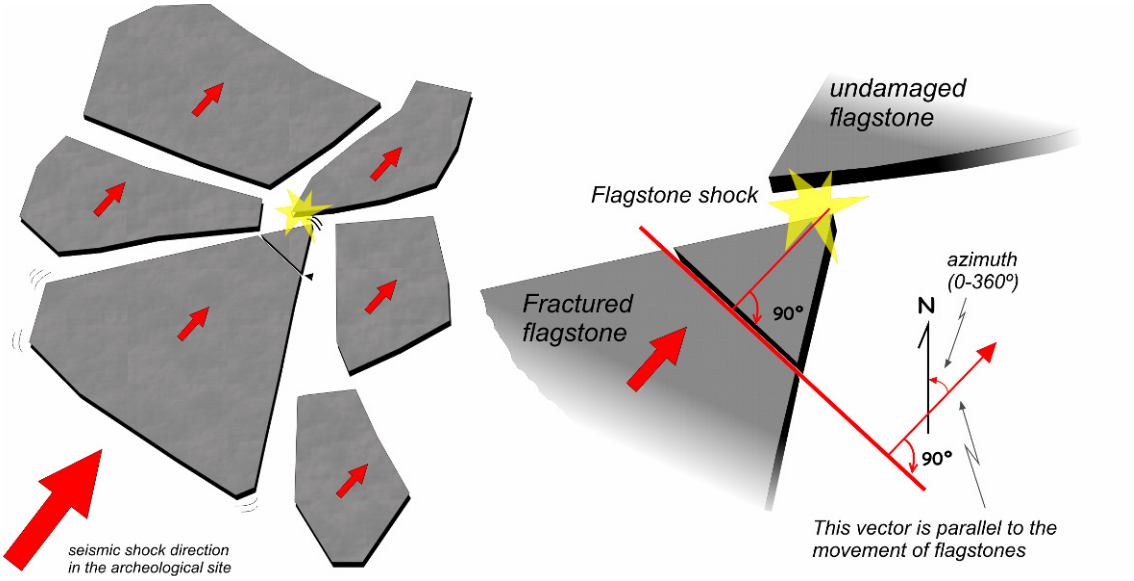

Fig. 3.9: Shock breakouts in flagstones. The slip vector of the seismic shaking is orthogonal to the base of the resulting triangle.

II. Tilted, Displaced and Folded Walls

Tilted wall

Tilted walls are common in ancient cities and remains. Earthquakes may be the origin of this tilting. In general, wall tilting is a consequence of horizontal movement of the ground foundation and the seismic waves produce such vibrations. Photos 15 and 16 are two examples of tilted walls at Baelo Claudia. The azimuth of the incoming seismic ray ranges between 0° and 90° in relationship with the orientation of the wall. Several works noticed that the azimuth of tilting (L2) is opposite to the azimuth of the incoming seismic ray (Stiros, 1996; Kovach, 2004; Silva et al, 2009a) (Fig. 3.10 and 3.11).

Nevertheless, a tilted wall by seismic phenomena exhibits a differential displacement among the bricks of the wall (Fig. 3.10, side view).

By using several tilted walls, we can estimate the range of the possible seismic shock paths (Fig. 3.11b), whenever all of the walls have similar fabric features and being located closer each other.

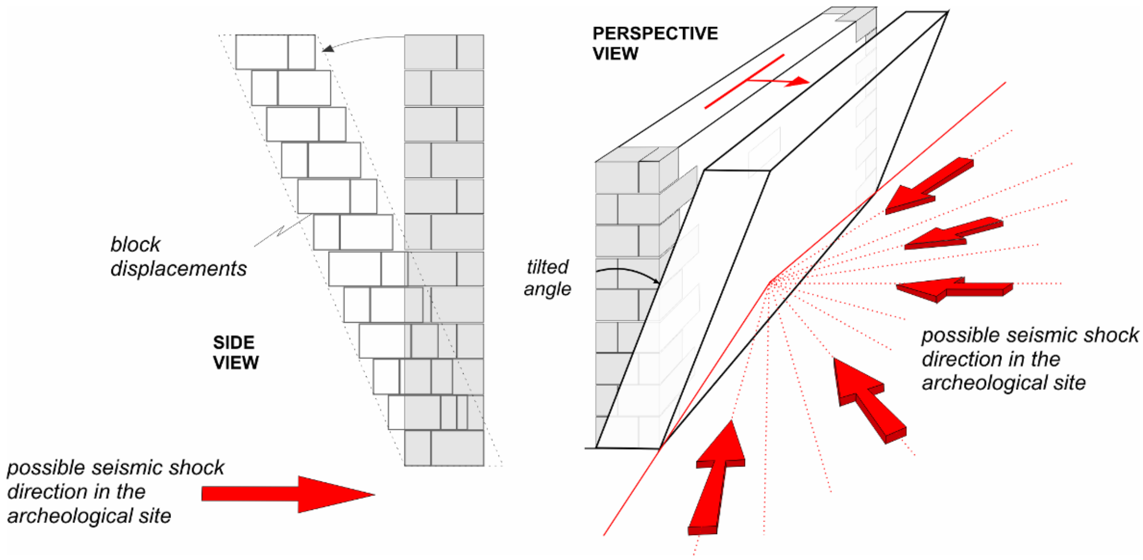

Fig. 3.10: Wall tilting related to the incoming seismic ray (Lawson, 1912; Urbina and Camacho, 1916; Stiros, 1996; Kovach, 2004; Silva et al., 2009). Accordingly, the orientation of the wall defines an interval of 180° for the possible seismic incoming path. The angle of tilting is defined by the differential displacement among the bricks in each row of the wall (side view).

Furthermore, the inclination plane of the wall is not constant, increasing the angle from the lateral to the central part of the wall. This is the *anchor effect* (Fig. 3.13). It will recommend that the measure of the tilted wall (α) will be performed at the maximum inclination point of the wall.

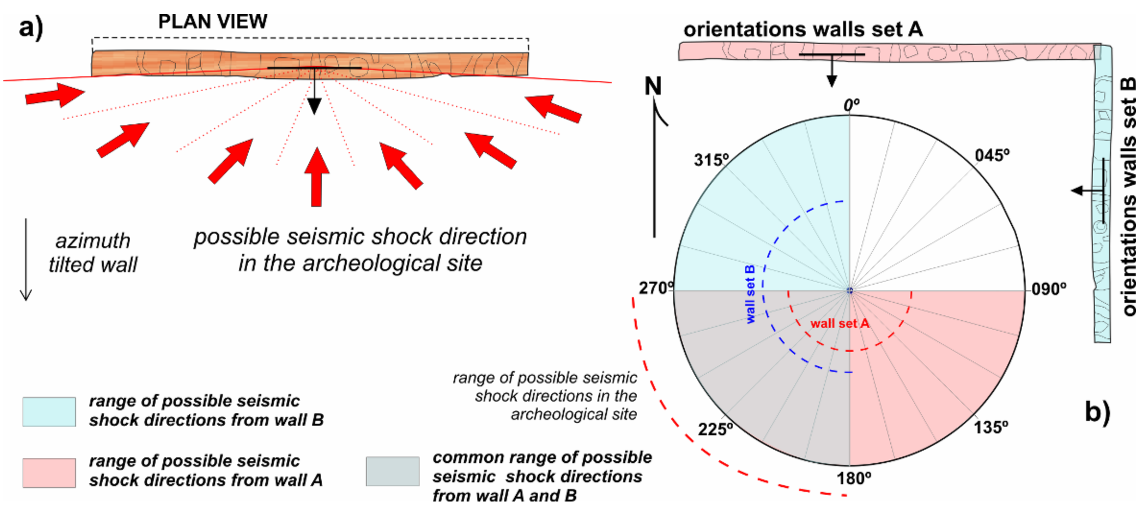

Fig. 3.11: (a) A tilted wall defines a range of 180° of possible seismic azimuths (L2, range of orientations). For one building, we ordinary have two orthogonal intervals for this range. (b) Plotting together in a rose-type diagram both ranges, we can calculate the common range for this building (complementary data).

In other cases, the ground deformation produces tilting in walls as well. In this case, the mechanical behaviour of the affected walls works as a rigid solid. However, if the ground materials change its geotechnical properties due to an earthquake (i.e. liquefaction) the wall can either be tilted or even totally collapsed. As aforementioned, the sense of the wall tilting is related to the sense and direction of the seismic ray (azimuth). This kind of EAE is similar those displayed by folded walls and described in the next section.

Folded wall

Other typical EAE defined in archaeological sites are folded walls. We have classified two types of folds in relationship with the plunge of the axis fold, (a) Axis fold with plunge smaller than 45° (Type A, î <45°) and (b) Axis fold with plunge greater than 45° (Type B, î >45°) (Fig. 3.12).

(a) Type A (î <45°)

These folds are related with the lack of space in the wall during the vibration. This feature appears when the corners of the building have a more resistant behaviour during the ground motion (e.g. masonry walls), and the freedom degrees of the oscillations are limited (Fig 3.12b). This fact generates a lack of the space during the vibration of the wall and induces a fold in the wall (in example, shops walls in the Foro, *work plan 7*; Photo 18).

(b) Type B (î >45°)

These folds are related with the differential movement throughout the wall. The end part of the wall acts as an anchor and the movement is here smaller than at the central part of the wall (Korjenkov and Kaiser, 2003) (Fig. 3.13). The maximum displacement of the wall is therefore located at the central part of the wall and the vibration is transverse to the wall longitude (Photo 17).

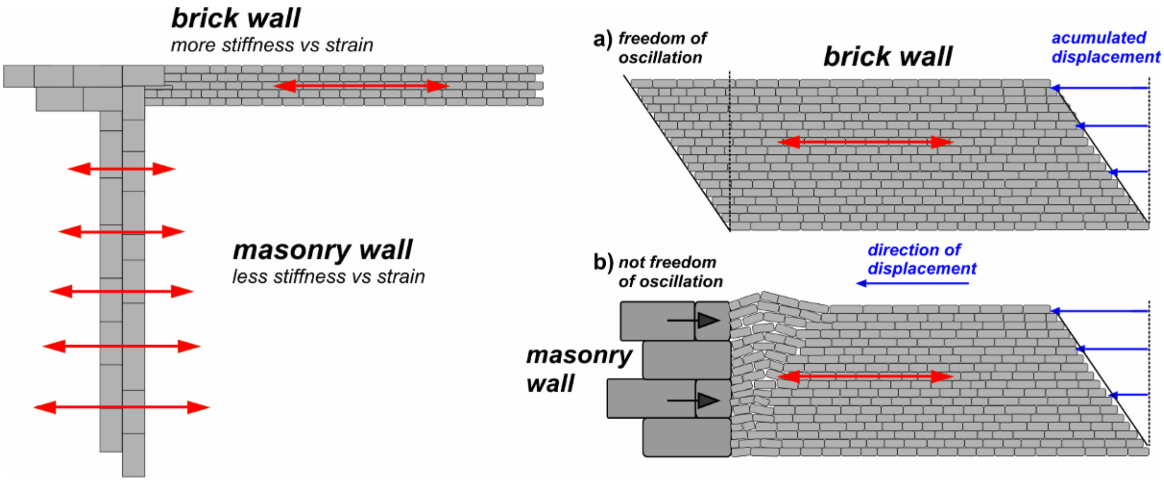

Fig.3.12: Folding in walls by differential behaviour of the wall fabric. The presence of more resistant masonry blocks decrease the oscillations of the wall and induce a holding. Examples in the shops N-S walls at the east part of the Foro place.

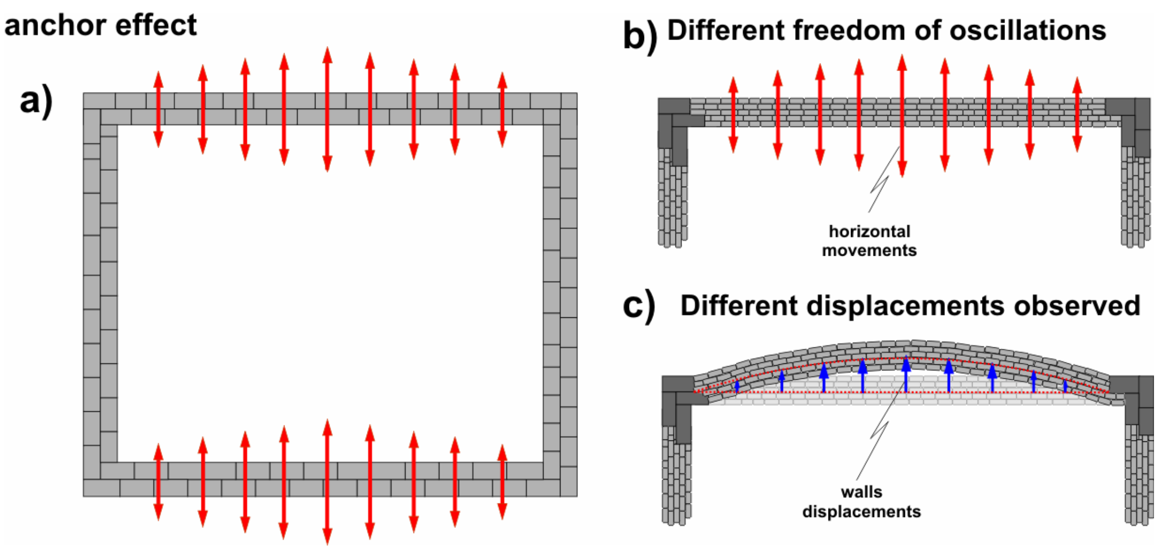

Fig. 3.13: Anchor effect in walls. (a) Different degree of freedom for the wall oscillating from a seismic wave. The central part of the wall undergoes the maximum oscillation whereas the wall-ends show smaller vibration due to the anchor effect of the orthogonal walls (after Korjenkov and Kaiser, 2003). (b) The anchor effect buffers the vibration of the wall-end. (c) Differential movement of the wall is more relevant in the central part of the wall. Furthermore, this effect is increased for brick walls and with small size for bricks.

Walls of bricks experience a differential vibration from the ending to the central part of the wall (Fig. 3.13b).

Two sections of a bended wall are represented in the Fig. 3.14.1. Section AA' is located in the distal part of the wall and the section BB' is located at the central one (Fig. 3.14.2). Both sections illustrate the differential movement of the bricks. However, section AA' the movement is smaller than the section BB' due to the degree of freedom is constrained by the anchor effect. This effect produces the apparent folding or bending of the wall.

There are other effects due to the aforementioned differential movement (Fig. 3.14.3)

- The tilting of the walls increases from the distal part to the central part of the wall.
- The rotation of bricks is greater in the distal part than the rotation of bricks within the central part of the wall. This rotation accommodates the differential displacement among bricks.

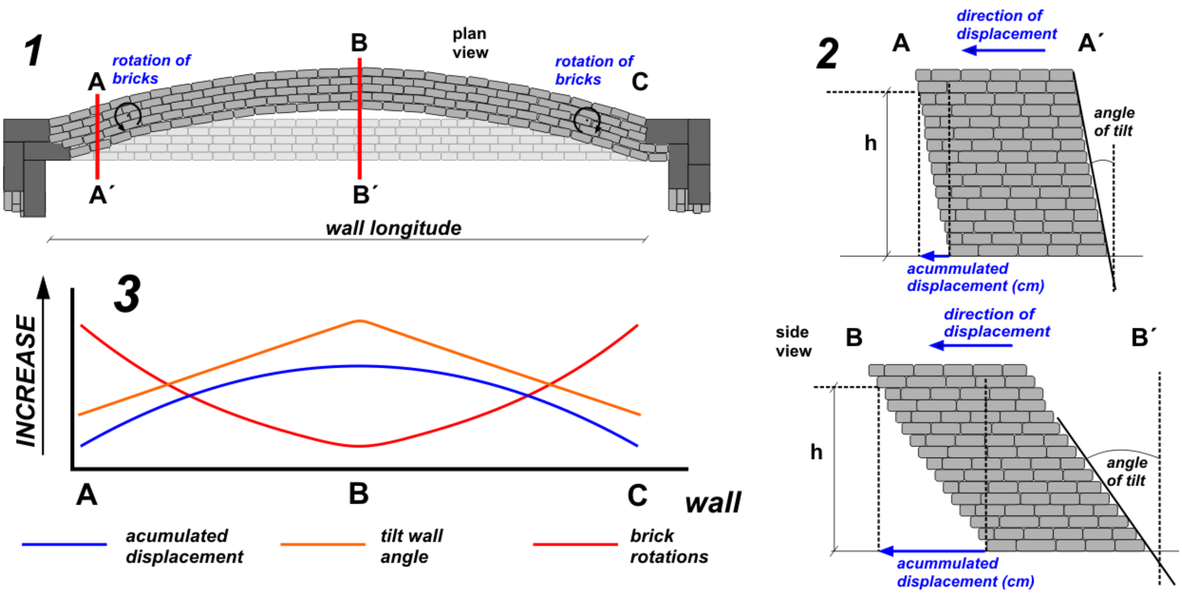

Fig. 3.14: (1) Sketch of wall displaying the anchor effect. Section AA' is closer to the wall-end than the section BB'. The rotation of bricks is more relevant close to the wall-end. (2) Idealized sections of a folded wall. Note that the horizontal displacement of bricks in the section AA' is smaller than section BB'. In the last case, the accumulated horizontal displacement is greater. (3) Idealised representation of the different degrees of freedom for brick rotation within the wall fabric. These degrees represent the accumulated displacement among bricks and the vertical angle of the tilted wall and the rotation (in degrees) of the bricks. These values increase or decrease in relationship the distance of the wall to the border (anchor effect).

The anchor effect is a relevant parameter for the quantification of the strain from tilted walls. This building effect affects the tilting angle of the walls. Therefore, the angle of tilting depends on (Fig. 3.14):

The longitude value of the wall: this value defines the distance between the border of the wall and points with anchor effects. Walls with similar fabric features as size of bricks and type of foundation, for example, as longer are as greater displacement show and, consequently, they have a greater value for the angle of tilting.

The position of the measurement: Depending on the position where we place either the compass of the clinometer, we can obtain different values because of the larger value is for the central part of the wall.

Displaced wall (Photos 19-20)

These EAEs are more common in brick-walls. On the contrary Masonry walls hold higher values of rigidity and are more resistant to ground oscillations. The rigidity increases as the brick/block size increases as well.

The oscillation of the wall produces a strain that is accommodated by brick rotations even near to the anchors of the walls. However if the ground vibration outsized, the wall breaks and it is displaced.

Korjenkov and Kaiser (2003) concluded that folds, rotations of bricks and fractures in walls depend on the orientation of the wall with respect to the main horizontal component of the seismic vibration. In this work, we propose that the way that the wall accommodates the seismic strain is the main factor controlling the type of resulting EAE. In addition this strain accommodation depends on the foundation of the wall, the size of bricks or blocks, presence of large masonry blocks, presence of mortar between bricks, type of lateral anchors, etc.

III. Fallen and Oriented Columns (Photo 25)

Fallen and oriented columns within archaeological sites are a common feature of destruction associated to the seismic phenomena (Nur and Ron, 1996, Stiros, 1996). Moreover, these authors stated that the orientation of the longitudinal axis of the columns is in relation with the seismic ray propagation. However, other authors review this statement and include other factors which are relevant for the orientation of the collapsed columns, such as the quality of the building stone, anthropic destructions, etc. (Ambraseys, 2006; Marco, 2008), and topographic constrains, such as slopes and geomorphic scarps (Silva et al., 2009a).

If we assume that the oriented fallen columns are due to seismic phenomena, we have to consider that the azimuth of the longitudinal axis of the whole of the fallen columns (L2) are parallels to the seismic wave propagation but in opposite sense (Fig. 3.15).

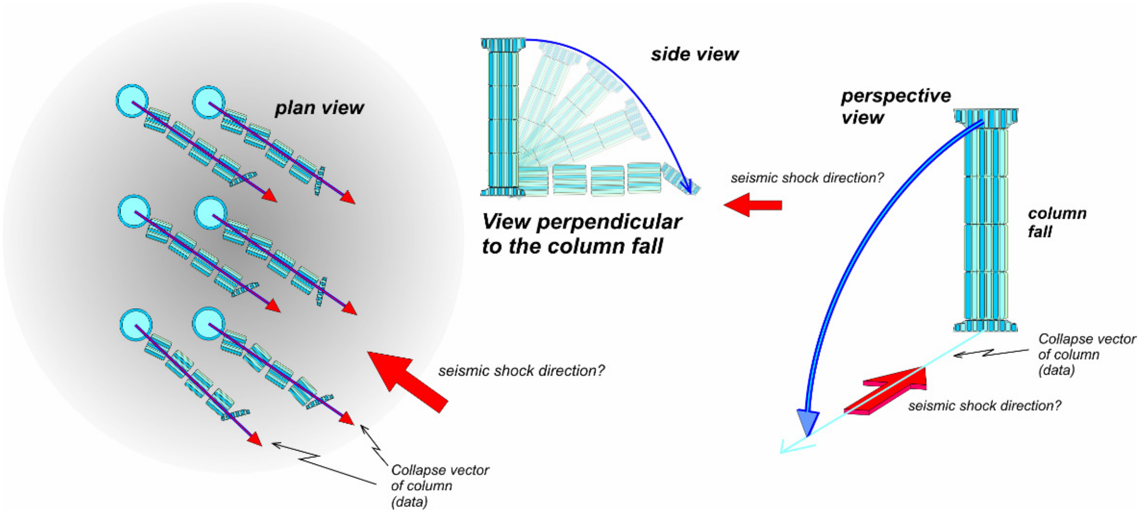

Fig. 3.15: Sketch showing the relationships between the longitudinal axes of the oriented fallen columns and the seismic wave propagation. One key factor to assign as seismic origin to oriented fallen columns are the occurrence of "slices of Salami" or the Domino arrangement for drums defined by Stiros, 1996.

IV. Dropped Keystone in Arch or Lintel in Windows and Doors

(Photos 27-29)

In many cases, disruptions of arches and lintel blocks of doors and windows are assumed as a seismic origin (Marco, 2008; Silva et al., 2009a). In these cases, downward slid keystones are common in earthquake-stricken regions (Marco, 2008). Kamai and Hatzor (2007) applied the finite elements technique for true cases to conclude that, only strong earthquakes can produce the downward sliding of keystones and therefore this EAE constitutes an archaeoseismic evidence for strong earthquakes. Moreover, these authors stated that the walls of the arches experience a decreasing of load to develop this EAE. However, other causes can produce structural damage in arches (Fig. 3.16), although these can be differentiated from structural damage of seismic origin.

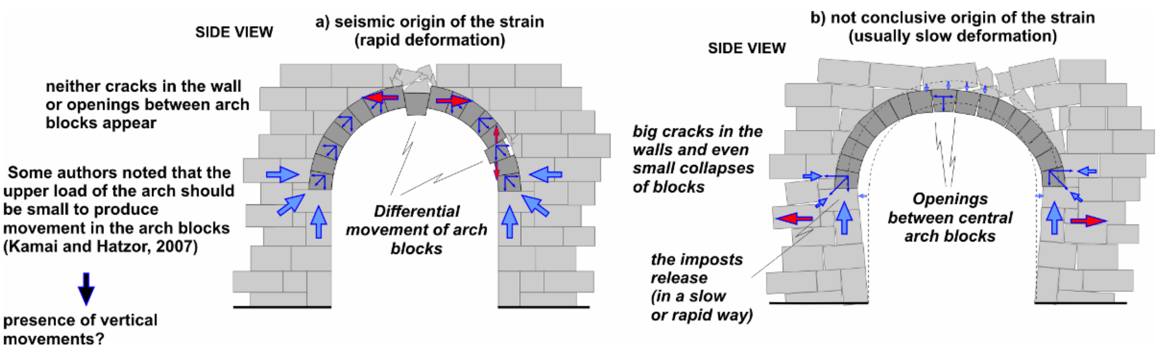

Fig. 3.16: Structural damage of arches in side view. (a) Structural damage from seismic origin showing a general scheme of the strain distribution within the arch blocks. (b) Structural damage of arches with not conclusive origin of the strain.

Structural damage from seismic origin is evidenced by the sliding of the key stone, although other adjacent blocks can also slide (Fig. 3.17; Photo 28) (Marco, 2008). Also differential horizontal movements of the arch blocks may occur during the seismic damage of arches (Photo 29).

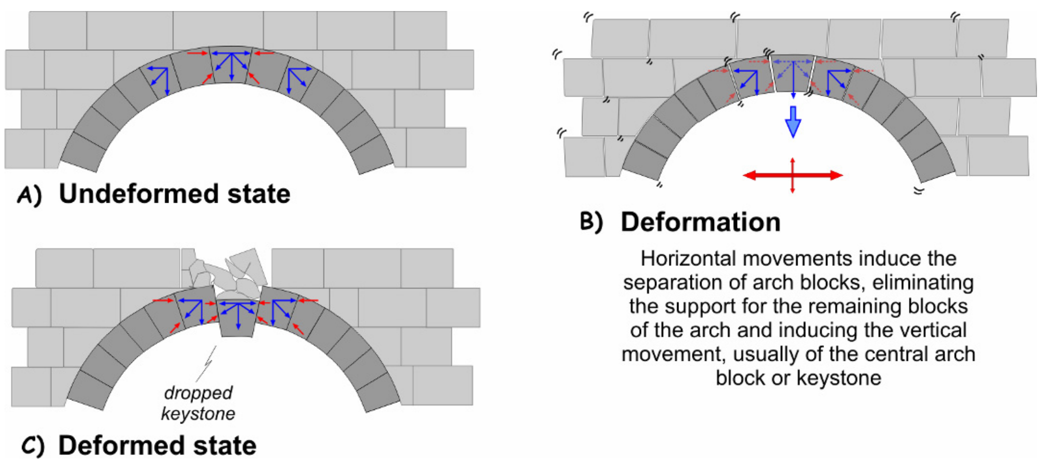

Fig. 3.17: Side view of the strain evolution along the arch blocks by vertical movements.

There is a relation between the vertical downwards sliding of the key stone and the seismic shock direction. This relation shows that the angle (L1, range of orientations) between the seismic ray and the arch is smaller than 45°. If this angle is greater than 45°, the orthogonal component of movement of the arch wall increases and the key stone does not slide downwards.

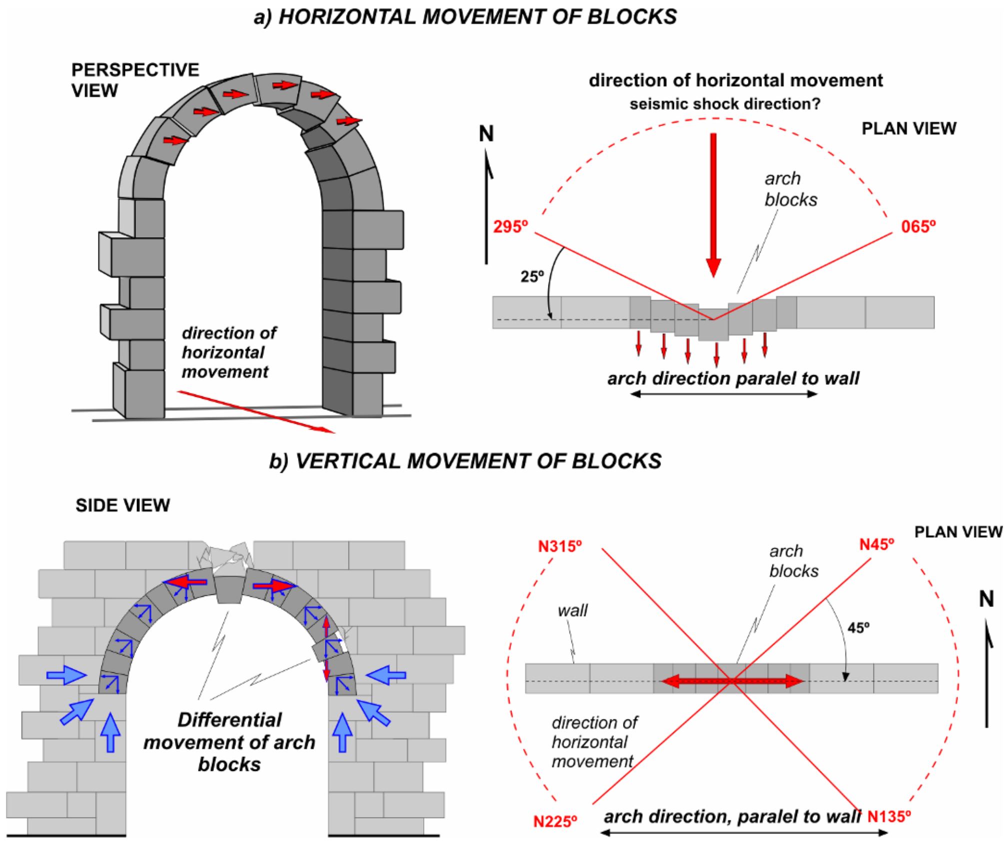

Fig. 3.18: Evolution of the strain deformation generated by the vertical movements of the arch blocks. See the typical vertical movement downward of the key stone, although other blocks can slide out of the arch line.

We can apply a similar analysis for arch damage than for tilted walls. We assume that the seismic ray is the responsible of the displacement of the arch blocks. Therefore, we obtain a range of angle intervals of 130° in relationship with the orientation of the longitudinal axis of the arch wall (Fig. 3.18a) for horizontal movement of the arch blocks, whilst for vertical movements the range of interval for the seismic ray propagation is ± 90° of the longitudinal axis of the arch wall (Fig. 3.18b). In both cases, these data can be classified as type L2 (See Fig. 2 and section 3.1 for further explanation of the format of L2).

In some cases, a particular arch can show both vertical and horizontal displacement of arch blocks, so we can define a common interval of movements allowing a more accurate determination of the movement direction (complementary data) (Fig. 3.19).

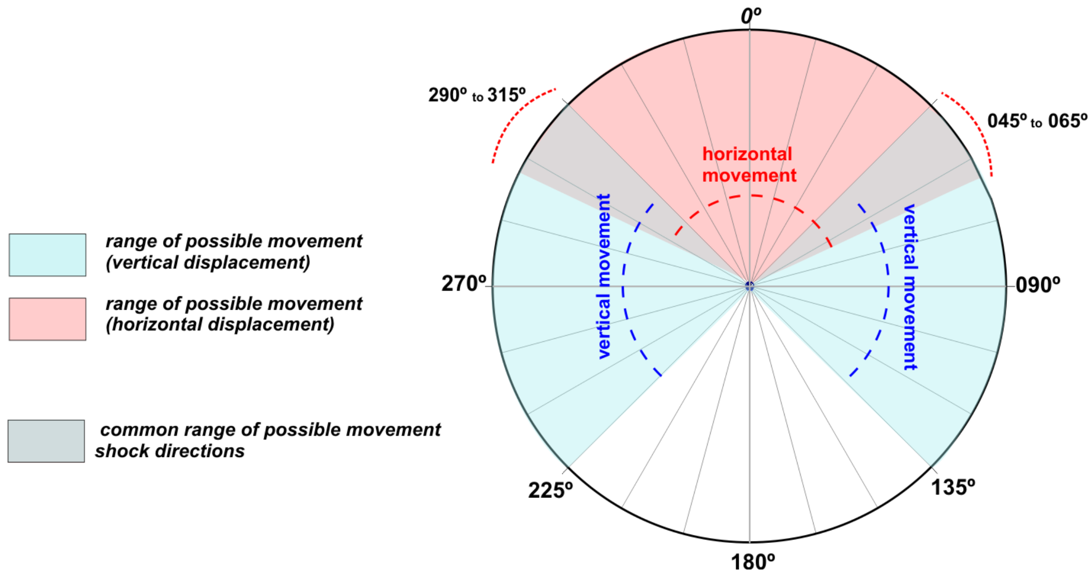

Fig. 3.19: Representation of data by a rose-type diagram in order to determine the likelihood geographical quadrant for the incoming seismic rays. Both horizontal and vertical data sets can be represented together due to both ranges represent complementary data. This example represents the orientation for seismic damage of the arch of the Fig. 3.18.

V. Impact Block Marks

Impact marks appear as result of fallen heavy blocks on pavements (Photos 31, 32). These marks can indicate the collapse of the top part of buildings by horizontal movement of seismic origin. However, this EAE must to be interpreted in the overall context of building damage showing others EAE and not as an isolate data to attribute ancient earthquakes.

This EAE is analysed in a similar way than those for tilted walls. It is necessary to determine the original position of the block.

Then, we consider two intervals of 180° limited by the orientation of the fallen trajectory. The seismic ray direction can be included within the orientation range defined by the impact marks on pavements (Fig. 3.20).

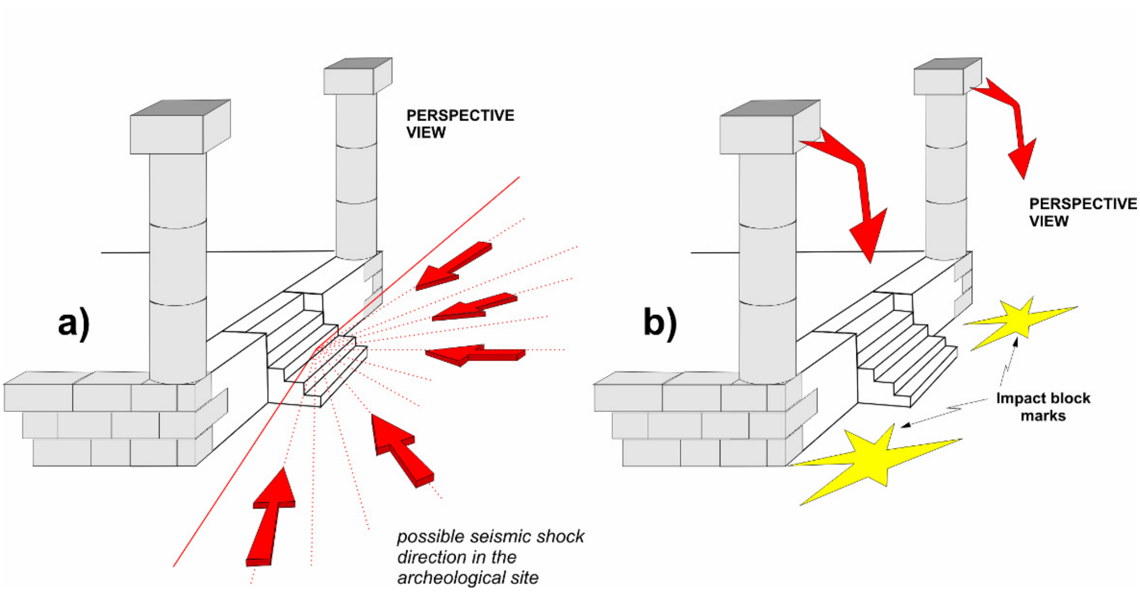

Fig. 3.20: a) Potential seismic shock azimuth in relation with the probable fallen block. b) Block marks generated from the incoming seismic ray drawn in (a).

VI. Dipping Broken Block-Corner (Photo 33)

Dipping broken corner or chipping marks (Urbina y Camacho, 1913; Stiros, 1996; Marco, 2008) represents EAE of triangular fractures generated by a vertical oscillatory movement of blocks or drums in columns and/or masonry walls. Vertical movement between blocks repeatedly shakes the corner (Fig.21a) and triggering a triangular faceted rupture. These triangular fractures usually are dipping 45°.

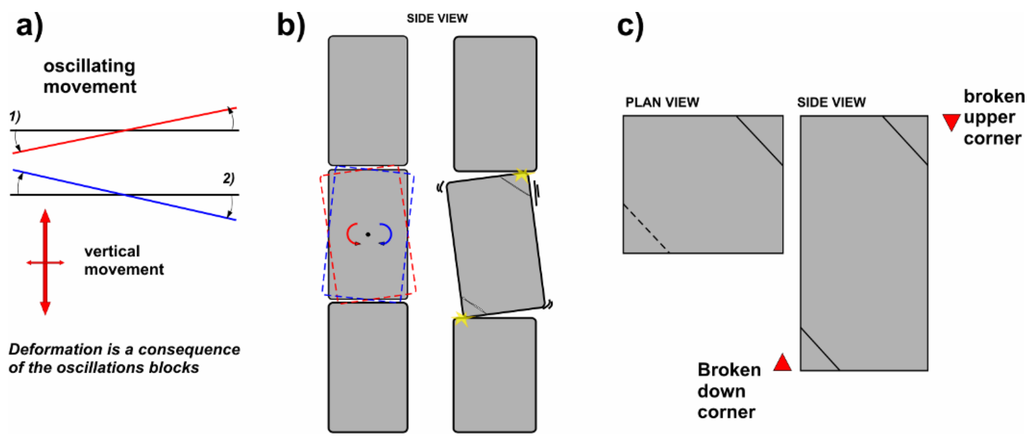

Fig. 3.21: a) Oscillatory movement between blocks and proposed mechanism for broken corners. b) Side view of the oscillating blocks and/or drums. The movement has been exaggerated to underline the mechanism of rupture. c) Location of the faceted corners in plan view and side view.

The dip sense of the faceted block-corner is parallel to the seismic shock main direction. Moreover, the faceted block-corners occur in opposite sides of the block, one in the lower and other in the upper part (See Fig. 3.21c). This fact implies that we have to indicate if the faceted block-corner is located either at the upper or the lower part of the block (Fig. 3.22).

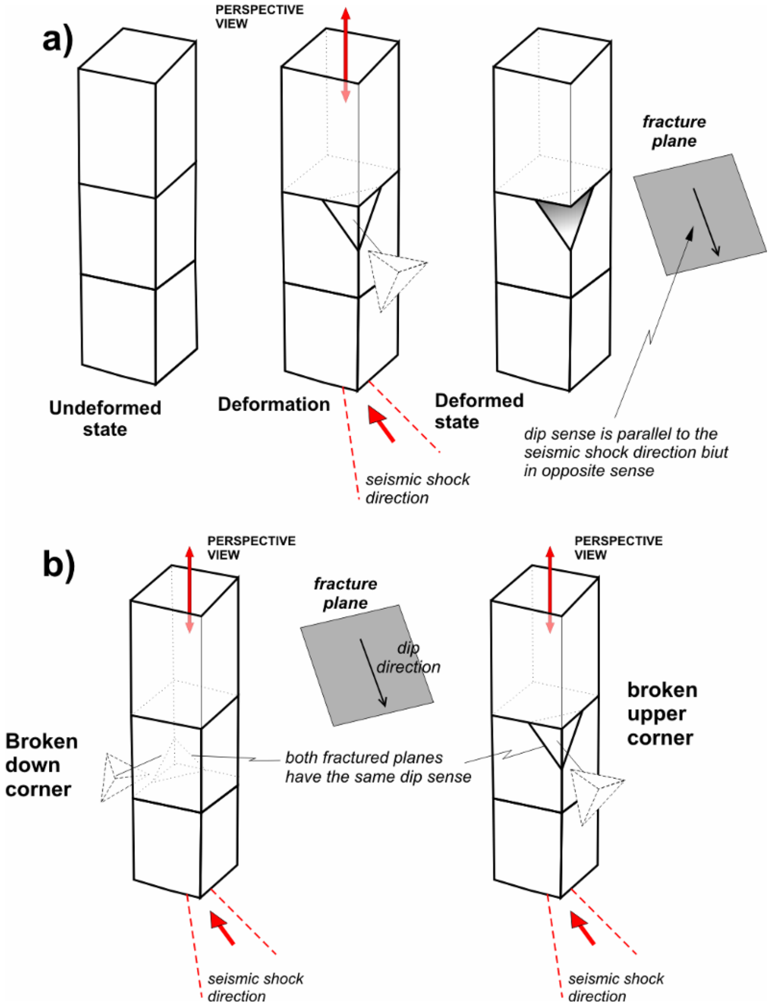

Fig. 3.22: a) Sketch showing the formation of a dipping corner fracture: undeformed state, deformation (broken corner), deformed state (dip sense of the triangular facet coincides with seismic shock direction. b) Correct location of the broken corners and relationship with the seismic shock direction.

3.4 STRAIN FIELD *VS* PREVIOUS ANISOTROPY

The scale factor is a relevant parameter to be considered in the strain analysis proposed here. This scale affects both the field work as the eventual data representation. As aforementioned, the strain tensor varies with the scale of representation (Giner-Robles et al., 2003) and local strain tensors can display switch off between the principal axes (Pérez-López et al., 2007).

3.4a Geological data

In structural geology the anisotropy is a key concept to study strain/stress fields from rock structures (e.g. Pérez-López et al., 2005). In addition, this anisotropy can produce variations of the strain field effect on rocks in comparison with the strain field acting on isotropic rocks. This anisotropy can be faults, joints, lithological contacts, mineral lineations, etc. Fig.3.23 shows several strain tensors acting on the same structure in relation with the strain field described by *El Asnam* strong earthquake (1980, Ms>7) (Phillip and Cisternas, 1983).

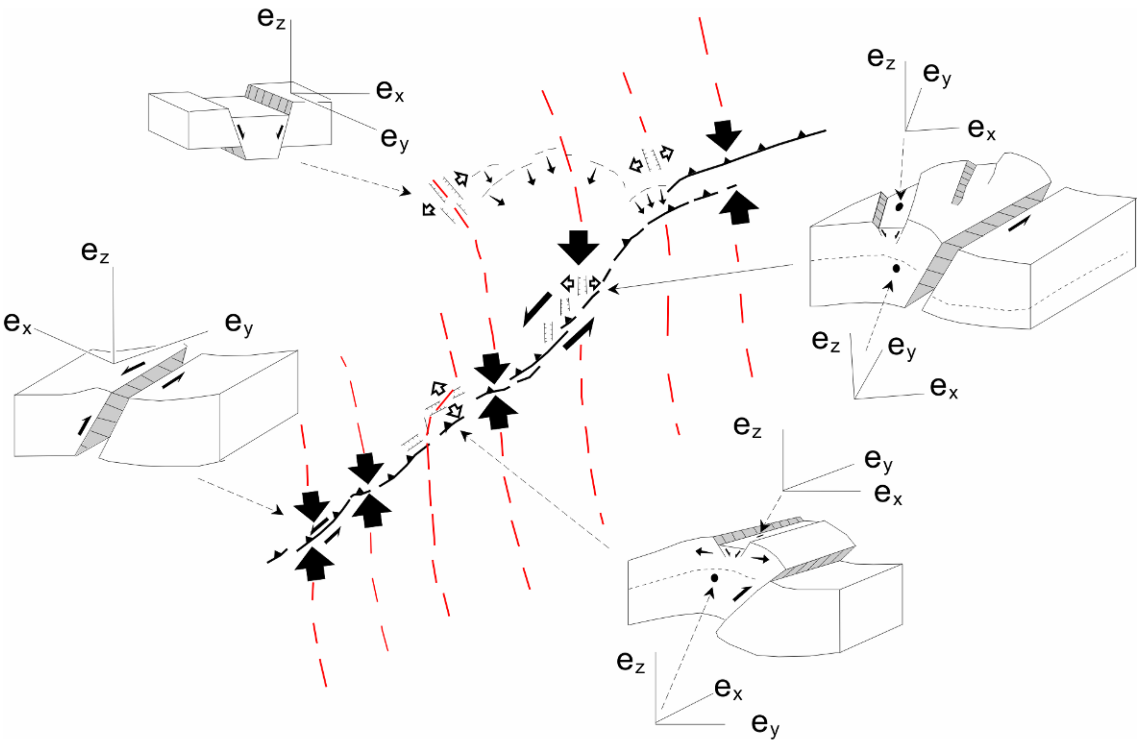

Fig. 3.23: Compatible strain tensors of a strain field, defined by superficial structures reactivated and/or neoformed Turing the El Asnam strong earthquake (1980). We can see switch off of the principal axes of the strain field, changing the direction of the maximum horizontal shortening (ey) (red lines) (After Phillip and Cisternas, 1983).

3.4b Anisotropy induced by archaeological structures

Archaeological sites have several structures (walls, pavements, etc...) that represent anisotropies under a strain field. These structures produce rotations in the ey trajectory (plan view) and therefore a different shape factor of the resulting strain tensor. Common structures as underground drainages, canalizations, ancient masonry, etc., determine variations for the orientation in the ey trajectory. Furthermore, the type of the structure as regular or irregular flagstone pavement also impact on the orientation of the resulting ey trajectory (Fig. 3.24).

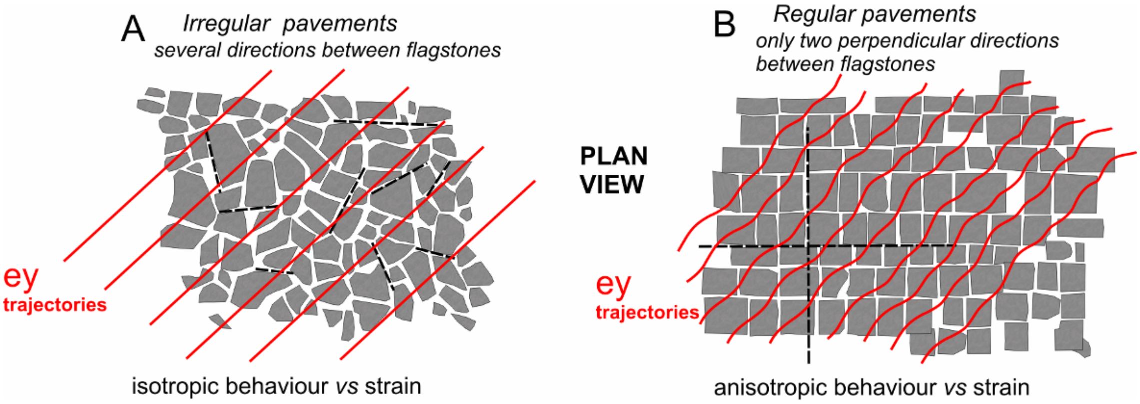

Fig. 3.24: Geometry of the ey trajectory for two types of flagstone pavements: A) Irregular pavements have an isotropic behaviour of the strain (several directions between flagstones). B) Regular pavements have an anisotropic behaviour of the strain (pavements defined by two principal and orthogonal directions between flagstones).

Accordingly, all structural and architectural factors must to take in account to obtain the strain tensor associated to potential earthquake damage, showing a dispersion dataset for EAEs (Fig. 3.25).

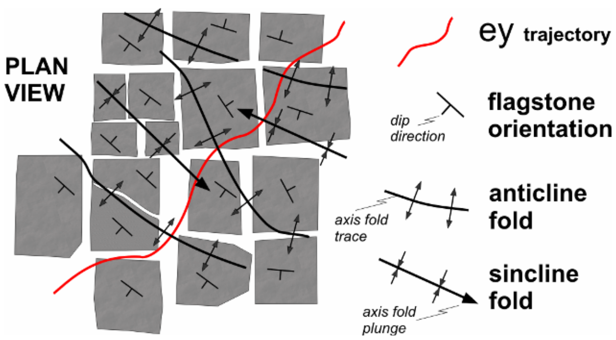

Fig. 3.25: Idealized distribution and orientation of folds in a flagstone pavement.

This is the reason why we have to apply statistics analysis for the interpreted EAE to calculate the strain tensor. Moreover, we have to divide the archaeological site in sectors, which exhibits homogeneous EAE spatial distribution (Fig. 3.5).

In some cases can be complicated to sectorize the site. In these cases, we have to perform a precise description of each EAE including a detailed description of the architectonic context as well. For example, the wall behaviour under a strain field depends on the orientation of the wall. Regular spatial distribution of streets and buildings, two orthogonal main directions control the anisotropy to generate EAE (e.g. Baelo Claudia). Otherwise, if the archaeological site exhibits an irregular spatial distribution, the whole of the site acts as an isotropic area under the strain field.

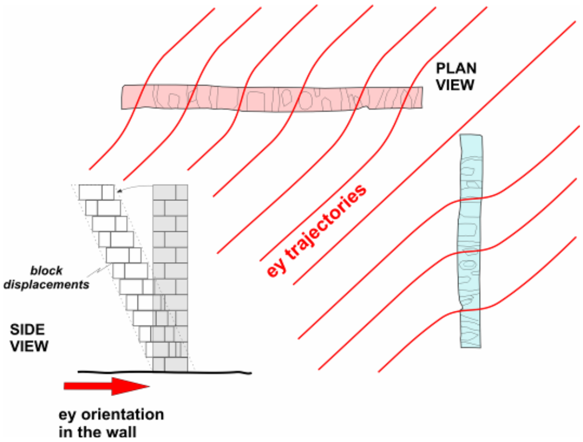

Fig. 3.26 shows the rotation of the ey trajectory for a strain field in relation with two orthogonal wall directions. The variation of the strain orthogonally accommodates the strain within the wall. Other sources of anisotropy can be underground drainages, ancient buried masonry blocks, etc. (Fig. 3.27).

Fig. 3.26: Variation of the ey trajectory in relationship with two orthogonal directions.

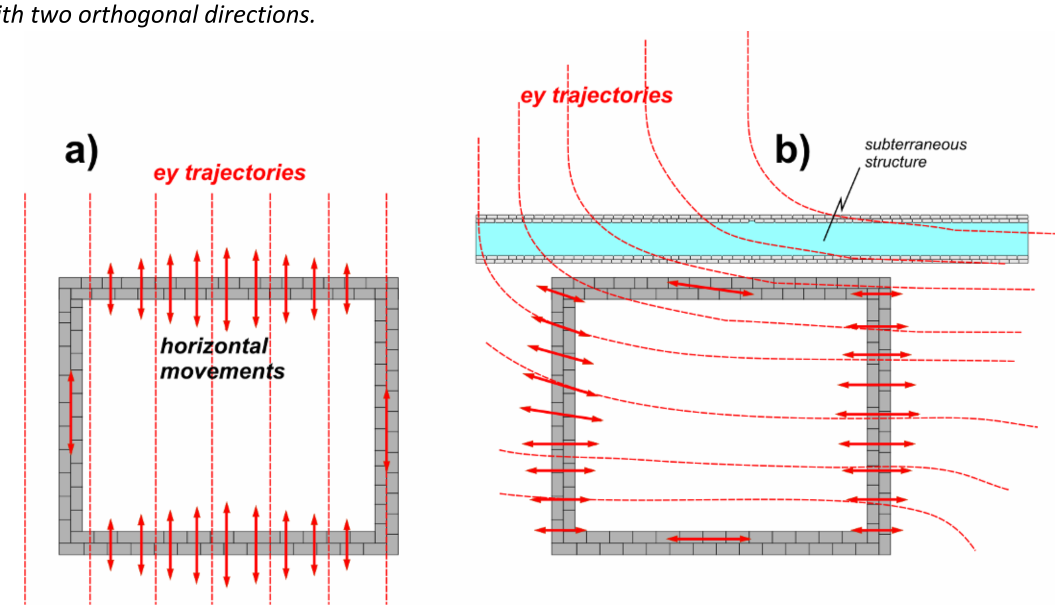

Fig. 3.27: Plan view for ey trajectory variations: a) building without underground structures. b) building with underground structures. In the last case, the ey trajectory is reoriented indicating the horizontal movement responsible for the building damage.

3.5 CONCEPTUAL EXAMPLE OF THE FINAL RESULT OF THIS COURSE

Figure 3.28 illustrates a conceptual example of the abilities that the assistant can reach by performing the course on Structural Analysis applied on Earthquakes Archaeological effects. This figure represents an idealized map of an Archaeological site with structural damage. Cartographic symbols proposed here correspond with symbols indicated in each sheet of the EAEs.

This examples exhibits a set of EAEs generated by a single earthquake of a normal fault trending NW-SE. The focal mechanism solution and the strain tensor are synthetic and illustrate the orientation of the maximum horizontal shortening (Ey) with NE-SW trending.

We have represented the structural damage using the cartographic symbols proposed to each EAE. Field sheets of the next sections compile eight selected EAEs (*1. folded mortar pavements; fractures, folds & pop-ups; 2. shocks breakouts in flagstones; 3. tilted walls; 4. folded walls; 5. fallen and oriented columns; 6. dropped keystones in arches or lintels in windows and doors; 7. dipping broken corners and 8. building reconstruction*). In these sheets a detailed description of the structural damage in relation with the ey orientation is indicated. In this sense, Fig. 2.28 idealizes several EAEs displaying the anisotropy that would be generated for this synthetic earthquake and assuming and seismic intensity greater than VI (MSK, EMS, etc.).

Therefore, the ultimate goal of course is the acquisition of a systematic methodology in the quantification of the seismic deformation from structural damage affecting ancient buildings and findings in archaeological sites.

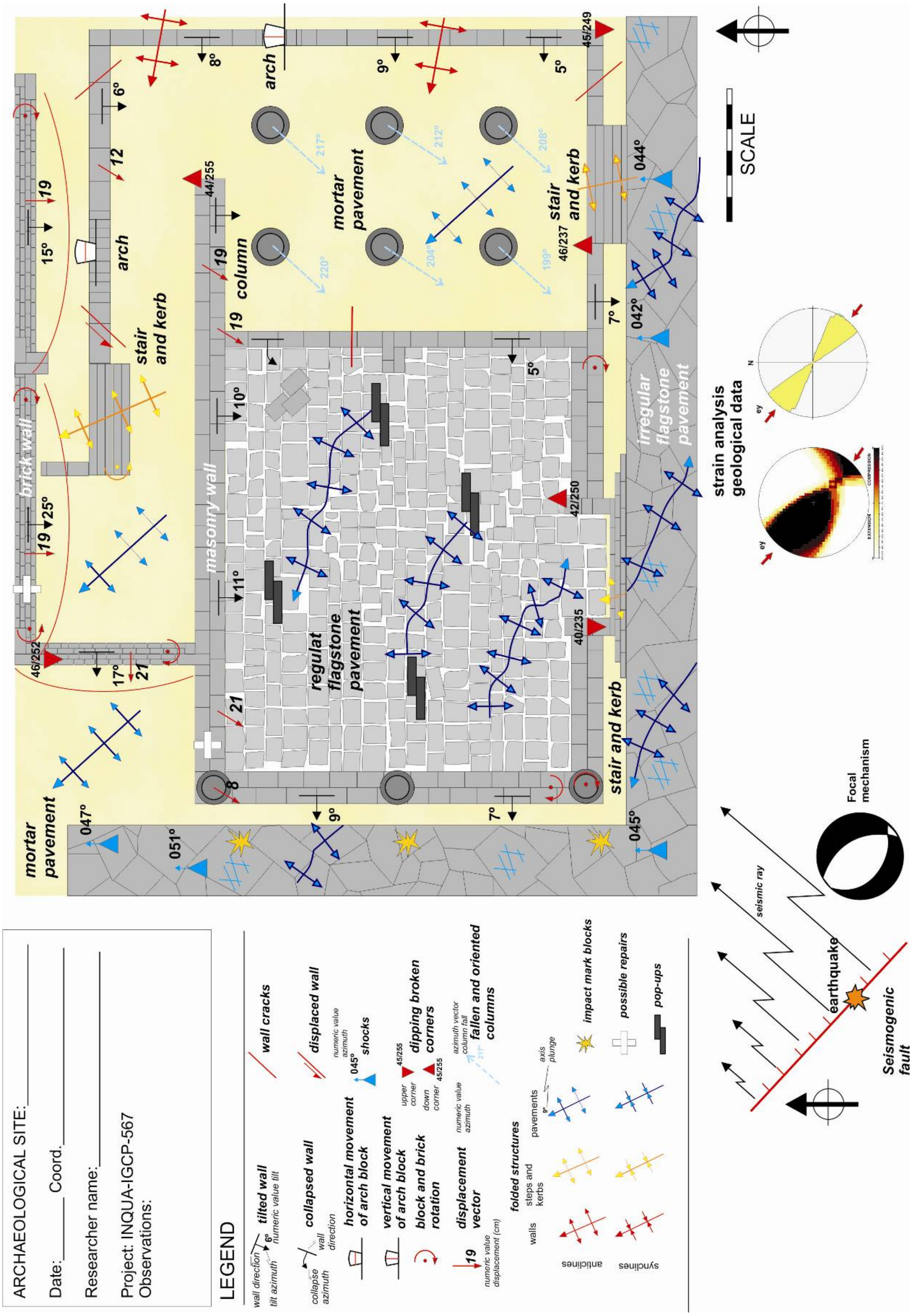

Fig. 3.28. *Example of the final result of EAE analysis performed at an idealized archaeological site.*

4. FIELD SHEETS FOR SELECTED EAE

structure name: FOLDED PAVEMENTS

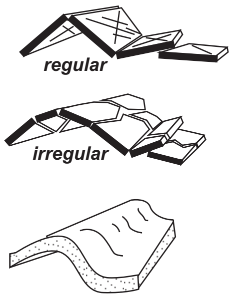

		behaviour vs strain	common structures
flagstone pavements	regular	anisotropic	folds fractures pop-ups
	irregular	isotropic	folds fractures pop-ups
mortar pavements		isotropic	folds

morphology.

Folded pavement with pop-ups in flagstones and fracture sets.

interpretation.

Seismic waves arrival bends the basement and "performs" foldings in the pavement. Pavements with irregular fabric behaves different under a strain field than pavements with regular fabric (i.e. regular flagstones).
The ey orientation os perpendicular to the axis fold (both syncline as anticline).

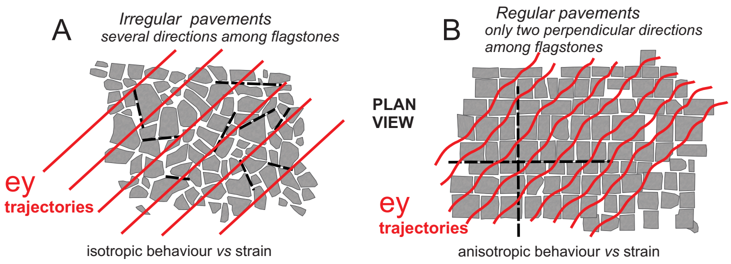

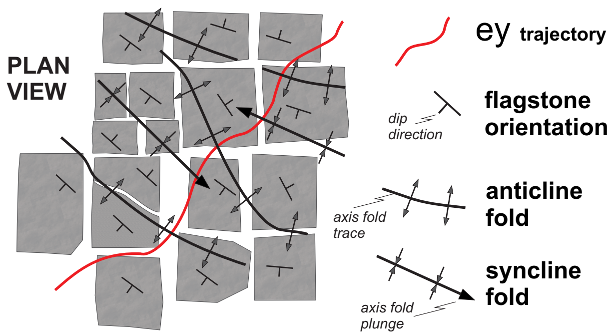

Pavements of regular flagstones behave as anisotropic material under a strain field. This fact implicates variations fo the strain tensor, the fold axis is dashed and can arise interference folding (dome and basin).

Folding in steps and kerbs are similar in mechanism that pavements of regular flagstones and their axes are also perpendicular to the ey direction.

measurement and representation

Quantification of strain from fold pavement is in relationship with the orientation of the axis fold and does not depend on the type of pavement (regular or irregular). We can obtain the axis fold direction either by direct measurement the axis fold or by differrent measurements on both limbs of the fold. Other measurement is the plunge of the axis fold, generated in general by interference of folding. Thrust movement between flagstone produces pop-up arrays in pavements. The direction of the thrust is the slip vector and it is parallel to the ey direction.

cartographic symbol

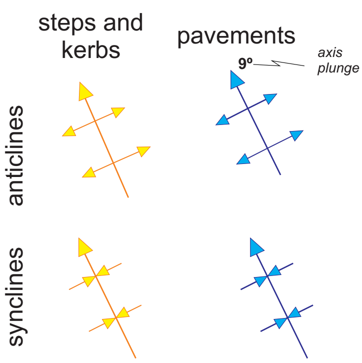

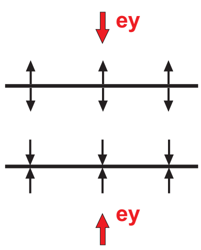

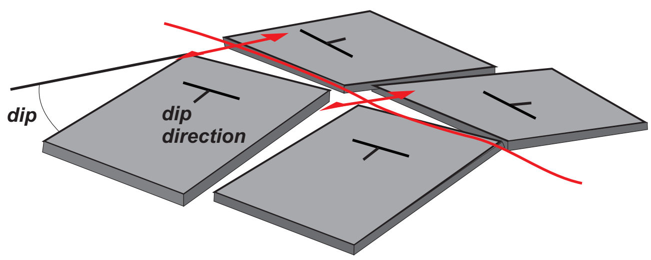

type of data

line (L1)
single orientation
single data

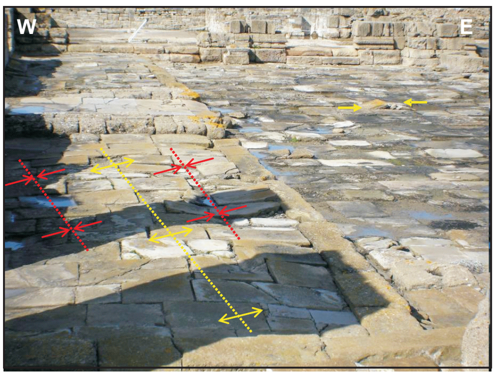

References

Altunel (1998),
Rodriguez-Pascu et al.(2009a)
Silva et al. (2009a),

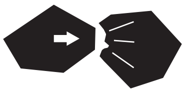

structure name: SHOCK

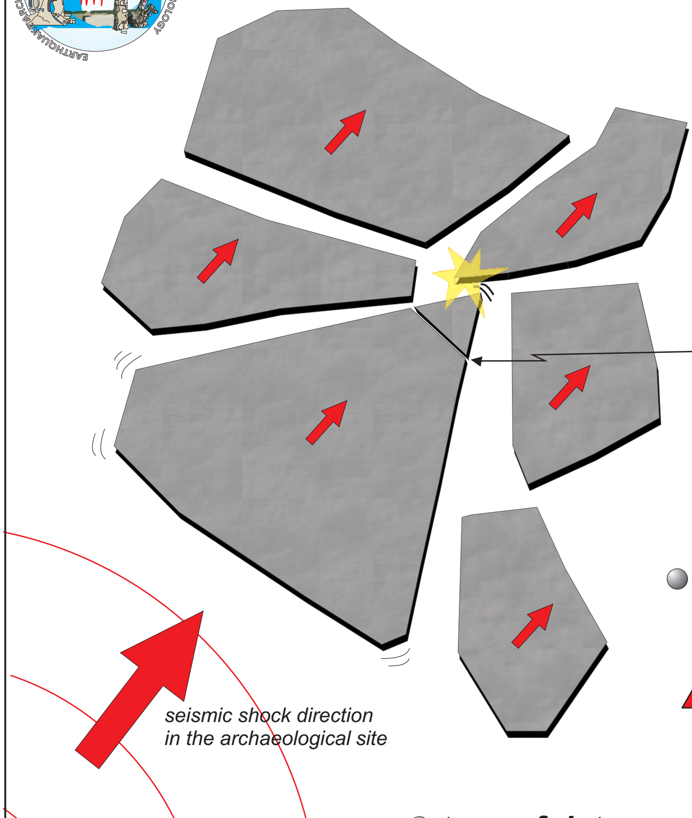

wave front

- ***morphology.*** **Triangular rupture in the corner-edge of the flagstones. For a better interpretation in situ preservation of the broken piece is desired. Size: usually cm (exceptionally dm).**

- ***interpretation.*** **Horizontal movement due to seismic waves induces collision between flagstones giving place to the rupture of their corner-edges. The rectilinear rupture outlines a perfect triangle.**

- ***measurements and representation***
Movement of flagstones is perpendicular to the base of the triangle pointing to the undamaged flagstone.

- ***cartographic symbol***

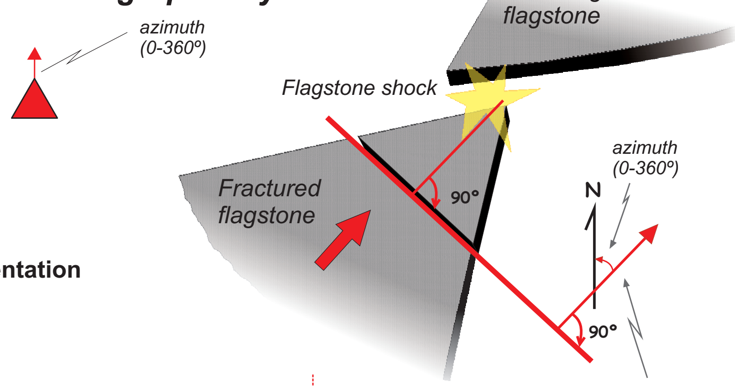

- ***type of data***
Line (L2), single orientation and single data

application sites

The most concluding results are obtained in irregular flagstone-pavements, with variable size and shape of flagstones. Results will not depend on the prevailing directions existing in regular pavements.

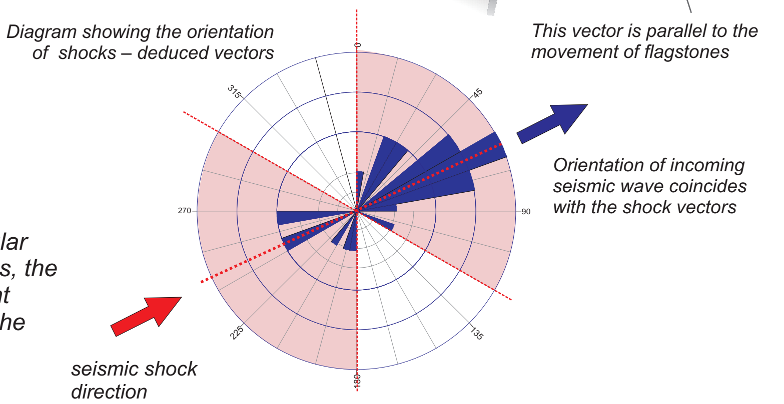

Irregular pavements
several directions between flagstones

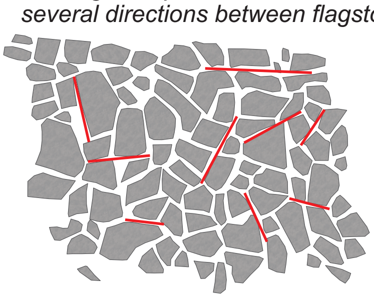

In the case of irregular flagstone-pavements, the existence of different orientations allows the correct analysis of this structure.

Regular pavements
only two perpendicular directions between flagstones

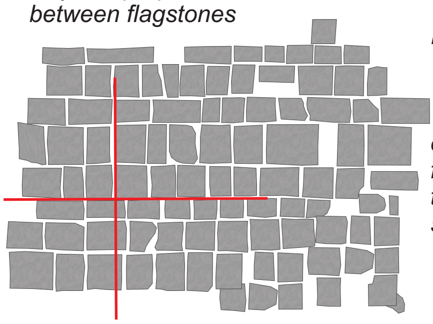

In this case, the presence of these structures is subordinated to the orientation of the flagstones with regard to the incoming seismic wave.

- ***examples in Baelo Claudia***

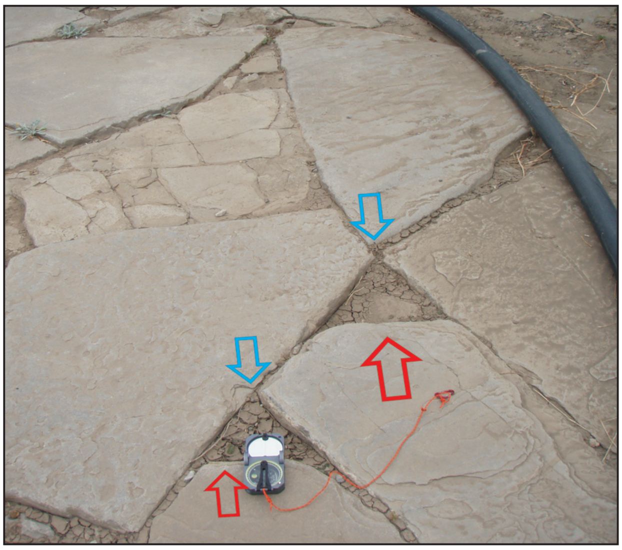

References
Stiros (1996), Boer and Hale (2000), Korjenkov et al. (2003), Silva et al. (2005), Marco (2008) Rodriguez-Pascua (2009a), Silva et al. (2009a)

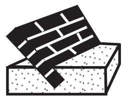

structure name: TILTED WALL

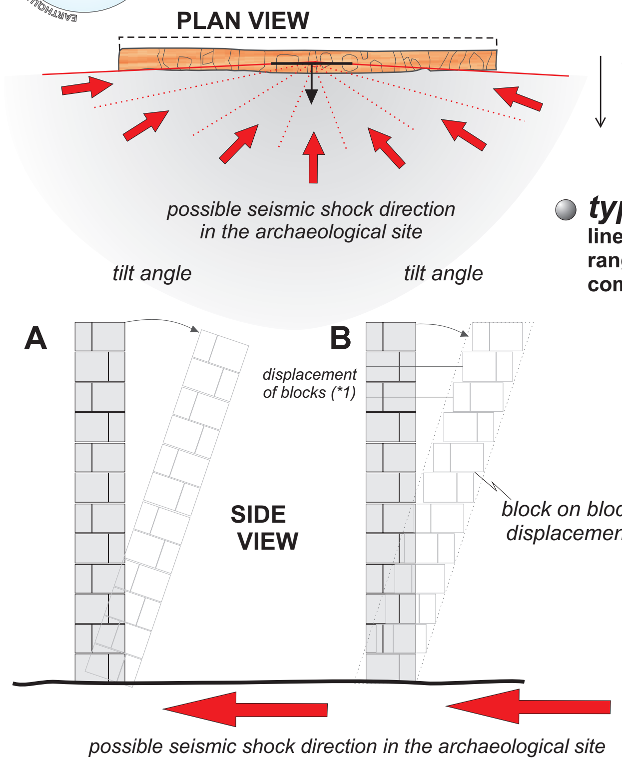

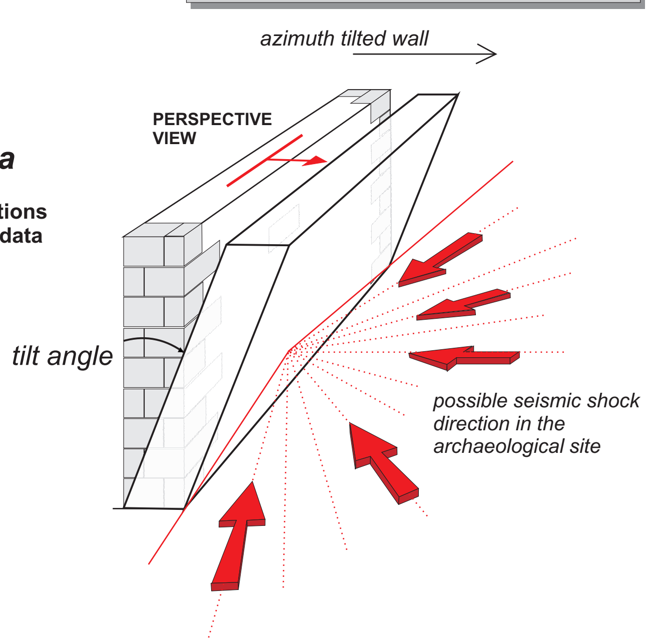

type of data

line (L2)
range of orientations
complementary data

interpretation.

The movement of seismic waves triggers the tilting or collapse of the walls. The sense of the tilt gives information about the possible seismic shock direction in the archaeological site.

morphology.

Tilted walls, either as a unit (A) or by displacement between blocks (B) or mixed. The displaced walls that give more information ar the mixed ones.

cartographic symbol

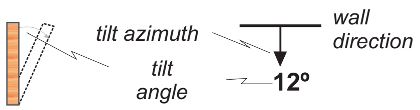

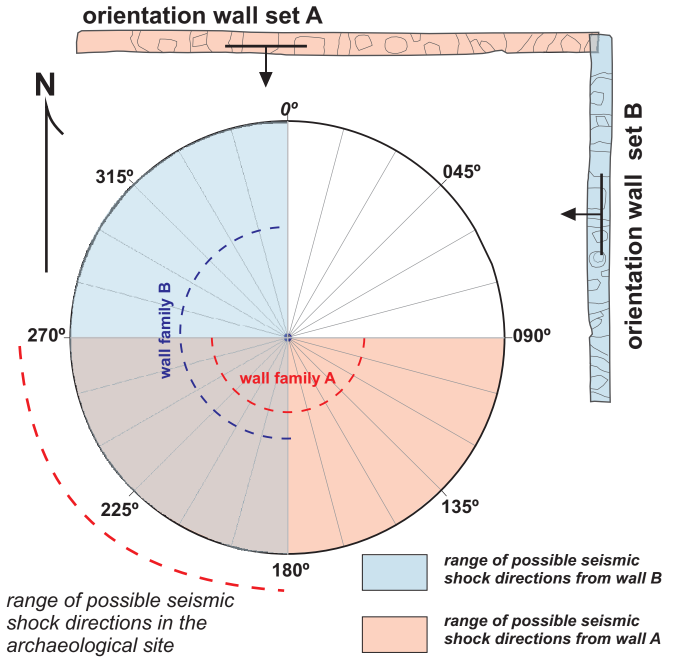

range of possible seismic shock directions from wall B

range of possible seismic shock directions from wall A

range of possible seismic common shock directions from wall A and B

measurement and representation

The orientation of the wall denes two elds of possible azimuths, the sense of the tilt points to the interval where the most probable seismic shock direction comes from. In this case, the range of azimuths is interval 2 (090º to 270º)

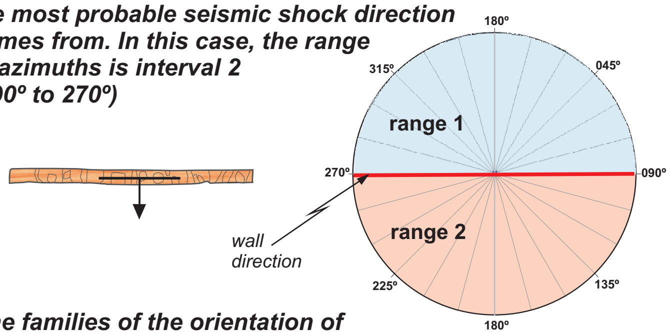

The families of the orientation of tilted walls must be stated for the archaeological site (families A and B in the example on the left). The combination of intervals for each family will dene the possible common azimuths of the seismic shock for the entire archaeological site

examples in Baelo Claudia

References

Stiros (1996), Korjenkov and Kaiser (2003), Korjenkov et al. (2003), Kovach (2004), Monaco and Tortorici (2004), Binda and Saisi (2005), Silva et al. (2005), Ambraseys (2006), Marco (2008), Silva et al. (2009a), Rodriguez-Pascua et al. (2009a),

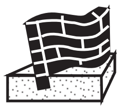

structure name: FOLDED WALL (I)

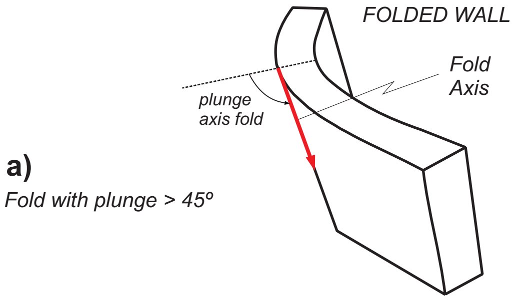

morphology

Folded walls. There are two type of folded walls:
(1) Fold with the axis fold plunge > 45º and
(2) Fold with the axis fold plunge < 45º.

ANCHOR EFFECT

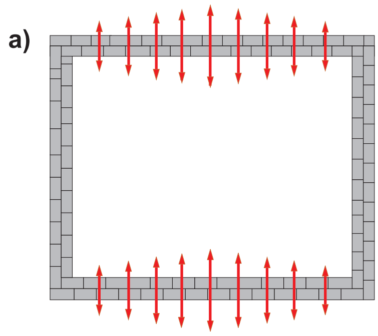

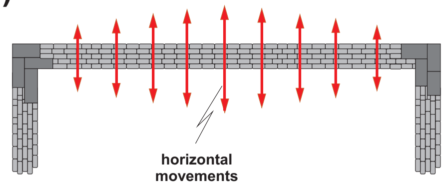

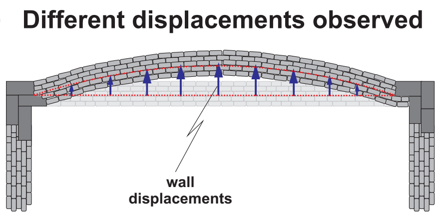

interpretation

Differential movement of the wall is due to the anchor effect, the bricks into the wall have a differential movement also and finally, the wall is folded.

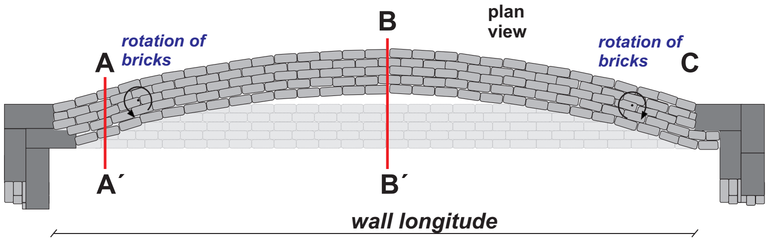

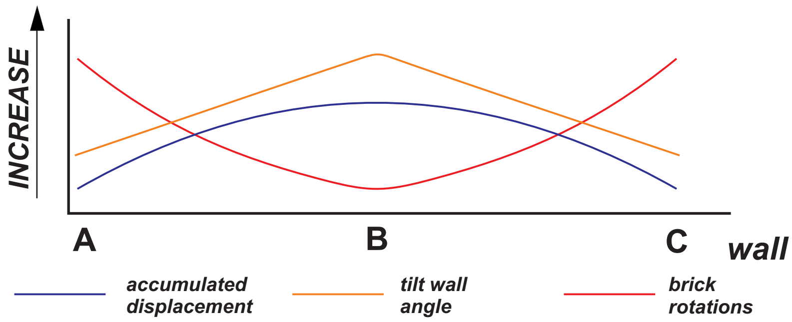

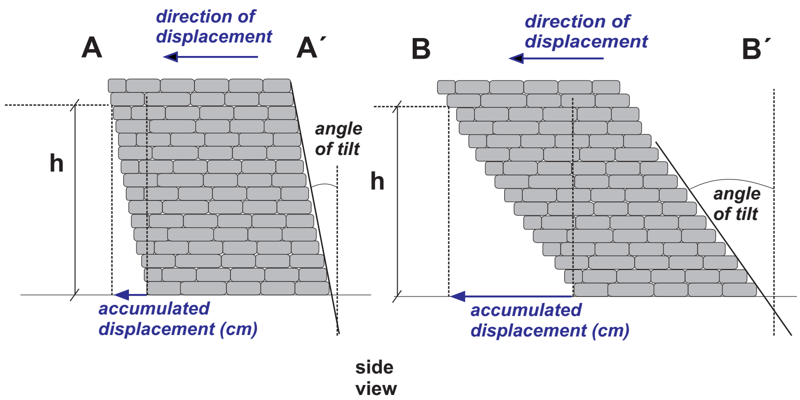

measurement and representation

We have to measure the maximum tilt angle of the wall and the maximum displacement. Both values are in relationship and increase from the lateral to the central part of the wall

We can measure two parameters:
-tilt angle
-accumulated displacement

Both parameters (angle and displacement) must to be weighted with the longitude of the wall.

The accumulated displacement of walls are related with the hight of the wall. For this reason and with the aim to compare different displacements from differents walls, is strongly recommended to obtain the maximum displacement of each wall at the same hight. Moreover, a set of displacement for different hights for a wall is desired.

cartographic symbol

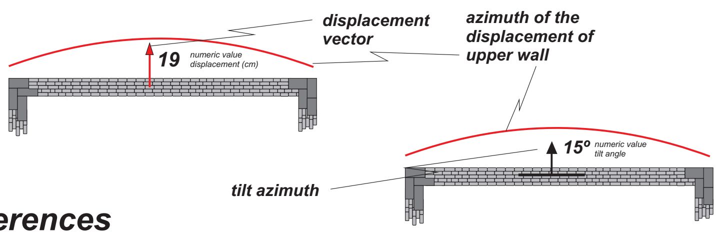

type of data

line (L1, axis fold),
line (L3, displacement vector)
single orientation
complementary data

References

Stiros (1996), Boer and Hale (2000), Korjenkov et al. (2003), Korjenkov and Kaiser (2003), Silva et al. (2005), Ambraseys (2006), Marco (2008), Rodriguez-Pascua et al. (2009a), Silva et al. (2009a)

structure name: FOLDED WALL (II)

b) *Folding with axis plunge (i) < 45º*

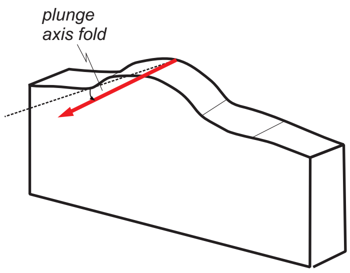

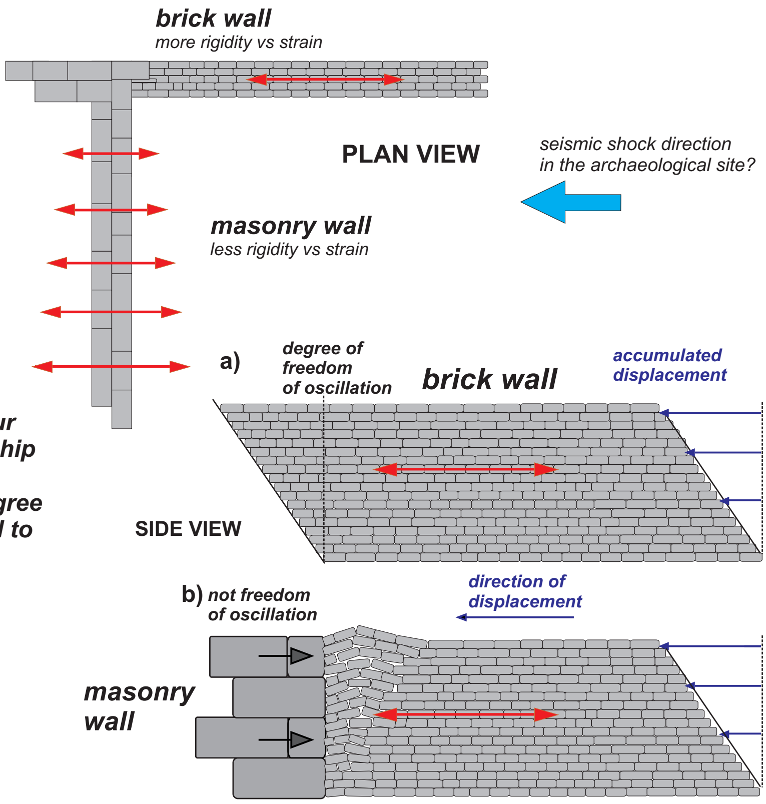

interpretation

This structure is generated by a different behaviour of the wall during the deformation and in relationship with the fabric of the wall. The presence of rigid masonry blocks with other blocks reduces the degree of freedom of the wall oscillations, folding the wall to accommodate the deformation.

measurement and representation

In this type of EAE, we direct obtain the measure of the axis fold. The direction of the maximum horizontal shortening (ey) is perpendicular to the axis fold orientation.

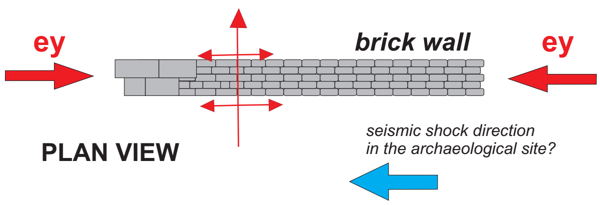

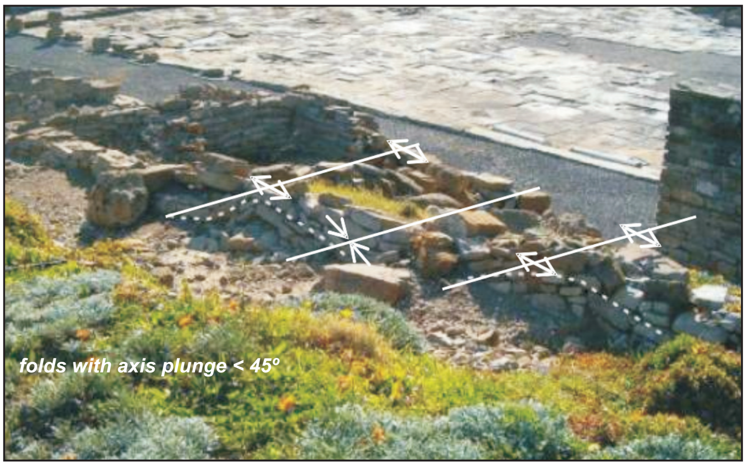

implementation

These folds usualy appear in brick walls and/or mortar walls. Walls of rigid masonry walls hardly are folded, instead the bricks of the lateral part of the wall rotate and present cracks and fractures.

type of data

line (L1)
single orientation
single data

cartographic symbol

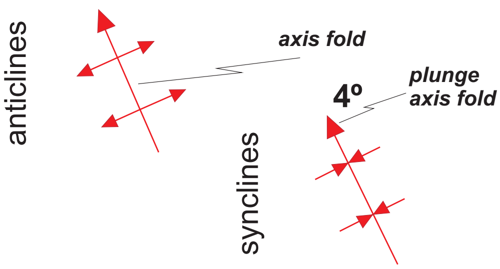

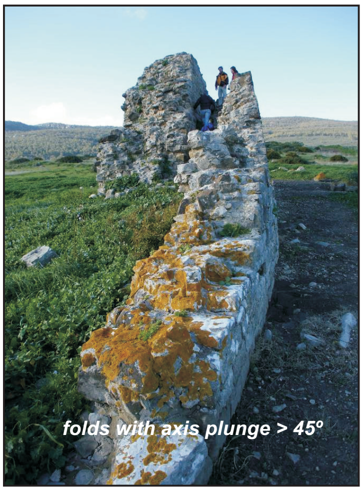

structure name: ORIENTED COLUMN FALLEN

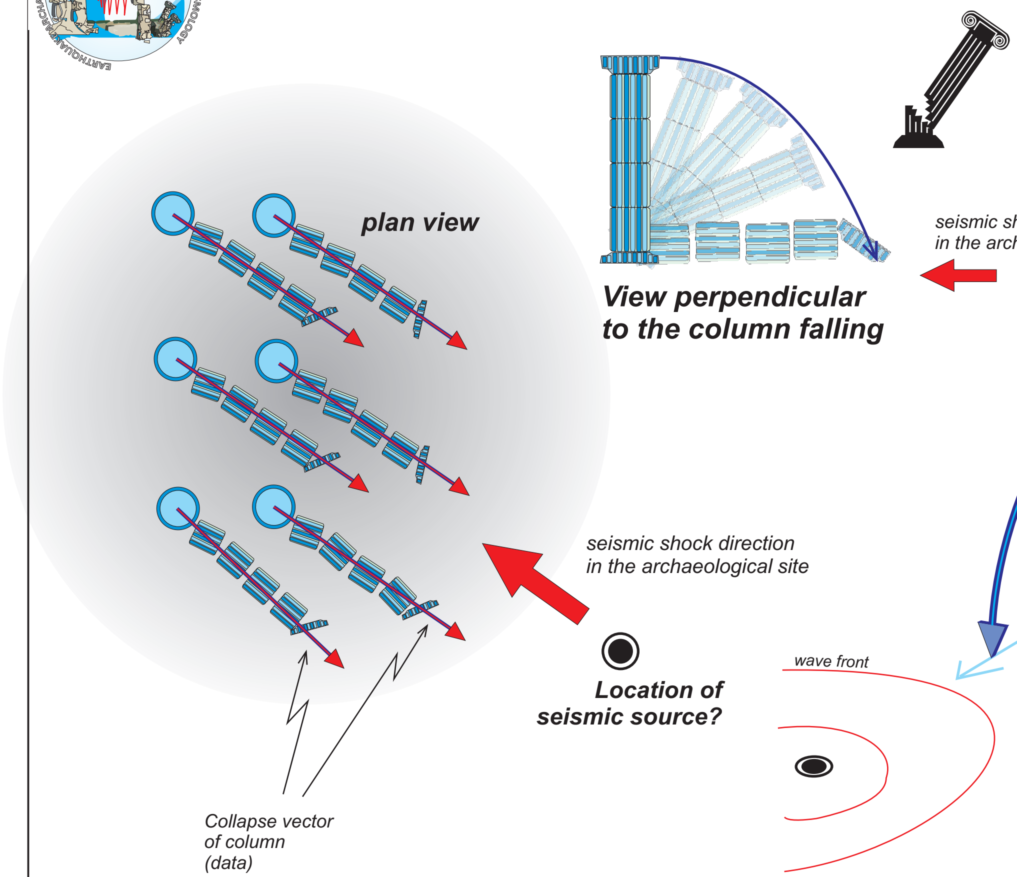

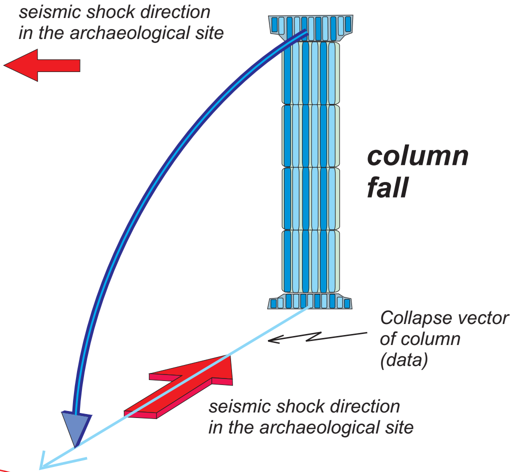

type of data
Line (L2), single orientation and single data

morphology
Oriented fallen columns in the archaeological site

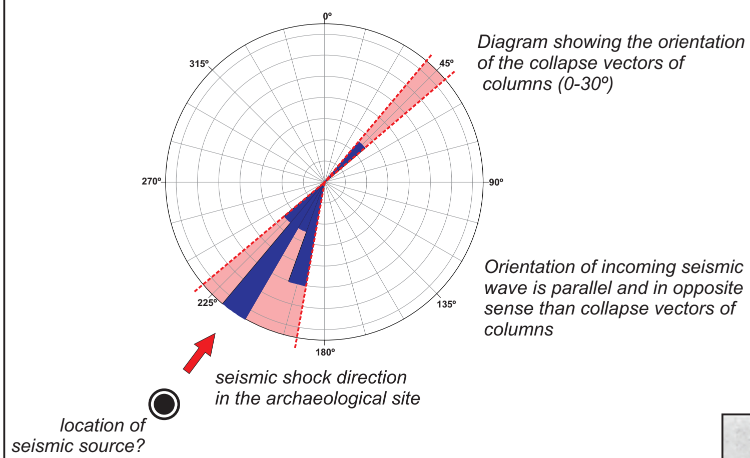

interpretation.
The movement induced by seismic waves provokes the collpase of columns. All the columns in the archaeological site fall in the same direction, pointing to a common genetic cause for the collapse.

measurements and representation
The columns collapse in the same direction but opposite sense than the incoming waves in the archaeological site. Orientation of collapse vectors (0-30º) of columns point to the seismic source.

cartographic symbol

Dip direction collapse of columns (0-360º)

application sites
This indicator can be applied to any distribution of independent columns, not attached to any wall. The results are more reliable when the collapse orientation does not coincide with the main orientation of buildings or structures where they are located. Downslope collpases are not concluding either.

examples in Baelo Claudia

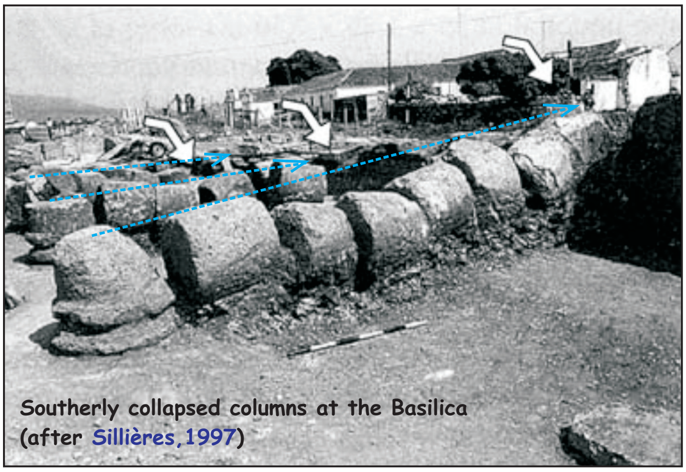

Southerly collapsed columns at the Basilica (after Sillières,1997)

references

Nur and Ron (1996), Stiros (1996), Sillières (1997), Altunel (1998), Altunel et al. (2003), Korjenkov, et al. (2003), Binda and Saisi (2005), Silva et al. (2005), Ambraseys (2006), Marco (2008), Rodriguez-Pascua et al. (2009a); Silva et al. (2009a)

structure name: SLIDING OF ARCH BLOCKS (I)

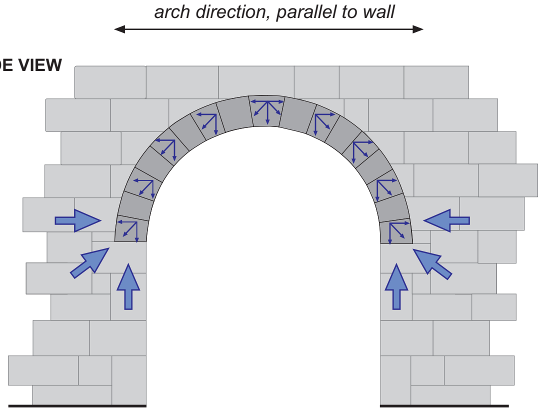

General scheme of the strain distribution within the arch blocks

- **morphology.** Differential displacement of arch blocks
- **interpretation.** Due to the movement induced by seismic waves, a differential displacemetn of arch blocks takes place. Horizontal, vertical or mixed displacements, and without collapse of the arch.

VERTICAL MOVEMENT OF BLOCKS

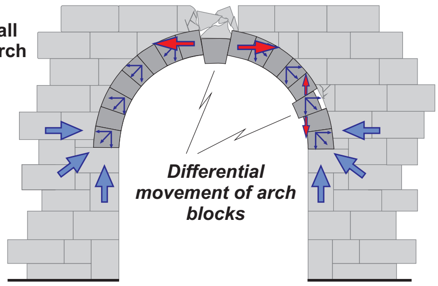

Some authors noted that the upper load of the arch should be small to produce movement in the arch blocks (Kamai and Hatzor, 2007)

presence of vertical movements?

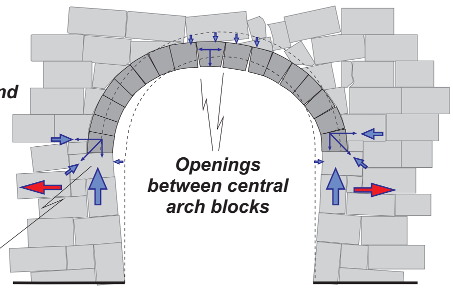

Side view of strain evolution (*A*, *B* and *C*)

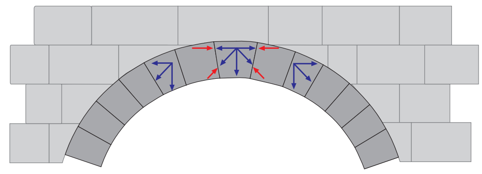

A) Undeformed state

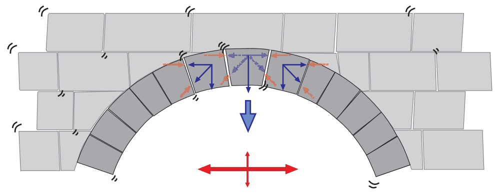

B) Deformation

Horizontal movements induce the separation of arch blocks, eliminating the support for the remaining blocks of the arch and inducing the vertical movement, usually of the central arch block or keystone

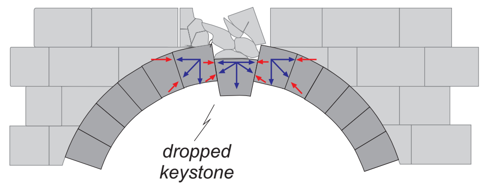

C) Deformed state

- ***measurement and representation***

At first approximation, and without any other data to compare, we can just define the most probable orientation of the movement that has induced this kind of structure.

In the case of differetnial vertical movement of arch blocks we can consider that: the angle between the direction of movement and the wall where the arch is located, should not exceed 45º.

In this example, the direction of the movement must be between N45ºE and N135ºE, and in any case we can state the sense of movement.

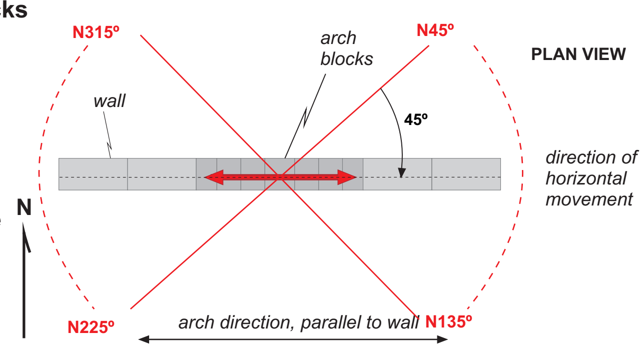

structure name: SLIDING OF ARCH BLOCKS (II)

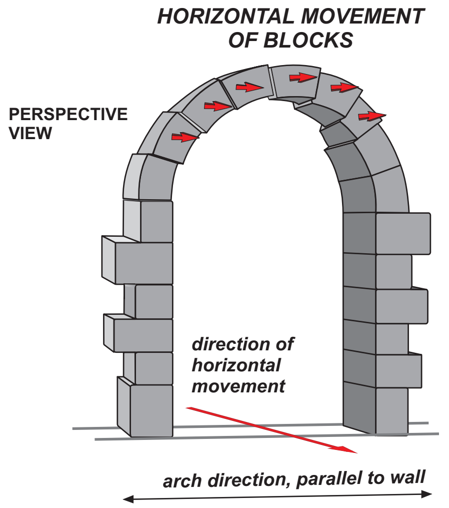

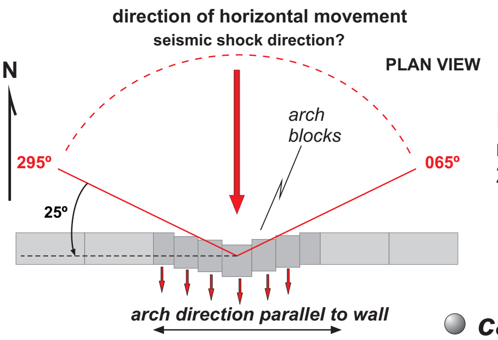

In this example, the direction of movement must range between 295º and 065º

cartographic symbols

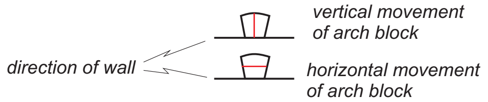

measurement and representation

In the case of differential horizontal movement of arch blocks, the angle between the direction of movement and the wall that contains the arch, must be higher than 25º. Diverging from the previous case (vertical movement of arch blocks), in this case we can state the sense of movement, since it will be the same than the arch blocks displacement. This could be tentetively interpreted as the seismic shock direction.

In some cases, a given arch can show both vertical and horizonal displacement of arch blocks, so we could state a common interval of movements that allow a more precise determination of the movement direction.

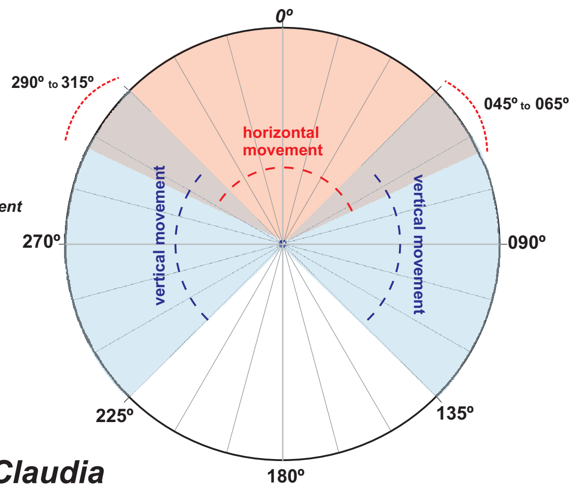

range of possible movement (vertical displacement)

range of possible movement (horizontal displacement)

common range of possible movement shock directions

type of data

Line (L1, L2), range of orientations and complementary data

examples in Baelo Claudia

Arch blocks with horizontal displacements in arch of an entrance to Theatre

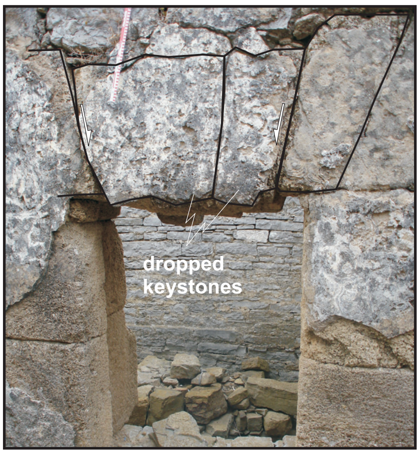

Dropped keystone in the lintel windown in the west side of Curia (public building)

Dropped keystone in the arch of the North Bastion´s gate in the east wall city

References

Stiros (1996), Binda et al., (1999), Altunel et al. (2003), Korjenkov, et al. (2003), Kovach (2004), Luca et al. (2004), Binda and Saisi (2005), Silva et al. (2005), Kamai and Hatzor (2007), Marco (2008), Rodriguez-Pascua et al. (2009a), Silva et al. (2009a),

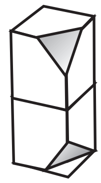

structure name: DIPPING BROKEN CORNERS

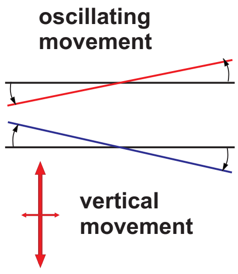

The deformation in walls appears from the blocks oscillation movement.

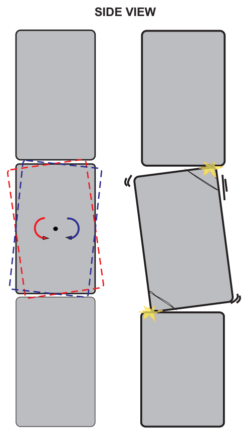

morphology

Broken corners in masonry blocks and pillars. In general the fracture dip angle is close to 45º.

interpretation

Seismic waves produce an oscilllating movement in the vertical plane. This movement displaces the blocks of the wall.

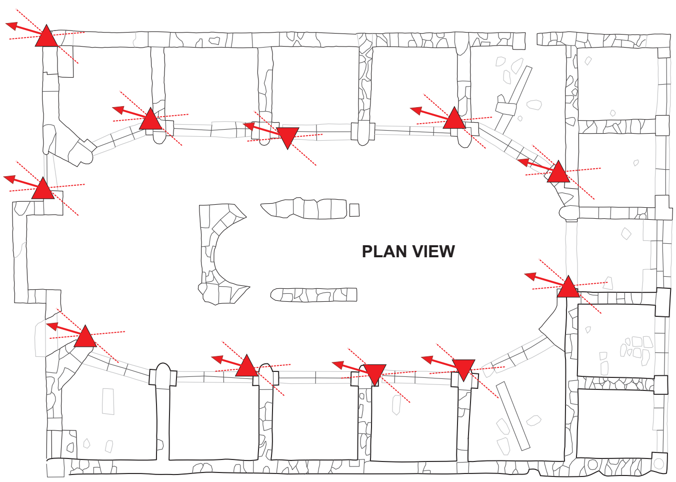

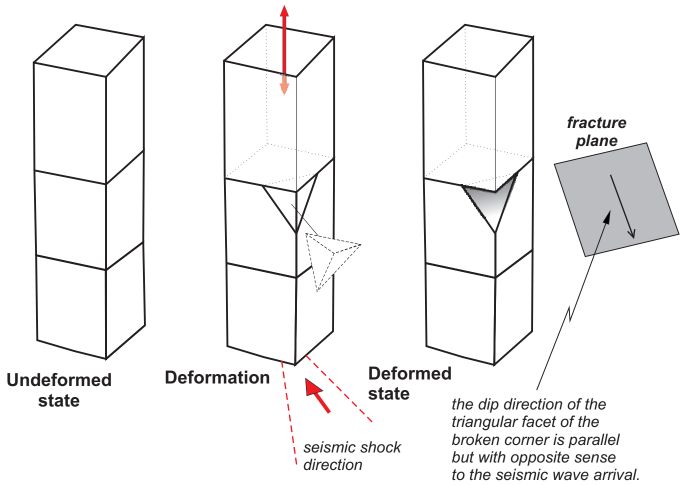

Triangular facets of broken corners appear both in the top as the bottom of the block. Therefore, we have to describe the up or down position of the broken corner.

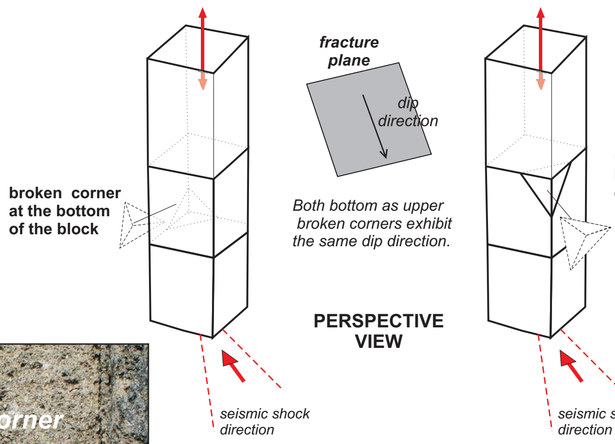

type of data

plane or line (L2)
single orientation
single data

cartographic symbol

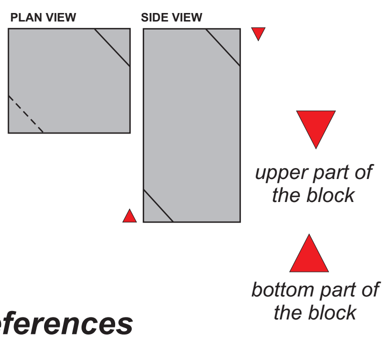

examples in Baelo Claudia

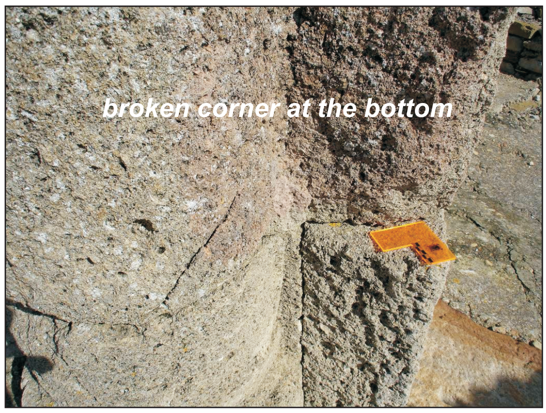

References

Stiros (1996), Korjenkov, et al. (2003), Marco (2008), Rodriguez-Pascua (2009a), Silva et al (2009a)

structure name: RECONSTRUCTION

morfología.

The identification of reconstructions in archaeological sites from seismic damage is based on contrasted information. Sliding downward keystone of arches and/or vaults is a common feature to be rebuilding. However, single reparations are not conclusive for supporting the theory of seismic damage and even single seismo-resistant buildings. Is recommended that other reparations potentialy assigned to seismic damage should be supported by writing chronicles and archaeological findings.

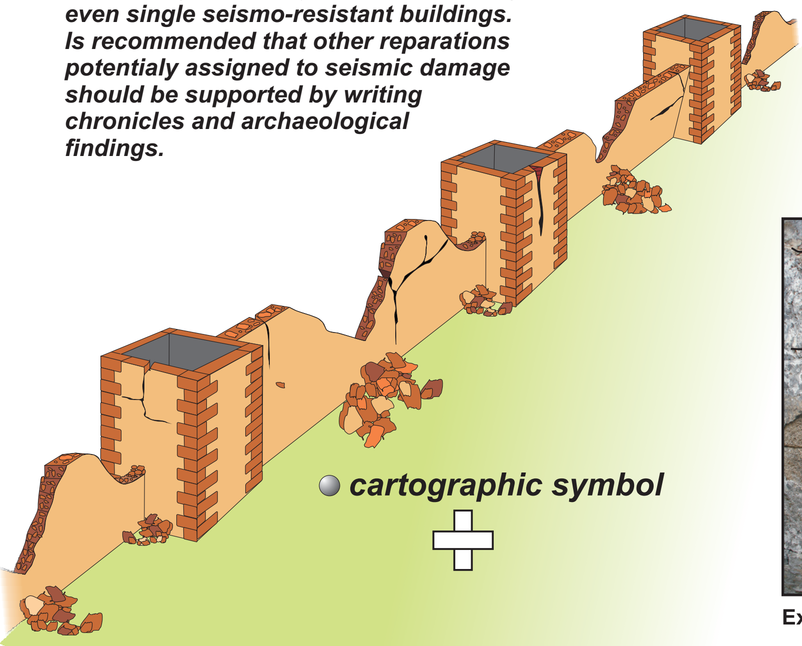

cartographic symbol

examples in Baelo Claudia

1) From the late 1st century AD to early 2nd century AD reparation, reinforcement and thickening of the 1st century city wall. However, this repairs cannot be attributed only to a seismic single event.

2) Reparation of the sliding downward keystone in the lintel of a window and attributed to the seismic origin. Only repaired the external dintel, the internal dintel is not repaired.

External view (repaired) Internal view (not repaired)

3) Possible reconstruction of the keystone of the arch-door affected by , at least, a single earthquake and located in the North Bastion:
A) Original position.
B) Carving of the sliding keystone to repair the stone door frame.
C) Final result at present (photos 1 and 2)

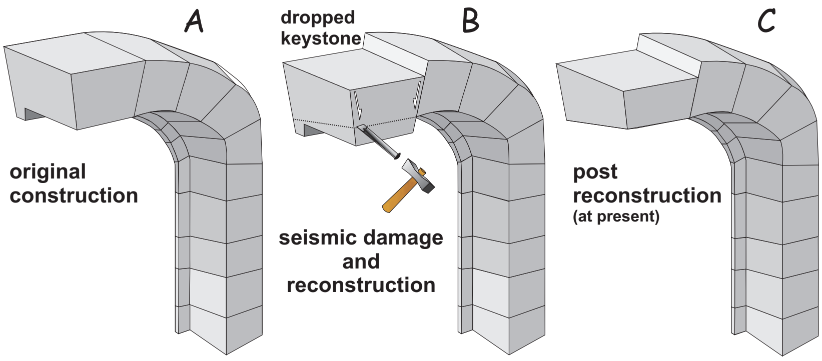

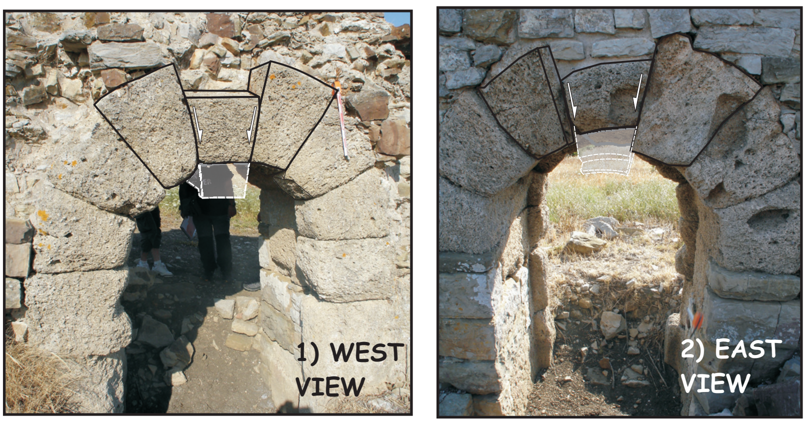

4) Reconstruction of the wall close to the fish factories, by using recycled stones.

References

Stiros (1996), Korjenkov, et al. (2003), Binda and Saisi (2005), Marco (2008), Rodriguez-Pascua et al.(2009a), Silva et al. (2009a)

5. REFERENCES

References

Altunel, E. (1998). Evidence for Damaging Historical Earthquakes at Priene, Western Turkey. *Turkish Journal of Earth Sciences*, 7: 25-35.
Altunel, E., Stewart, I. S., Barka, A., Piccardi, L. (2003). Earthquake Faulting at Ancient Cnidus, SW Turkey. *Turkish Journal of Earth Sciences*, 12: 137-151.
Ambraseys (2006). Earthquakes and archaeology. *Journal of Archaeological Science*, 33: 1008-1016.
Angelier, J., and P. Mechler (1977). Sur une methode graphique de recherche des contraintes principals egalement utilisable en tectonique et sismologie:La methode des diedres droits, *Bull. Soc. Geol. Fr.,* 19(6): 1309-1318.
Binda L., Baronio G., Gavarini C., De Benedictis R., Tringali S. (1999). "Investigation on Materials and Structures for the Reconstruction of the Partially Collapsed Cathedral of Noto (Sicily)", *6° Int. Conf. Structural Studies, Repairs and Maintenance of Historical Buildings*, STREMAH 99, Dresden, Germany, pp. 323-332.
Binda L., Saisi A. (2005). Research on historic structures in seismic areas in Italy. *Progress in Structural Engineering and Materials, v 7, n 2*, April, 2005, pp. 71-85.
Boer J.Z. and Hale, J.R. (2000). The geological origins of the oracle at Delphi, Greece. In: *McGuire, W.J., Griffiths, D.R., Hancock, P.L. and I.S. Stewart. The Archaeology of Geological Catastrophes. Geological Society of London Special Publication*, 171, 45-70.
Bottari, C. (2003). Ancient constructions as markers of tectonic deformation and of strong seismic motions. Proceedings, *11th FIG Symposium on Deformation Measurements, Santorini*, Greece, 2003.
Bonsor, J. (1919). Photography of a skeleton of a man. *Jorge Bonsor y la recuperación de Baelo Claudia (1917-1921)*. Consejería de Cultura. Archivo General de Andalucia. Conjunto Arqueológico de Baelo Claudia. ISBN: 978-84-8266-889-5. 149p.
Buck, V. & Stewart, I. (2000). A critical reappraisal of the classical texts and archaeological evidence for earthquakes in the Atalanti region, central mainland, Greece. In: *McGuire, W.J., Griffiths, D.R., Hancock, P.L. and I.S. Stewart. The Archaeology of Geological Catastrophes*. Geological Society of London Special Publication, 171, 33-44.
Cejka, Jan (1978). Tonnengewólbe und Bogen ¡slamischer Architektur. Wolbungstechnik und Form. *Dissertation: München. Techn. Univ. Fachbereich Architektur.*
Chatzipetros. A. and Pavlides, S. (2009). A rare case of preserved earthquake ruptures in an archaeological site: Mikri Doxipara – Zoni, NE Greece. In: *R. Pérez-López, C. Grützner, J. Lario, K. Reicherter and P.G. Silva (eds). Archaeoseismology and Palaeoseismology in the Alpine-Himalayan Collisional Zone*. Abstracts Volume of the 1st INQUA-IGCP 567 International Workshop on Earthquake Archaeology and Palaeoseismology, 7th-13th September, p. 20. Baelo Claudia, Spain.
De Vicente, G. (1988). *Análisis Poblacional de Fallas: El sector de enlace Sistema Central-Cordillera Iberica, PhD*, Univ. Complutense de Madrid, Madrid.
Evans, A. (1928). *The Palace of Minos at Knossos II.* MacMillan. London.
Galadini, F., Hinzen, K.-G. and Stiros, S.C. (2006). Achaeoseismology at the Beginning of the 21st Century. *Journal of Seismology*, 10 (4), Special Issue. P 393-537.
Galadini, F., K. G. Hinzen, and S. C. Stiros (2006). Archaeoseismology: methodological issues and procedure. *Journal of Seismology*, 10: 395–414.
Giner-Robles, J.L.; González-Casado, J.M.; Gumiel, P. & García-Cuevas, C. (2003). Changes in strain trajectories in three different types of plate tectonic boundary deduced from earthquake focal mechanisms. *Tectonophysics*, 372: 179-191.
Guidoboni, E. (1989). I terremoti prima del Mille in Italia e nell´area Mediterranea: storia, archaeologia, sismologia. Bologna. SGA-Instituto Nazionale di Geofisica.
Guidoboni, E., Muggia, A. & Valensise, G. (2000). Aims and methods in territorial archaeology: possible clues to a strong fourth-century AD earthquake in the Straits of Messina (southern Italy). In: *McGuire, W.J., Griffiths, D.R., Hancock, P.L. and I.S. Stewart. The Archaeology of Geological Catastrophes. Geological Society of London Special Publication*, 171, 45-70.
Guidoboni, E., Muggia, A., Marconi, C., Boschi, E., (2002). A case study in archaeoseismology. The collapses of the Selinunte temples (Southwestern Sicily): two earthquakes identified. *Bulletin of the Seismological Society of America* 92: 2961–2982.
Hancock, P.L., Chalmers, R.M.L., Altunel, E., Çakir, Z. & Becher-Hancock, A. (2000). Creation and destruction of travertine monumental stone by earthquake faulting at Hierapolis, Turkey. *In: McGuire, W.J., Griffiths, D.R., Hancock, P.L. and I.S. Stewart. The Archaeology of Geological Catastrophes.* Geological Society of London Special Publication, 171, 1-14.
Hinzen, K.G. (2009). Dynamic response of simple structures. *In: R. Pérez-López, C. Grützner, J. Lario, K. Reicherter and P.G. Silva (eds). Archaeoseismology and Palaeoseismology in the Alpine-Himalayan Collisional Zone.* Abstracts Volume of the 1st INQUA-IGCP 567 International Workshop on Earthquake Archaeology and Palaeoseismology, 7th-13th September, p. 47. Baelo Claudia, Spain.
Hinzen, K.G., Fleischer, C., Reamer, S.K., Schreiber, S., Schütte, S. and Yerli, B. (2009). Quantitative methods in archaeoseismology. *In: R. Pérez-López, C. Grützner, J. Lario, K. Reicherter and P.G. Silva (eds). Archaeoseismology and Palaeoseismology in the Alpine-Himalayan Collisional Zone*. Abstracts Volume of the 1st INQUA-IGCP 567 International Workshop on Earthquake Archaeology and Palaeoseismology, 7th-13th September, p. 50. Baelo Claudia, Spain.
Jones, R.E. & Stiros, S.C. (2000). The advent of archaeoseismology in the Mediterranean. *In: McGuire, W.J., Griffiths, D.R., Hancock, P.L. and I.S. Stewart. The Archaeology of Geological Catastrophes.* Geological Society of London Special Publication, 171, 25-32.
Jin, K., Lee, M. and Kim, Y.S. (2009). Archaeoseismological approach on stone heritages in Gyeongju Area, SE Korea. *In: R. Pérez-López, C. Grützner, J. Lario, K. Reicherter and P.G. Silva (eds). Archaeoseismology and Palaeoseismology in the Alpine-Himalayan Collisional Zone.* Abstracts Volume of the 1st INQUA-IGCP 567 International Workshop on Earthquake Archaeology and Palaeoseismology, 7th-13th September, p. 63. Baelo Claudia, Spain.
Karcz, I., Kafri, U. (1978). Evaluation of supposed archaeoseismic damage in Israel. *Journal Archaeological. Science*, 5: 237– 253.

Kamai, R. and Hatzor, Y.H. (2007). Numerical analysis of block displacements in ancient masonry structures: a new method to estimate historic ground motions: *International Journal for Numerical and Analytical Methods in Geomechanics.* 32, 1321-1340.

Karcz, I., (2004). Implications of some early Jewish sources for estimates of earthquake hazard in the Holy Land. *Annals of Geophysics*, 47, 759–792.

Korjenkov, A. and Kaiser D. (2003). Historical-macroseismic study of the town church in Wittstock, northern Germany. In: *Proceedings, 11th FIG Symposium on Deformation Measurements*, Santorini, Greece.

Korjenkov, , K. Baipakov, C. Chang, Y. Peshkov & T. Savelieva (2003). Traces of Ancient Earthquakes in Medieval Cities Along the Silk Road, Northern Tien Shan and Dzhungaria. *Turkish Journal of Earth Sciences*, 12, 241-261.

Korres, M. (1996). Seismic damage of the Monuments of the Athenian Acropolis. *In: Stiros and Jones, Archaeoseismology.* British School at Athens. Fitch Laboratory Occasional Paper nº 7. p. 69-74.

Kovach, R. L. (2004). *Early earthquakes of the Americas*. Cambridge University Press. Cambridge. 268 p.

Lanciani, R. (1918). Segni di Terremoti negli edifizi di Roma Antica. *Bull. Della Comm. Arch*. Communale Roma, 1-30.

Lawson, A.C. (1908). *The California earthquake of April 18, 1906. Report of the state earthquake investigation commission in two volumes and atlas.* Published by the Carnegie Institution of Washington. Vol. 1, 451 p; Vol.2, 192 p; Atlas: 40 p.

Marco, S. (2008). Recognition of earthquake-related damage in archaeological sites: Examples from the Dead Sea fault zone. *Tectonophysics*, 453, 148-156.

McGuire, W.J., Griffiths, D.R., Hancock, P.L. and Stewart, I.S. (2000). *The Archaeology of Geological Catastrophes.* Geological Society of London Special Publication, nº 171. 417pp.

Michetti, A.M. et al. (2007). Intensity Scale ESI-2007. *Memorie Descriptive Della Carta Geologica D'Italia*, 74. APAT, SystemCart Srl, Roma, Italia.

Mistler, M., Butenweg, C., Meskouris K. (2006). Modelling methods of historic masonry buildings under seismic excitation. *Journal of Seismology*, 10, 497-510.

Monaco, C. and Tortorici L. (2004). Faulting and effects of earthquakes on Minoan archaeological sites in Crete (Greece). *Tectonophysics*, 382, 103– 116.

Nikonov, A. 1988. On the metholology of archaeoseismic research into historical monuments*. In: Engineering Geology of Ancient Works, Monuments and Historical Sites (G. Marinos and G. Koukis, Eds.).* Balkema, Roterdam. 1325-1320.

Nur, A. and Ron, H. (1996). And the Walls Came Tumbling Down: Earthquake History in the Holyland. *In: Stiros and Jones, Archaeoseismology.* British School at Athens. Fitch Laboratory Occasional Paper nº 7. p. 75-86.

Nur, A. and H. Ron. (1997). Armageddon's Earthquakes. *International Geology Review*, 39, 532-541.

Nur, Amos and Cline, Eric H., (2000). Poseidon's horses: Plate tectonics and earthquakes storms in the Late Bronze Age Aegean and Eastern Mediterranean. *Journal of Archaeology Science*, 27, 43-63.

Nur, A. and Burgess, D. (2008). *Apocalypse: Earthquakes, Archaeology and the Wrath of God*. Princeton University Press. Princeton and Oxford. 309 p.

Pérez-López, R., Paredes, C. and Muñoz-Martín, A. (2005). Relationship between the fractal dimension anisotropy of the spatial faults distribution and the paleostress fields on a Variscan granitic massif (Central Spain): the F-parameter. *Journal of Structural Geology* , 27(4), 663-677.

Pérez-López, R., J.L. Giner-Robles, J.J. Martínez-Díaz, M.A. Rodríguez-Pascua, M. Bejar, C. Paredes and J. M. González-Casado (2007). Active strain field on Deception Island (West-Antarctica): a new approach to the collapsed volcanic caldera from the fractal anisotropy of fracture sets. *U.S. Geological Survey and The National Academies; USGS Open File Report;* USGS OFR-2007-1047 (Short Research Paper 086).

Philip, H and Cisternas, A. (1983). El terremoto del Asnam del 10 de octubre de 1980. *En: Mecanismo de los terremotos y tectónica. Eds: Udías, A.; Muñoz, A. y Buforn*, E. Ed. U.C.M. 175-196. Madrid.

Rapp, G. 1982. Earthquakes in the Troad. *In: Troy: The archaeological Geology (G. Rapp and J.A. Gifford, Eds.).* Princenton. 43-58.

Reches, Z. (1983). Faulting of rocks in three-dimensional strain fields, II, Theoretical analysis, *Tectonophysics,* 95, 133-156.

Rodríguez-Pascua, M.A., R. Pérez-López, J. P. Calvo and M. A. García del Cura (2008). Recent seismogenic fault activity in a Late Quaternary closed-lake graben basin (Albacete, SE Spain). *Geomorphology*, 102, 169-178.

Rodríguez-Pascua, Miguel Angel, Raúl Pérez-López, Jorge L. Giner-Robles, Pablo G. Silva, Victor H. Garduño-Monroy and Klaus Reicherter. (2009a). A comprehensive classification of Earthquake Archaeological Effects (EAE) for structural strain analysis in Archaeoseismology. In: *R. Pérez-López, C. Grützner, J. Lario, K. Reicherter and P.G. Silva (eds). Archaeoseismology and Palaeoseismology in the Alpine-Himalayan Collisional Zone*. Abstracts Volume of the 1st INQUA-IGCP 567 International Workshop on Earthquake Archaeology and Palaeoseismology, 7th-13th September, p. 110. Baelo Claudia, Spain.

Rodríguez-Pascua, M.A., Abad Casal, L., Pérez-López, R., Gamo Parra, B., Silva, P.G., Garduño-Monroy, V.H., Giner-Robles, J.L., Israde-Alcántara, I., Bischoff, J. and Calvo,Garduño-Monroy, V.H., Giner-Robles, J.L., Israde-Alcántara, I., Bischoff, J. and Calvo, J.P. (2009b). Roman, visigoth and islamic evidence of earthquakes recorded in the archaeological site of El Tolmo de Minateda (Prebetic Zone, Southeast of Spain). In: *R. Pérez-López, C. Grützner, J. Lario, K. Reicherter and P.G. Silva (eds). Archaeoseismology and Palaeoseismology in the Alpine-Himalayan Collisional Zone.* Abstracts Volume of the 1st INQUA-IGCP 567 International Workshop on Earthquake Archaeology and Palaeoseismology, 7th-13th September, p. 114. Baelo Claudia, Spain.

Rodríguez-Pascua, M.A., J. Bischoff, V.H. Garduño-Monroy, R. Pérez-López, J.L.Giner-Robles, , I. Israde-Alcántara, (2009c). Estimation of the tectonic slip rate from Quaternary lacustrine facies within the intraplate Albacete province (SE of Spain). Sedimentary Geology (*in press*).

Schaub, A., Reicherter, K., Grützner, C. and Fernández-Steeger, T. (2009). Evidence for a medieval earthquake in the Aachen area (Germany), revealed by structural damage in the cathedral. In: *R. Pérez-López, C. Grützner, J. Lario, K. Reicherter and P.G. Silva (eds). Archaeoseismology and Palaeoseismology in the Alpine-Himalayan Collisional Zone.* Abstracts Volume of the 1st INQUA-IGCP 567 International Workshop on Earthquake Archaeology and Palaeoseismology, 7th-13th September, p. 132. Baelo Claudia, Spain.

Schreiber, S., Hinzen, K.G. and Fleischer, C. (2009). An application of 3D laser scanning in archaeology and archaeoseismology: the Medieval Cesspit in the Archaeological Zone Cologne, Germany. In: *R. Pérez-López, C. Grützner, J. Lario, K. Reicherter and P.G. Silva (eds). Archaeoseismology and Palaeoseismology in the Alpine-*

Himalayan Collisional Zone. Abstracts Volume of the 1st INQUA-IGCP 567 International Workshop on Earthquake Archaeology and Palaeoseismology, 7th-13th September, p. 136. Baelo Claudia, Spain.

Silva, P.G., Borja, F., Zazo, C., Goy, J.L., Bardají, T., De Luque, L., Lario J., Dabrio, C.J. (2005). Archaeoseismic record at the ancient Roman City of Baelo Claudia (Cádiz, south Spain). *Tectonophysics*, 408 (1-4): 129-146.

Silva, P.G., Reicherter, K., Grützner, Ch., Bardají, T., Lario, J., Goy, J.L., Zazo, C. and Becker-Heidmann, P. (2009a). Surface and subsurface palaeoseismic records at the ancient Roman city of Baelo Claudia and the Bolonia Bay area, Cádiz (south Spain). *Geological Society of London, Special Publication*, 316: 93-121.

Silva, P.G., Rodríguez Pascua, M.A., Pérez López, R., Giner-Robles, J.L., Lario, J., Bardají, T., Goy, J.L. and Zazo, C. (2009b). Geological and archaeological record of the 1504 AD Carmona earthquake (Guadalquivir Basin, South Spain): a review after Bonsor, 1918. In: *R. Pérez-López, C. Grützner, J. Lario, K. Reicherter and P.G. Silva (eds). Archaeoseismology and Palaeoseismology in the Alpine-Himalayan Collisional Zone.* Abstracts Volume of the 1st INQUA-IGCP 567 International Workshop on Earthquake Archaeology and Palaeoseismology, 7th-13th September, p. *139. Baelo Claudia, Spain.*

Sintubin, M. and Stewart, I. S. (2008). A Logical Methodology for Archaeoseismology: A Proof of Concept at the Archaeological Site of Sagalassos, Southwest Turkey. *Bulletin of the Seismological Society of America*, 98 (5), 2209–2230.

Sintubin, M., Stewart, I.S., Niemi, T. and Altunel, E. (2009). Archaeoseismology: past, present and future. In: *R. Pérez-López, C. Grützner, J. Lario, K. Reicherter and P.G. Silva (eds). Archaeoseismology and Palaeoseismology in the Alpine-Himalayan Collisional Zone.* Abstracts Volume of the 1st INQUA-IGCP 567 International Workshop on Earthquake Archaeology and Palaeoseismology*,* 7th-13th September, p. 143. Baelo Claudia, Spain.

Sillières (1997). *Baelo Claudia: Una ciudad Romana de la Bética*. Junta de Andalucía- Casa de Velázquez, Madrid.

Stiros, S. 1988a. Earthquake effects on Ancient Constructions. *In: New Aspect of Archaeological Science in Greece (R.E. Jones and H.W. Catling, Eds.)*. British Schools at Athens, Fitch Occasional Paper, 3, 1-6.

Stiros, S. 1988b. Archaeology, a tool to study active tectonics – The Aegean as a case study. *Eos, Trans. Am. Geophys. Union.* 13, 1636-1639.

Stiros, S. and Jones, R.E. (1996): Archaeoseismology. Institute of Geology and Mineral Exploration. Fitch Laboratory Occasional Paper. Stiros S., and Jones, R.E., Eds. Atenas. 268 p.

Stiros, S. C. (1996). Identification of Earthquakes from Archaeological Data: Methodology, Criteria and Limitations. *In: Stiros, S. and Jones, R., eds., Archaeoseismology.* Fitch Laboratory Occasional Paper 7. British School at Athens: 129-152.

Urbina, F. y Camacho, H. (1913). La zona megaseismica Acambay – Tixmadege, estado de México, movida el 19 de noviembre de 1912. *Boletín del Instituto Geológico de México,* 32, 125 p.

Yerli , B., Schreiber, S., Hinzen, K.G., ten Veen, J.H. and Sintubin, M. (2009). Testing the hypothesis of earthquake-related damage in structures in the lycian ancient city of Pinara, SW Turkey. In: *R. Pérez-López, C. Grützner, J. Lario, K. Reicherter and P.G. Silva (eds). Archaeoseismology and Palaeoseismology in the Alpine-Himalayan Collisional Zone.* Abstracts Volume of the 1st INQUA-IGCP 567 International Workshop on Earthquake Archaeology and Palaeoseismology*,* 7th-13th September, p. 173. Baelo Claudia, Spain.

Zang, B., Liao, Y., Guo, S., Wallace, R. Buckham, R. and Hanks, T. (1986). Fault scarps related to the 1739 earthquake and seismicity of the Yinchuan graben, Ningxia Zizhiqu, China. *Bull. Soc. America*. 76, 1253-1287.

APPENDIX – WORK PLANS OF BAELO CLAUDIA

A Theatre
B West Decumanus Maximus
C Central Decumanus Maximus
D East Decumanus Maximus
E Market
F Baths
G Archive, Temple
H Shops
I Foro
J Basilica
K Temple of Minerva
L Temple of Jupiter
M Temple of Juno
N Temple of Isis

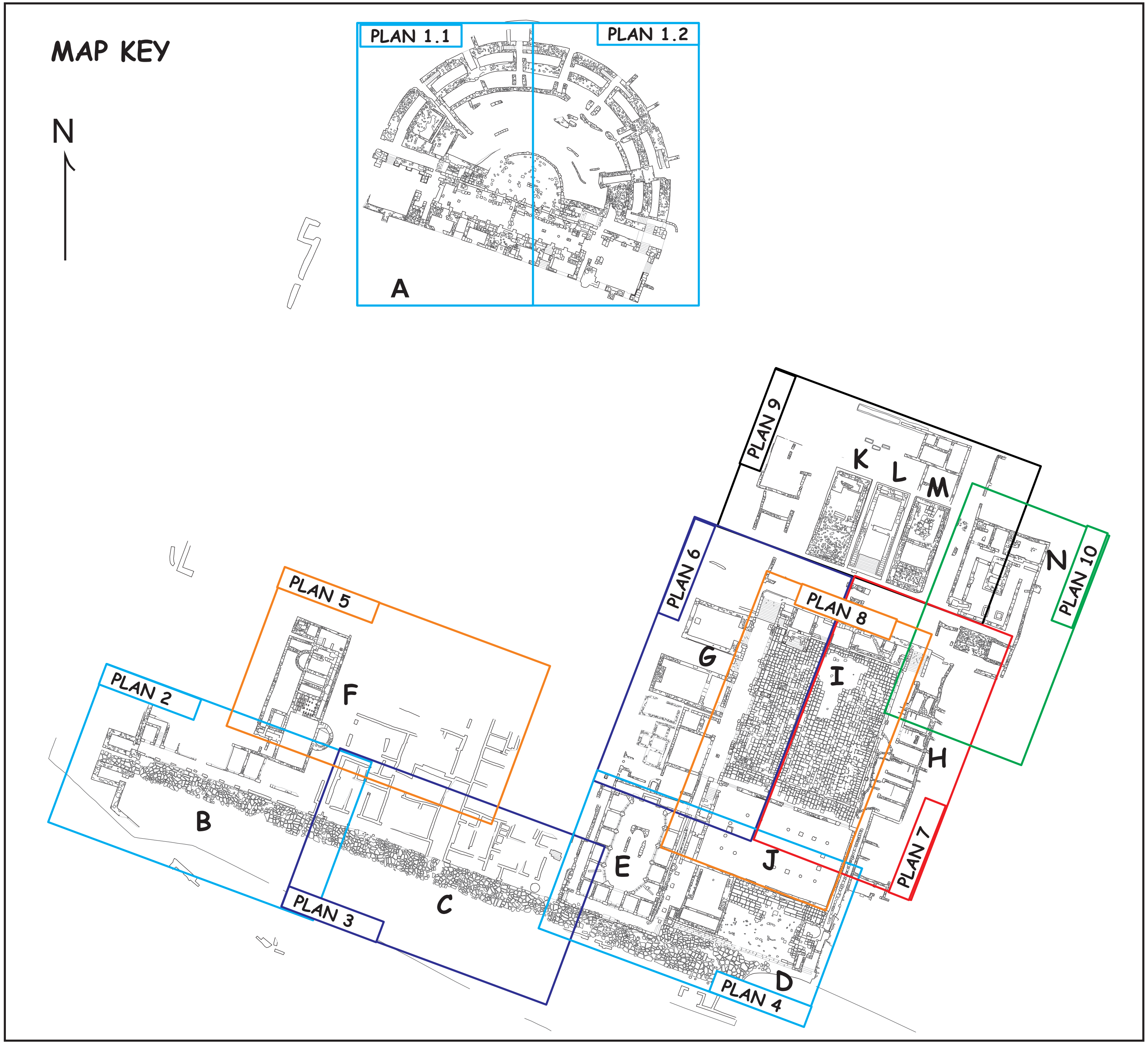

DATA

NOTES and DRAFTS

MAP 1.1
grid 1mx1m
BAELO CLAUDIA. THEATRE. WEST SIDE
0 5 10 15 m
graphic scale
N
1.1
25,683

DATA

NOTES and DRAFTS


MAP 1.2
grid 1mx1m
BAELO CLAUDIA. THEATRE. EAST SIDE
1.2
N
0
5
10
15 m
graphic scale

DATA

NOTES and DRAFTS

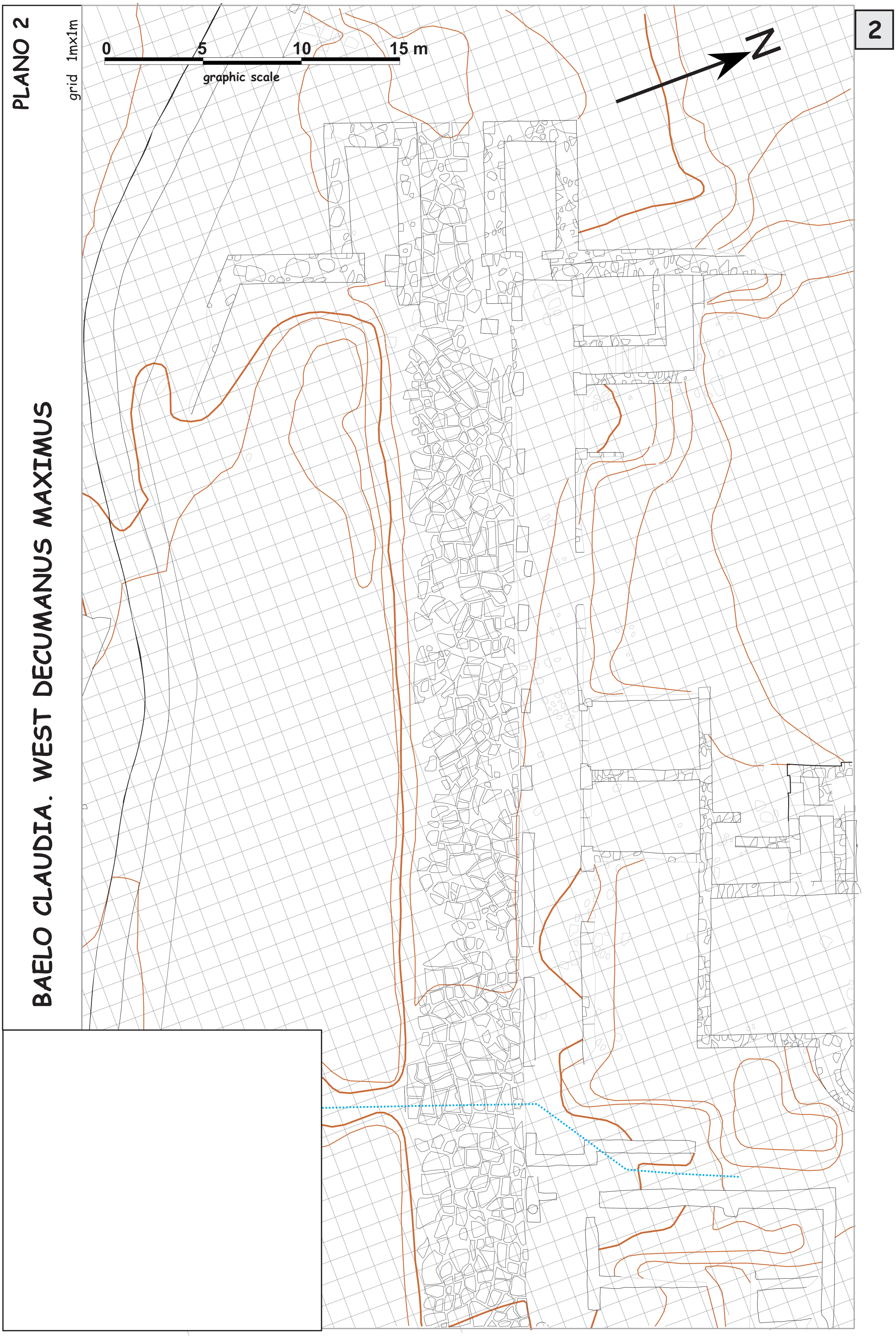
PLANO 2
grid 1mx1m
BAELO CLAUDIA. WEST DECUMANUS MAXIMUS
0
5
10
15 m
graphic scale
N
2

DATA

NOTES and DRAFTS

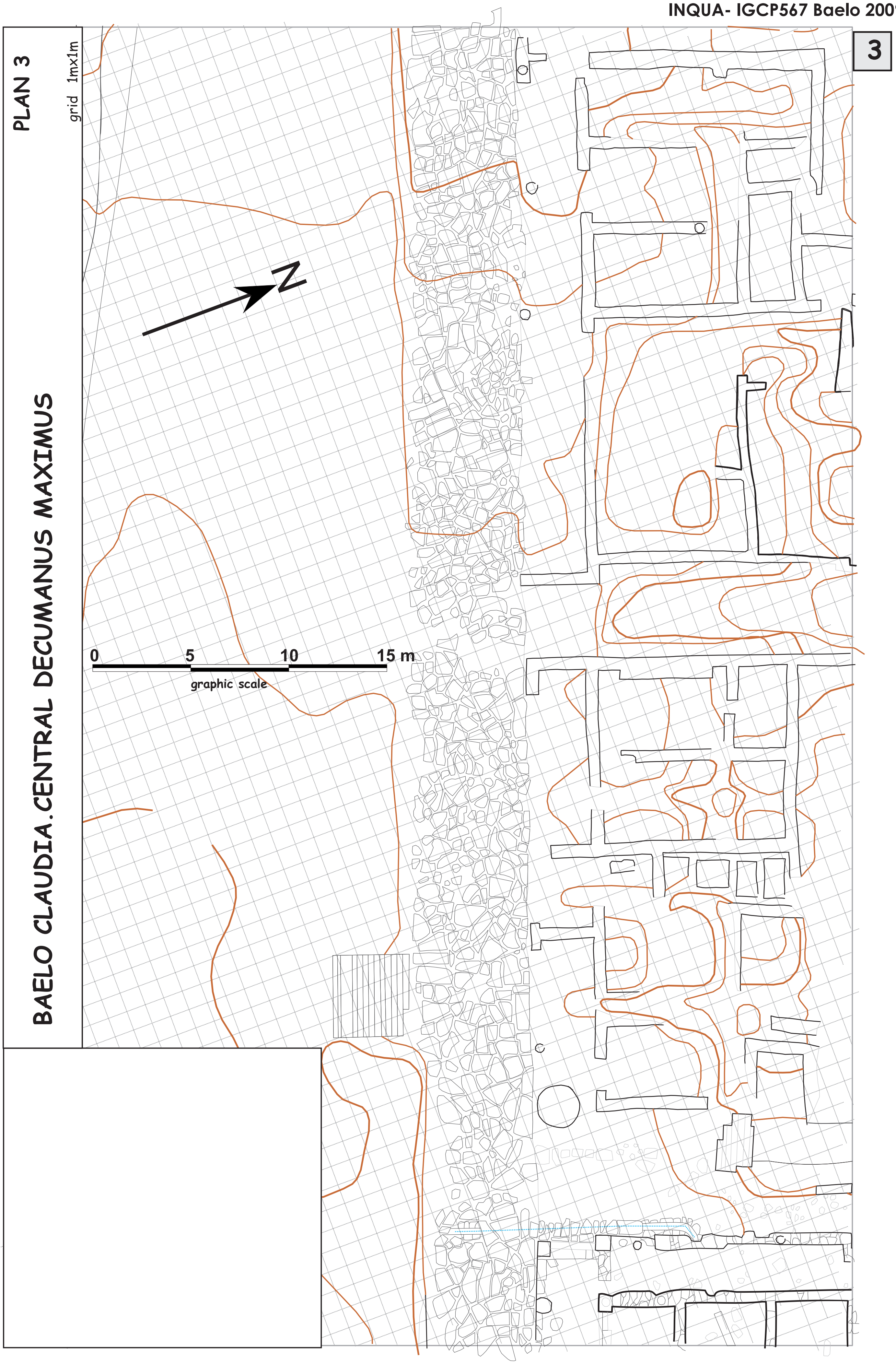
3
PLAN 3
grid 1mx1m
BAELO CLAUDIA.CENTRAL DECUMANUS MAXIMUS
N
0
5
10
15 m
graphic scale

DATA

NOTES and DRAFTS

PLAN 4

grid 1mx1m

EAST DECUMANUS MAXIMUS. MARKET. SOUHT PLACE. CURIA

DATA

NOTES and DRAFTS

PLAN 5

grid 1mx1m

BAELO CLAUDIA. BATHS

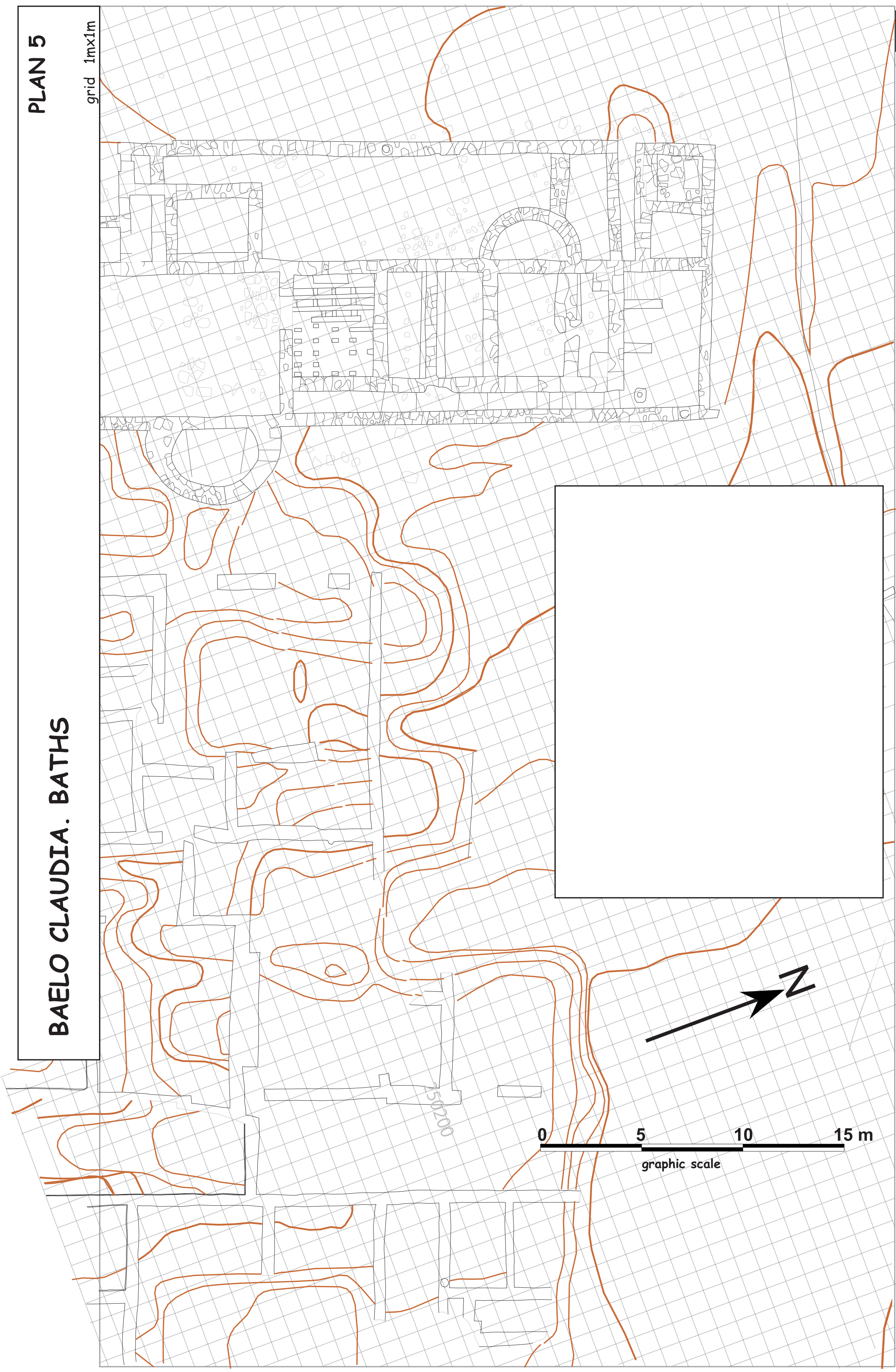

DATA

NOTES and DRAFTS

6

PLAN 6

grid 1mx1m

BAELO CLAUDIA. WEST FORO. TEMPLE. ARCHIVE.

DATA

NOTES and DRAFTS

BAELO CLAUDIA. EAST FORO. SHOPS

PLAN 7

grid 1mx1m

DATA

NOTES and DRAFTS

BAELO CLAUDIA. FORO. BASILICA

PLAN 8

0 5 10 15 m
graphic scale

grid 1m×1m

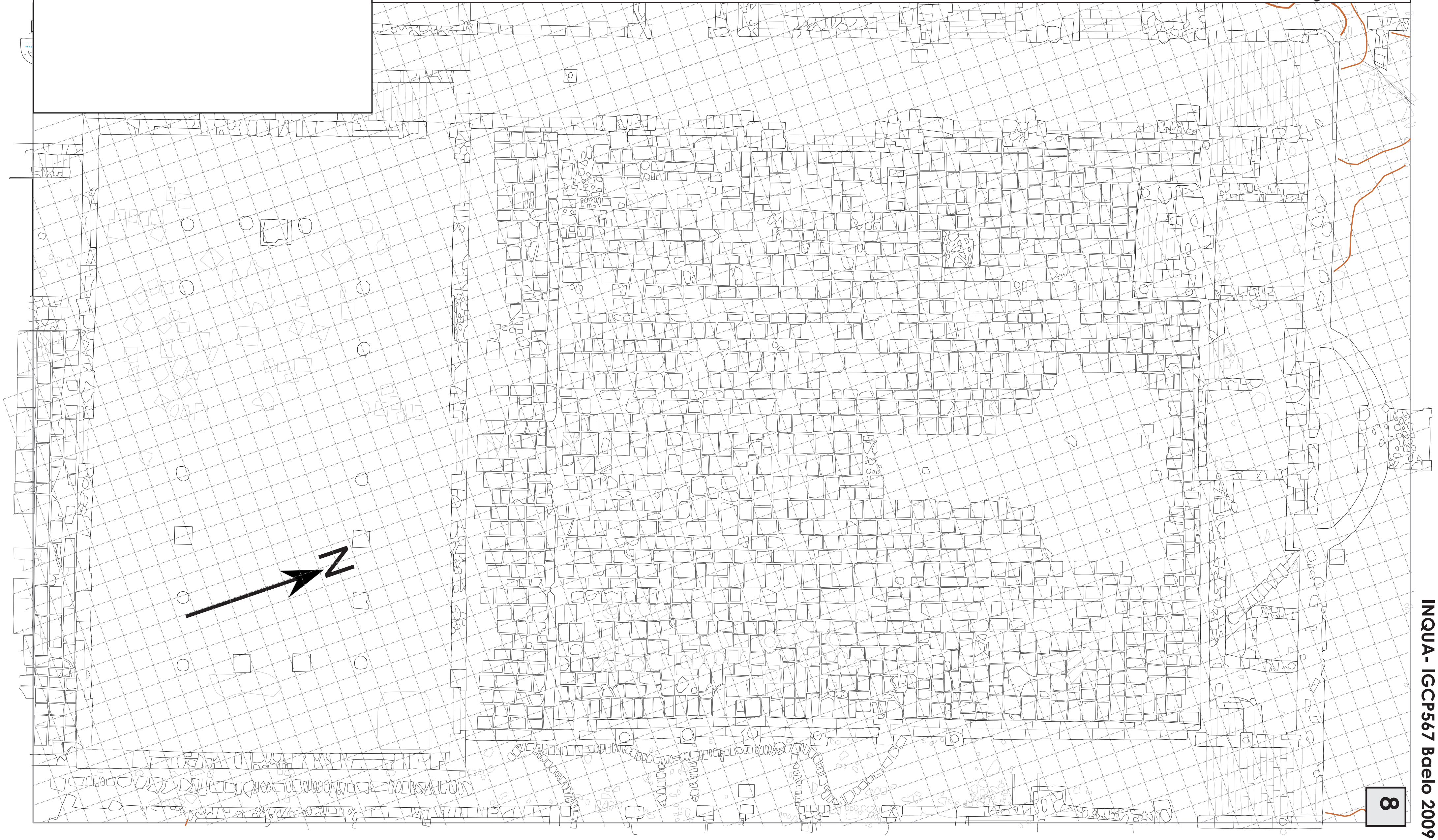

DATA

NOTES and DRAFTS

THE CAPITOLIUM: TEMPLES OF MIERVA, JUPITER AND JUNO

PLAN 9

grid 1m×1m

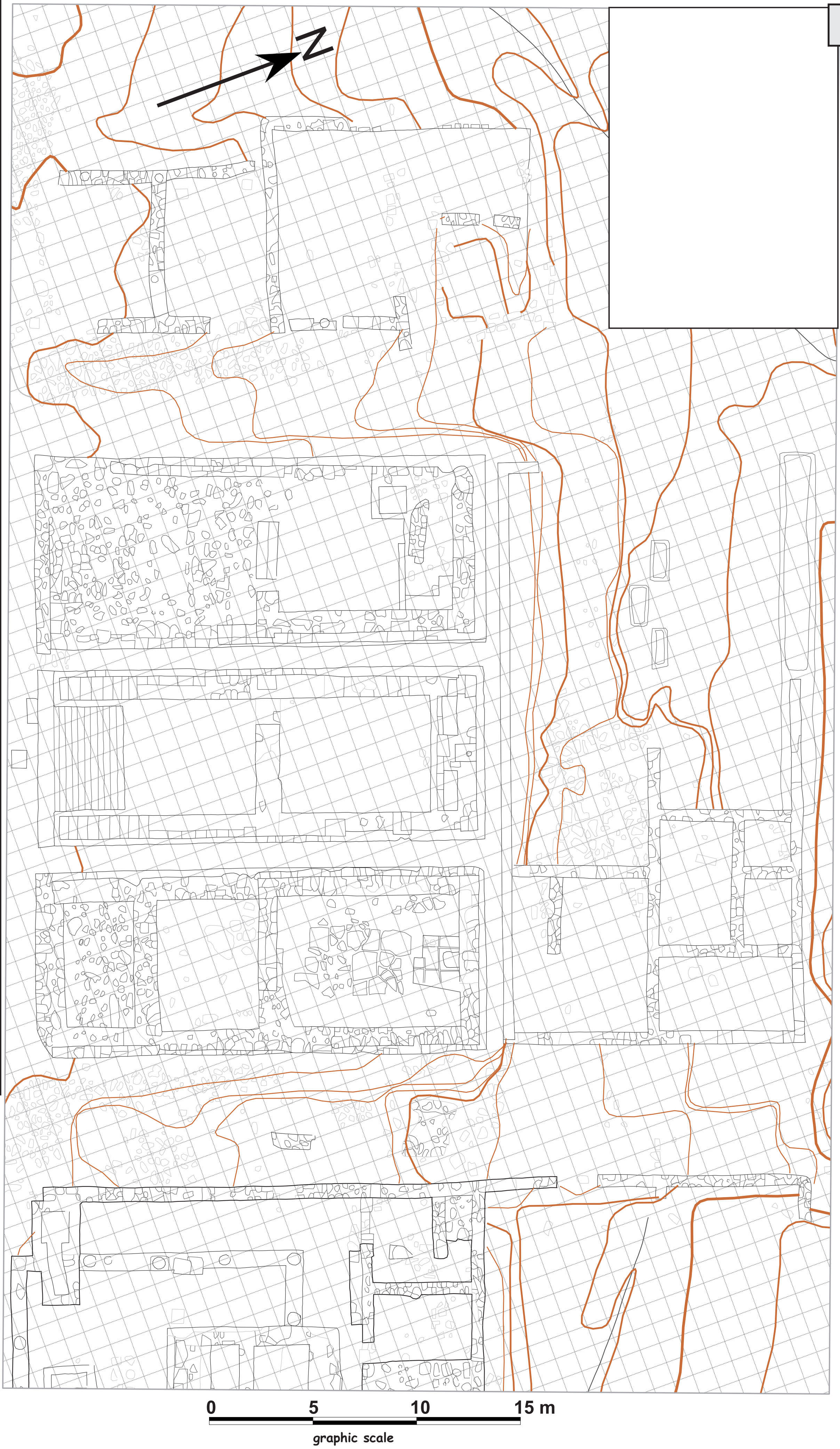

DATA

NOTES and DRAFTS

PLAN 10

grid 1mx1m

BAELO CLAUDIA. TEMPLE OF ISIS

Notes

BAELO 2009

INQUA PALEOSEISMOLOGY

IGCP-567

EARTHQUAKE ARCHAEOLOGY

PALEOSEISMOLOGY

VOLUME 2

RWTH AACHEN UNIVERSITY

VNiVERSiDAD D SALAMANCA

UNED

Instituto Geológico y Minero de España

INQUA

IUGS UNESCO IGCP

AEQUA

JUNTA DE ANDALUCIA
CONSEJERIA DE CULTURA

CSIC

GOBIERNO DE ESPAÑA

MINISTERIO DE CIENCIA E INNOVACIÓN